

“ DEVELOPING A PREDICTIVE CORRELATION MODEL BETWEEN AGGREGATE PROPERTIES AND MARSHALL PARAMETERS IN ROAD PAVEMENT ASPHALT MIXTURES”

RESEARCH DISSERTATION

Submitted by
SHEMA Richard (Registration No: 220017899)

Under the Guidance of
Supervisor: Assoc. Prof. MBEREYAHU Léopold

Submitted in partial fulfillment of the requirements for the award of
MASTER OF SCIENCE DEGREE
IN
HIGHWAY ENGINEERING AND MANAGEMENT

July 2025



**UNIVERSITY of
RWANDA**

COLLEGE OF SCIENCE AND TECHNOLOGY

SCHOOL OF ENGINEERING

P.O. Box: 3900 Kigali, Rwanda.

**DEPARTMENT OF CIVIL ENVIRONMENTAL AND GEOMATICS ENGINEERING
(CEGE)**

DECLARATION

I, Richard SHEMA, hereby declare that the dissertation titled “Developing a predictive correlation model between aggregate properties and Marshall parameters in road pavement asphalt mixtures” submitted in partial fulfillment of the requirements for the Master of Science degree at University of Rwanda, is my own original work.

To the best of my knowledge, it contains no material previously published or written by another person, nor material accepted for the award of any other degree at this or any other institution, except where due acknowledgment has been made in the text.

Names: SHEMA Richard

Registration Number: 220017899

Signature:

Date: 25th July 2025

CERTIFICATION

This is to certify that this dissertation work titled “Developing a predictive correlation model between Aggregate properties and Marshall parameters in road pavement asphalt mixtures” was carried out by Richard SHEMA under my Supervision.

Supervisor names: **Assoc. Prof. MBEREYAHO Léopold**

Department of Civil, Environmental and Geomatics Engineering

University of Rwanda, College of science and Technology

P.O. BOX 3900, KIGALI

Signature:.....

Date: 25th July 2025

ACKNOWLEDGEMENTS

I am profoundly grateful to my supervisor, Assoc. Prof. MBEREYAHU Léopold, whose steadfast guidance and timely feedback have shaped every stage of this research. Despite his busy schedule, he consistently provided constructive comments and unwavering encouragement.

My heartfelt appreciation extends to the University of Rwanda, College of Science and Technology, Department of Civil, Environmental and Geomatics Engineering, whose excellent teaching and resources laid the foundation for my growth as an emerging researcher.

I am equally thankful to my classmates, now cherished friends, whose collaboration, discussion, and camaraderie made this Master's journey both possible and enjoyable.

Finally, my deepest gratitude goes to my wife, ABAYO Albertine, and our beloved children. Your constant love, patience, and encouragement have been invaluable to me. Thank you for everything.

SHEMA Richard

Table of Contents

DECLARATION	i
CERTIFICATION	ii
ACKNOWLEDGEMENTS	iii
LIST OF FIGURES	ix
LIST OF TABLES	x
LIST OF ABBREVIATIONS AND ACCRONYMS	xi
ABSTRACT	xiv
CHAPTER ONE: GENERAL INTRODUCTION	1
1.1 Background of study	1
1.2 Problem Statement	2
1.3 Objectives of the research	3
1.3.1 Main Objective	3
1.3.2 Specific Objectives	3
1.4. The Project Scope.....	4
1.5 Justification of the project	4
1.6 Organization / structure of the research thesis	5
CHAPTER TWO: LITERATURE REVIEW	7
2.1 Introduction	7
2.2 Constituent materials of asphalt mixtures	7
2.2.1 Tests performed on bituminous roads	7
2.2.2 Aggregates	9
2.2.2.1 Specific Gravities.....	10
2.2.2.2 Gradation.....	11
2.2.3 Asphalt Binder	11
Binder content and its effects.....	12
2.2.4 Volumetric Parameters	12
2.2.4.1 Bulk density determination (G_m).....	16
2.2.4.2 Theoretical specific gravity of the mix G_t	17
2.2.4.3 Bulk specific gravity of mix G_m	17

2.2.4.4 Air voids percent V_v	17
2.2.4.5 Percent volume of bitumen V_b	18
2.2.4.6 Voids in mineral aggregate VM A.....	18
2.2.4.7 Voids filled with bitumen VFB.....	18
2.3 Marshall Mix Design Framework	18
2.3.1 Apparatus	19
2.3.2 Sampling.....	20
2.3.3. Determination of Marshall stability and flow Marshall	22
Apply stability correction	23
2.3.4 Graphical plots.....	23
2.3.5 Determination of optimum bitumen content	23
Volumetric Parameters.....	25
2.4 Evolution of mix design methodologies.....	27
2.4.1 Superpave Mix Design Approach.....	27
2.4.2 Balanced Mix Design (BMD).....	27
2.5 Influence of Aggregate properties on Marshall parameters	28
2.5.1 Specific Gravity Effects.....	28
2.5.2 Gradation and Packing.....	28
2.5.3 Volumetric Interplay.....	28
2.6 Predictive Modelling of Marshall Stability and Flow	28
Linear and Non-Linear Regression.....	28
2.7 Engineering Modelling.....	29
Problem Definition	29
Data Collection & Literature Review	29
Modeling Approach Selection.....	29
Model Formulation and Model Implementation	30
Model Simulation, Validation and Calibration.....	30
2.8 The gap in the previous research.....	31
CHAPTER THREE: STUDY METHODOLOGY	32
3.1 Study Description.....	32
3.2 Aggregates and volumetric properties data collected	32

3.2.1	Aggregates properties	32
3.2.2	Volumetric Properties.....	33
3.2.3	Asphalt binder type data collected.....	33
3.2.4	Asphalt mixtures.....	33
3.3	Data collection.....	34
3.3.1	Data collection strategy	34
3.3.2	Data Verification Protocol.....	34
3.3.3	Training vs Validation split	35
3.4	Data processing and statistical analysis	35
3.4.1	Descriptive statistics	35
3.4.2	Correlation analysis	36
3.5	Regression Modelling	36
	Model Development via Stepwise Regression	36
3.6	Model validation.....	36
CHAPTER FOUR: RESULTS AND DISCUSSION		38
4.1	Data collection and verification	38
4.1.1	Dataset Overview	38
4.1.2	Descriptive Statistics Procedure	38
4.1.3	Binder content (Pb) Dispersion analysis	40
4.1.4	Aggregate- and Mix-Density Characteristics	41
4.1.5	Volumetric-Parameter Distribution	42
4.1.6	Marshall Performance Indices	43
4.2	Correlation analysis.....	44
4.2.1	Findings from the Correlogram	45
	Density cluster (Gsb, Gmm, Gmb, Gse)	45
	Air-void effects	45
	Binder-related variables	46
	Volumetric balance	46
4.2.2	Interrelationships among aggregate properties.....	46
	Strong positive Correlations:	46
	Negative Correlations:	46

4.2.3 Relationships with Marshall Parameters:	47
Marshall Stability (MS):	47
Marshall Flow (MF):.....	47
4.2.4 Scatter plot analysis	47
4.2.4.1 Asphalt Content (Pb) vs Marshall Parameters	48
4.2.4.2 Bulk Specific Gravity of Aggregate (Gsb) vs Marshall Parameters	48
4.2.4.3 Maximum Theoretical Specific Gravity (Gmm) vs Marshall Parameters	49
4.2.4.4 Bulk Specific Gravity of Compacted Mix (Gmb) vs Marshall Parameters	49
4.2.4.5 Air Voids (Va) vs Marshall Parameters	50
4.2.4.6 Voids in Mineral Aggregate (VMA) vs Marshall Parameters	51
4.2.4.7 Voids Filled with Asphalt (VFA) vs Marshall Parameters	52
4.2.4.8 Effective Specific Gravity of Aggregate (Gse) vs Marshall Parameters	52
4.3 Regression analysis	53
4.3.1 Regression Analysis for Marshall Stability (MS).....	53
□ Initial Stepwise Analysis	53
4.3.1.1 MS versus Pb, Gsb, Gmm, Gmb, Va, VMA, VFA, Gse	53
4.3.1.2 Regression Equation (MS).....	54
4.3.1.3 ANOVA analysis	54
4.3.2 MF versus Pb, Gsb, Gmm, Gmb, Va, VMA, VFA, Gse	54
4.3.2.1 Regression Equation (MF).....	55
4.3.2.2 ANOVA analysis	55
4.4 Model validation	56
4.4.1 MS Model validation	56
4.4.1.1 Analysis of Variance.....	56
4.4.1.2 Fits and Diagnostics for All Observations.....	56
4.4.1.3 Fits and Diagnostics for All Observations	58
4.4.2 MF Model Validation	61
4.4.2.1 Analysis of Variance.....	61
4.4.2.2 Fits and Diagnostics for All Observations	61
4.4.2.3 Fits and Diagnostics for All Observations	63
4.5 Model performance summary	66

4.6. Discussion of Results	66
4.6.1 Overview of Regression Findings	67
4.6.2 Interpretation of Key Predictors	67
4.6.3 Statistical Diagnostics.....	67
4.6.4 Practical Implications	67
4.6.5 Correlation-Based Predictive Capability of the Developed Models	68
CHAPTER FIVE: CONCLUSION AND RECOMMENDATIONS	69
5.1 CONCLUSIONS.....	69
5.2 RECOMMENDATIONS	70
References.....	71
APPENDICES	76
APPENDICE A.....	76
APPENDICE B	85

LIST OF FIGURES

Figure 2.1: Aggregate Characteristics Governing Marshall Response (Kunaev et al., 2025)	11
Figure 2.2: Effect of VMA on Marshall Stability (Awan et al., 2022).....	13
Figure 2.3: Effect of air void on fatigue (Lira et al., 2021)	14
Figure 2.4: Effect of VFA on Marshal Flow (Gul et al., 2022)	15
Figure 2.5: Marshal mould (a) and Specimen (b).....	16
Figure 2.6: Marshall Test apparatus.....	19
Figure 2.7: Marshal typical graphical plots (Abedal, 2014)	24
Figure 2.8: VMA - VFA design space and effect of $\pm 0.5\%$ Pb shift (Awan et al., 2022)	25
Figure 2.9: a, b, c and d are relationship between Voids Filled with Asphalt and Marshall Stability (compiled from (Asi et al., 2024), Based on calculations using marshal charts on Figure f obtained optimum asphalt content that meets the marshal parameters between 2% Asphalt buton and 4.2% Asphalt Pen 60/70, asphalt buton substitutes 32% use of asphalt Pen 60/70 as a binder.	26
Figure 4.1: Frequency distribution of binder content Pb	40
Figure 4.2: Frequency distribution of aggregate and Mix Density parameters	41
Figure 4.3: Frequency distribution of volumetric parameters	43
Figure 4.4: Frequency distribution of Marshal Flow	43
Figure 4.5: Frequency distribution of Marshal Stability.....	44
Figure 4.6: Pearson correlogram linking aggregate properties.....	45
Figure 4.7: Scatter plots of asphalt-binder content (Pb) against MS and MF with fitted 95 % CI regression lines.....	48
Figure 4.8: Bulk specific gravity of aggregate (Gsb) versus MS and MF.....	49
Figure 4.9: Maximum theoretical specific gravity (Gmm) versus MS and MF	49
Figure 4.10: Bulk specific gravity of compacted mix (Gmb) versus MS and MF	50
Figure 4.11: Air-void content (Va) versus MS and MF.	50
Figure 4.12: Voids in mineral aggregate (VMA) versus MS and MF	51
Figure 4.13: Voids filled with asphalt (VFA) versus MS and MF.	52
Figure 4.14: Effective specific gravity of aggregate (Gse) versus MS and MF.	52

LIST OF TABLES

Table 2.1: List of some tests performed on bituminous road materials (Mamlouk & Zaniewski, 2018)	7
Table 2.3: Binder and mix volumetric properties (Junaid et al., 2018)	12
Table 2.4: Summarises key parameters, their definitions, typical specification limits, and standard test methods (Kennedy et al., 1994).	16
Table 2.5: Correction factors for Marshal Stability values (Abedal, 2014).....	23
Table 2.6: Marshall mixes design specification (Abedal, 2014)	24
Table 3.1: Aggregate properties tests with their related standards (Abedal, 2014).....	Error!
Bookmark not defined.	
Table 4.1: Study parameter statistics summary	39
Table 4.2: Stepwise-regression elimination history for predicting MS from eight candidate variables	53
Table 4.3: Final MS regression coefficients, standard errors, confidence intervals and multicollinearity diagnostics.	54
Table 4.4: ANOVA for the MS regression model.	54
Table 4.5: Stepwise-regression elimination history for predicting MF from eight candidate variables	55
Table 4.6: Final MF regression coefficients, confidence intervals and VIF statistics.....	55
Table 4.7: ANOVA for the MF regression model.	56

LIST OF ABBREVIATIONS AND ACCRONYMS

AASHTO – American Association of State Highway and Transportation Officials

AC – Asphalt Concrete

ACV – Aggregate Crushing Value

AICc – Corrected Akaike Information Criterion

APA – Asphalt Pavement Analyzer

ASTM – ASTM International (formerly American Society for Testing and Materials)

BIC – Bayesian Information Criterion

BMD – Balanced Mix Design

BS – British Standard

CA/FA – Coarse-to-Fine Aggregate ratio

CDMA – Compacted Density of the Mixed Aggregate

CI – Confidence Interval

CV – Cross-Validation

EI – Elongation Index

EN – European Norm

Eqn – Equation

f/Pb – Filler-to-Bitumen ratio

FI – Flakiness Index

Gm – Bulk Specific Gravity of Mix

Gmb – Bulk Specific Gravity of Compacted Mix

Gmm – Maximum Theoretical Specific Gravity of Mix

Gsa – Apparent Specific Gravity of Aggregate

Gsb – Bulk Specific Gravity of Aggregate

Gse – Effective Specific Gravity of Aggregate

Gt – Theoretical Specific Gravity of Mix

HMA – Hot Mix Asphalt

HWT – Hamburg Wheel-Tracking Test

IDEAL-CT – Indirect Tensile Asphalt Cracking Test

ITS – Indirect Tensile Strength

JMF – Job-Mix Formula
LAAV – Los-Angeles Abrasion Value
MAE – Mean Absolute Error
MF – Marshall Flow
ML – Machine Learning
MLR – Multiple Linear Regression
MS – Marshall Stability
NMAS – Nominal Maximum Aggregate Size
OLS – Ordinary Least Squares (regression)
Pb – Asphalt-Binder Content by weight of mix (%)
Pba – Absorbed Binder Content
Pbe – Effective Binder Content
PG – Performance Grade
PRESS – Predicted Residual Error Sum of Squares
Ps – Percent Aggregate in Total Mix
Q–Q – Quantile–Quantile
RMSE – Root-Mean-Square Error
RTDA – Rwanda Transport Development Agency
SD – Standard Deviation
SEE – Standard Error of Estimate
SG – Specific Gravity
SGC – Superpave Gyratory Compactor
SHAP – SHapley Additive exPlanations
SHRP – Strategic Highway Research Program
TFOT – Thin Film Oven Test
TSR – Tensile Strength Ratio
Va – Air Voids in Compacted Mix (%)
Vb – Percent Volume of Bitumen
VFA – Voids Filled with Asphalt (%)
VFB – Voids Filled with Bitumen (%)
VIF – Variance Inflation Factor

VIM – Voids in the Mixture (%)

VMA – Voids in Mineral Aggregate (%)

V_v – Air Voids percent

WMA – Warm Mix Asphalt

XGBoost – eXtreme Gradient Boosting (ensemble ML algorithm)

ABSTRACT

The performance and longevity of asphalt pavements are fundamentally influenced by the properties of their constituent materials, particularly aggregates and asphalt binder. The conventional Marshall mix design method, while widely used, requires extensive laboratory testing to achieve optimal stability and flow, leading to increased costs and time constraints for road construction projects. This main objective of this study is to address these challenges by developing a predictive correlation model that links aggregate and volumetric properties directly to Marshall Stability and Marshall Flow parameters, aiming to streamline the mix design process and enhance pavement quality.

A total of 211 historical mix designs were collected from both public and private institutions, with 159 valid datasets retained after screening. Each record contained asphalt binder content (Pb), bulk specific gravity of aggregate (Gsb), maximum theoretical specific gravity (Gmm), bulk specific gravity of compacted mix (Gmb), air-voids (Va), voids in mineral aggregate (VMA), voids filled with asphalt (VFA), effective specific gravity of aggregate (Gse), and the corresponding Marshall test outputs (MS and MF).

Pearson correlation analysis showed that Gmb had the strongest positive correlation with MS ($r \approx +0.60$), while VFA exhibited the highest positive relationship with MF ($r \approx +0.68$). Regression models were developed using ordinary least squares with backward elimination, supported by a 70:30 training-to-testing data split and Mallows Cp/AICc criteria to avoid overfitting. The final MS model retained four predictors (Gsb, Gmb, VFA, Gse) with an adjusted R^2 of 53.3% and test R^2 of 48.8%, while the MF model included five predictors (Pb, Gsb, Gmb, VFA, Gse), yielding an adjusted R^2 of 56.3% and test R^2 of 53.9%.

- $MS \text{ (kN)} = -44.58 - 17.5 Gsb + 125.5 Gmb - 0.162 VFA - 66.4 Gse$
- $MF \text{ (mm)} = 2.58 - 0.276 Pb + 4.30 Gsb - 10.46 Gmb + 0.062 VFA + 3.86 Gse$

Both models were statistically significant ($F > 27$, $p < 0.001$), met regression assumptions, and demonstrated prediction errors of ± 2.42 kN (MS) and ± 0.28 mm (MF). Gmb emerged as the

dominant predictor, positively affecting MS and inversely influencing MF, while VFA served as a key moderating factor in both models.

It is concluded that aggregate and volumetric properties particularly Gmb, Gse, Gsb, VFA, and Pb can reliably predict Marshall Stability and Flow, offering a practical and cost-effective alternative to full-scale laboratory testing for performance-based asphalt mix design. Further research is recommended to incorporate environmental and traffic-loading variables, and to explore nonlinear or machine learning approaches for improving prediction accuracy and extending model applicability to broader pavement design contexts.

CHAPTER ONE: GENERAL INTRODUCTION

1.1 Background of study

Road pavements represent complex engineering systems where the interaction between constituent materials significantly influences overall structural integrity, durability, and long-term performance (Liu et al., 2024; Mendoza-Sanchez et al., 2024). Among various paving options, asphalt mixtures are globally favored due to inherent advantages including durability, flexibility, superior skid resistance, and relatively lower construction costs compared to alternative paving materials (Moghaddam et al., 2011; Pranav et al., 2020). However, the long-term performance of asphalt pavements heavily relies on critical material properties, especially those of aggregates and asphalt binder (Fang et al., 2019; Li et al., 2019).

Aggregate characteristics such as bulk specific gravity (G_{sb}), effective specific gravity (G_{se}), aggregate proportions in the total mix (P_s), asphalt binder content by weight (P_b), maximum specific gravity of paving mix (G_{mm}), bulk specific gravity of compacted mix (G_{mb}), percent air voids (V_a), voids in mineral aggregate (VMA), and voids filled with bitumen (VFA) significantly impact the strength, durability, and functional lifespan of asphalt pavements. Among these, aggregate gradation is critical, directly influencing the mixture's resistance to fatigue, rutting, and deformation under traffic and environmental stresses (Moghaddam et al., 2011; Pedersen et al., 2011). Weak or poor-quality aggregates often result in premature pavement distress, including rutting, cracking, and potholes, ultimately compromising roadway safety and serviceability (Shelar et al., 2022).

The Marshall test is a widely recognized laboratory evaluation for characterizing asphalt mixtures. Specifically, Marshall Stability (MS) measures the maximum load a compacted specimen withstands before permanent deformation, directly reflecting mixture stiffness and rutting resistance. Concurrently, Marshall Flow (MF) quantifies deformation at peak stability, indicating mixture flexibility and ductility under applied loads (Abedal, 2014; Sakshi & Duggal, 2023).

A high Marshall stability value indicates a stiffer and more stable asphalt mixture, which is desirable for pavement applications (Yan et al., 2022). On the other hand, Marshall Flow (MF) which is the vertical deformation of an asphalt specimen, measured in millimetres, at the maximum load point during a Marshall stability test, indicates the mixture's flexibility and ductility.

However, the direct relationship between aggregate strength and these Marshall parameters remains an area that requires further investigation (Awan et al., 2022).

Existing predictive models often face limitations such as region-specific datasets, constrained consideration of material variability, and insufficient representation of diverse climatic and traffic loading scenarios (Asi et al., 2024).

Therefore, this research is explicitly designed to bridge this critical knowledge gap by developing a statistically robust predictive correlation model, leveraging advanced analytical techniques to systematically correlate asphalt mixture properties with Marshall parameters. The outcomes of this research are anticipated to equip pavement engineers and designers with sophisticated predictive tools, thereby minimizing dependence on extensive laboratory testing, optimizing asphalt mixture designs, and contributing toward the construction of more resilient, durable, and cost-effective asphalt pavement infrastructures.

1.2 Problem Statement

Despite significant advancements in asphalt pavement technology, engineers continue to face considerable challenges in accurately predicting pavement performance due to limited understanding of the quantitative relationship between fundamental aggregates, volumetric properties with Marshall Stability and Flow parameters. Existing empirical methods predominantly depend on repeated laboratory trials that consume substantial resources, time, and financial investments. The lack of a scientifically robust and comprehensive predictive correlation model consequently hinders the optimization of asphalt mix designs, leading to less efficient use of materials and increased costs due to premature pavement failures (Gul et al., 2022; Lv et al., 2020).

Previous research efforts to establish predictive models have often utilized localised datasets and narrowly defined aggregate properties, resulting in limited generalizability and application across varied geographical regions and climatic conditions. These limitations significantly restrict their effectiveness and reliability when applied beyond specific local contexts (Asi et al., 2024; Gul et al., 2022). Hence, there exists a critical necessity for an innovative predictive approach that systematically integrates comprehensive aggregate characteristics to provide universal applicability and reliability.

Moreover, the absence of such a predictive correlation model forces pavement engineers and designers to rely predominantly on personal expertise and empirical rules, rather than scientifically validated methodologies, for asphalt mixture selection and pavement design. This practice inherently introduces subjective bias and inconsistency, adversely affecting pavement quality, durability, and cost-effectiveness. Addressing this limitation through rigorous scientific modeling would not only standardize the pavement design processes but also significantly enhance the reliability and accuracy of predicting pavement performance (Shah et al., 2020).

This study seeks specifically to fill this critical gap by developing a comprehensive, statistically rigorous predictive correlation model linking aggregate properties and volumetric parameters directly with Marshall stability and flow parameters. Through utilizing extensive datasets from diverse road construction projects and applying advanced statistical modeling techniques, this research promises to deliver a robust applicable predictive tool. Such a tool would provide pavement engineers and designers with practical, data-driven guidance, significantly reducing reliance on costly laboratory trials, streamlining mix design processes, enhancing pavement durability, and yielding substantial environmental and economic benefits (Gul et al., 2022).

1.3 Objectives of the research

1.3.1 Main Objective

The primary objective of this research is to develop a statistical model that could be used to predict the Marshall test parameters for road pavement asphalt mixtures.

1.3.2 Specific Objectives

The following specific objectives were set to achieve the main purpose of the study:

- a. Collect asphalt mix design data with aggregate, volumetric properties, and Marshall Test results.
- b. Analyze data patterns for preselecting suitable statistical models.
- c. Identify the best predictive model for reliable pavement performance forecasting.
- d. Validate the predictive model with independent data for reliability across construction projects.

1.4. The Project Scope

This study is focused on developing predictive regression models that establish reliable correlations between aggregate characteristics, volumetric mix properties, and Marshall performance parameters specifically, Marshall Stability (MS) and Marshall Flow (MF). The project does not attempt to revise or replace the Marshall mix design method, but rather to enhance its application by introducing statistically based tools that reduce dependency on extensive laboratory testing.

The analysis is based on validated above two hundreds asphalt mix design records collected from both public and private laboratories in Rwanda. The scope is restricted to road surface course mixtures, with predictor variables limited to routinely measured properties such as binder content (Pb), aggregate specific gravities (Gsb, Gse, Gmb, Gmm), and volumetric factors (VFA, VMA, Va). The models are intended for use during the preliminary stages of mix design and quality control, where time and resource efficiency are critical.

This work excludes performance modeling under long-term service conditions, such as fatigue cracking, rutting, or thermal susceptibility. Similarly, environmental variables, traffic loading data, and binder aging effects are beyond the scope of the current study. However, these aspects are acknowledged as valuable extensions for future research.

1.5 Justification of the project

- Currently, approximately 35% of road pavement failures are attributed directly to inadequate comprehension of how aggregate characteristics quantitatively affect asphalt performance indicators such as Marshall parameters (Lv et al., 2020). By bridging this knowledge gap, proposed model will enhance pavement performance predictions, significantly reducing pavement distress, maintenance requirements, and associated lifecycle costs.
- Moreover, the traditional method for determining Marshall Stability and Flow involves extensive laboratory testing, which is both resource-intensive and time-consuming (Gul et al., 2022). These laboratory processes require substantial investment in equipment, skilled

personnel, and considerable time delays, which adversely impact project timelines and budgets. A validated predictive model will substantially decrease dependence on physical tests, enabling faster and more cost-effective determination of optimal asphalt mix designs.

- The proposed predictive model also holds significant environmental implications. Pavement construction and maintenance contribute substantially to environmental impacts through resource consumption and carbon emissions (Department of Transport, 2023). Recent research demonstrates that optimizing asphalt mixtures based on precise predictive correlations can potentially reduce carbon emissions by up to 15% through decreased maintenance frequency, fewer construction activities, and improved material efficiency. Thus, the model's adoption would align pavement engineering practices with global sustainability objectives (Bressi et al., 2021).
- Economically, the absence of an effective predictive correlation model results in suboptimal use of construction resources and increased lifecycle costs. Studies by estimate potential cost savings ranging between \$2.50 and \$3.00 per square meter of pavement by employing optimized aggregate selection and mixture design processes informed by accurate predictive models. The implementation of this research model would thus significantly enhance economic efficiency and budget predictability for road infrastructure projects (Williams et al., 2019).
- Finally, the integration of a comprehensive and robust predictive model into standard engineering practice would enhance decision-making transparency and consistency in pavement design. By reducing subjective reliance on empirical practices and professional intuition, this model would facilitate more precise, scientifically grounded decisions. Consequently, it would lead to improved reliability, performance consistency, and sustainability in pavement construction, ultimately benefiting both infrastructure users and the broader community (Gul et al., 2022; Shah et al., 2020).

1.6 Organization / structure of the research thesis

This research report consists of five chapters successively structured as steps followed to achieve the specific research objectives. First chapter briefly explains the general introduction to the study. It introduces the background information on the study, states the research problem, and presents the research objectives. Furthermore, it presents the justification of the research and the structure of the thesis.

Chapter two presents a literature overview on prediction models between aggregate and volumetric properties with Marshall Parameters in hot asphalt mixtures. Third chapter describes the methodology used to achieve the study objectives; this chapter presents the study area and also identifies and details the methods and techniques used in data collection, data processing, and analysis.

Chapter four provides the research findings and their discussions. It explains the meaning of the findings, their importance, and implications. It also provides a comparison of findings related to the similar previous studies as discussions parts of this thesis while the last chapter presents conclusions and recommendations made from the results of this research. Finally, references and appendices are also included.

CHAPTER TWO: LITERATURE REVIEW

2.1 Introduction

The performance of asphalt pavements is governed by the complex interaction of aggregates, asphalt binder, and void structure in the compacted mix. Understanding how individual aggregate properties influence the Marshall Stability (MS) and Marshall Flow (MF) indices is much important for performance oriented mix design.

Although reliable, the repeated laboratory compaction and testing demanded by the Marshall procedure are time-consuming, equipment-intensive, and expensive. Recent moves toward performance-based design therefore emphasise predictive correlations that estimate MS and MF directly from readily measured aggregate properties and volumetric indices, saving both time and resources (Aliyu Yaro et al., 2024).

This chapter synthesises peer reviewed research, standards, and technical reports to define relevant aggregate and volumetric properties, discuss current mixture design frameworks, detail the Marshall test fundamentals, review empirical and data driven models that link aggregate properties to Marshall parameters, and identify knowledge gaps that motivate the present study.

2.2 Constituent materials of asphalt mixtures

2.2.1 Tests performed on bituminous roads

There are many tests performed to check if the specified criteria for the suitable mix design have been met, or to predict the performance of an asphalt pavement after construction. Various laboratory tests are essential to evaluate the engineering properties of road construction materials. These tests, categorized by material type aggregates, bitumen, and asphalt mixtures are summarized in Table 2.1, which highlights their purpose and relevance in pavement design.

Table 2.1: List of some tests performed on bituminous road materials (Mamlouk & Zaniewski, 2018)

<i>Tests on Aggregates</i>	<i>Purpose</i>
Sieve Analysis (Gradation)	Determines particle size distribution
Los Angeles Abrasion Test	Measures resistance to abrasion and wear
Aggregate Crushing Value (ACV)	Assesses resistance to crushing under gradually applied load
Flakiness Index	Evaluates particle shape – flaky particles affect compaction and strength
Elongation Index	Measures elongation; excessive elongation may lead to poor interlock

Specific Gravity (Bulk, Apparent, Effective)	Critical for mix design volumetric calculations (G_{sb} , G_{sa} , G_{se})
Water Absorption Test	Determines moisture susceptibility and binder demand
Soundness Test	Evaluates resistance to weathering (freeze-thaw or sulfate exposure)
Sand Equivalent Test	Indicates presence of clay-like fines
<i>Tests on Bitumen (Asphalt Binder)</i>	<i>Purpose</i>
Penetration Test	Determines hardness or softness of the bitumen
Softening Point Test	Indicates temperature at which bitumen softens (Ring and Ball test)
Ductility Test	Measures the stretchability before breaking
Flash and Fire Point Test	Determines temperature at which bitumen gives off vapors (safety measure)
Specific Gravity Test	Needed for volumetric calculations
Viscosity Test (Rotational or Saybolt)	Evaluates flow behavior at various temperatures
Solubility Test	Checks for purity and presence of non-bituminous materials
Thin Film Oven Test (TFOT)	Assesses aging characteristics due to heat exposure
Rolling Thin Film Oven Test (RTFOT)	Simulates short-term aging during mixing and compaction
<i>Tests on Asphalt mix</i>	<i>Purpose</i>
Marshall Stability and Flow Test	Measures strength and deformation characteristics under load
Hveem Stabilometer Test	Assesses mix stability using confined shear resistance
Gyratory Compactor Test	Simulates field compaction and measures compactability
Bulk Density Test (G_{mb})	Determines compacted density of asphalt specimens
Maximum Specific Gravity Test (G_{mm})	Required for calculating air voids, VMA, VFA
Air Voids Content (V_a)	Indicates percentage of air in compacted mix
Voids in Mineral Aggregate (VMA)	Indicates void space available in aggregate skeleton
Voids Filled with Bitumen (VFA)	Shows the degree of void filling by binder
Indirect Tensile Strength (ITS)	Measures tensile resistance – relates to cracking potential
Moisture Susceptibility (TSR)	Assesses durability and stripping potential
Rutting Resistance (Wheel Tracking Test)	Evaluates deformation under repeated loads
Fatigue Testing	Determines resistance to repeated flexural loading

2.2.2 Aggregates

Aggregates constitute roughly 90 % of the total mix mass and 80-85 % of the volume of Hot-Mix Asphalt (HMA). Key attributes include specific gravity, gradation, shape, angularity, surface texture, abrasion resistance, and absorption capacity (Omar et al., 2020). High bulk and effective specific gravities (G_{sb} , G_{se}) correlate with dense aggregate skeletons that enhance load transfer and reduce post-compaction densification (Moghaddam et al., 2011). Conversely, absorptive aggregates demand higher binder contents to achieve adequate film thickness, potentially lowering stability (Fang et al., 2019). To ensure the quality of aggregates used in asphalt mixtures, standard specification limits are followed. Standard specification limits that govern aggregate quality for asphalt mix design are provided in Table 2.2, based on international standards.

Table 2.2: Aggregate Characteristics Governing Marshall Response (Kunaev et al., 2025)

Sub-section	Key variables	Typical influence on MS/MF	Typical laboratory test
Gradation	% passing control sieves, Bailey ratios	Dense gradations enhance particle interlock, reducing air voids and raising MS; very fine or gap-graded mixes may raise MF	ASTM C136, EN 12697-2
Shape & Texture	Flakiness Index (FI), Elongation Index (EI), angularity	Angular, rough particles improve load transfer and MS but may increase MF if packing is poor	BS 812-105, ASTM D5821
Strength & Toughness	Aggregate Crushing Value (ACV), Los-Angeles Abrasion Value (LA AV)	Lower ACV/LAAV → tougher aggregate → higher MS and lower rutting susceptibility	BS 812-110, ASTM C131
Specific Gravities	Bulk (G_{sb}), Apparent (G_{sa}), Effective (G_{se})	Higher G_{sb} and lower water absorption correlate with dense packing and greater MS	ASTM C127/C128

2.2.2.1 Specific Gravities

Specific-gravity measurements translate the mass percentages of individual aggregate fractions into true volumes, making them indispensable for all volumetric parameters that govern Hot-Mix Asphalt (HMA) quality—particularly air-voids (Va), voids in mineral aggregate (VMA) and voids filled with asphalt (VFA). In European practice they are determined in accordance with EN 1097-6 (particle density and water absorption) and EN 1097-9 (bulk density of fines), while North-American laboratories rely on ASTM C127/C128 or AASHTO T 84/T 85. (Gashi et al., 2017), (Version, 2022).

Bulk specific gravity (Gsb) represents the ratio of oven-dry mass to volume, inclusive of impermeable pores. Apparent specific gravity (Gsa) excludes permeable pores. Effective specific gravity (Gse) accounts for the volume of absorbed binder and is critical for volumetric calculations. High-quality crushed igneous aggregates typically exhibit $Gsb \geq 2.70$, while sedimentary aggregates fall near 2.50-2.65, influencing mixture density and stiffness (Pedersen et al., 2011).

Recent modelling efforts confirm that Gmb, Va and VFA are the three strongest volumetric predictors of Marshall Stability, with correlation coefficients ($|r|$) often exceeding 0.70 (Aliyu Yaro et al., 2024).

Bulk specific gravity (Gsb) is the ratio of oven-dry mass to the total particle volume including both impermeable and permeable pores. Because those pores also hold asphalt during mixing, Gsb is the correct denominator for converting aggregate mass into volume in VMA calculations. A mis-measured Gsb can shift optimum binder content by $\pm 0.5\%$ and VMA by more than 1%, with direct consequences for durability and rut resistance (Gashi et al., 2017).

Apparent specific gravity (Gsa) excludes permeable pores, representing only the solid mineral lattice. Gsa therefore exceeds Gsb for any porous rock. Although it is **not** used directly in HMA design, the gap between Gsa and Gsb acts as a porosity indicator and flags aggregates that may suffer excessive asphalt absorption or moisture damage.

Effective specific gravity (Gse) occupies the middle ground: it removes the volume of pores that eventually fill with asphalt binder but retains the impermeable pore space. Gse is derived from the theoretical-maximum mixture density (Gmm) and is vital for calculating absorbed-binder content

(Pba) and, by extension, effective binder content ($P_{be}=P_b-P_{ba}$) the quantity that actually coats the aggregate skeleton and controls durability.

2.2.2.2 Gradation

Gradation controls aggregate interlock, permeability, and binder demand. Well-graded dense mixes minimise voids in mineral aggregate (VMA) and reduce susceptibility to rutting, whereas gap-graded or stone-mastics utilise a rich mortar matrix to resist cracking (EN 12697-2:2023). Studies show that shifting the gradation curve toward the finer side of the control envelope decreases MS but improves MF, reflecting enhanced flexibility (Kalaitzaki et al., 2015). Figure 2.1 illustrates the influence of gradation, shape, texture, and strength parameters on Marshall Stability and Flow, as observed by Kunaev et al. (2025).

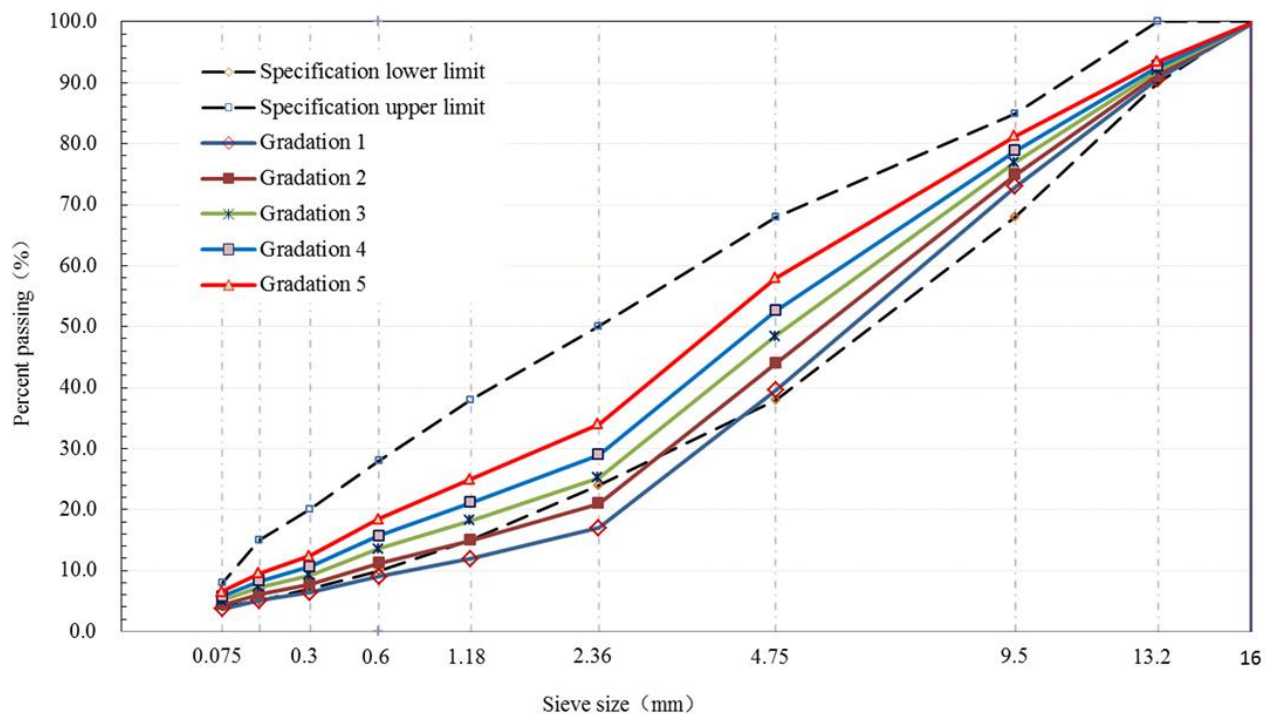


Figure 2.1: Aggregate Characteristics Governing Marshall Response (Kunaev et al., 2025)

2.2.3 Asphalt Binder

The asphalt binder, often termed bitumen, is the primary binding agent in hot mix asphalt (HMA), importantly for coating aggregates and providing cohesion, flexibility, and durability to the pavement. The physical and chemical properties of the asphalt binder directly influence the performance characteristics of asphalt mixtures, including Marshall parameters, which are essential indicators of pavement quality and longevity (Li et al., 2019).

Binder content and its effects

Binder content (% by weight of total mix) significantly impacts the volumetric and mechanical properties of asphalt mixtures. Optimal binder content ensures adequate coating of aggregate particles, minimizes air voids, and achieves a balance between stability and flexibility. Too little binder can result in poor cohesion and raveling, while excessive binder can lead to bleeding and rutting (Kassem et al., 2011). Table 2.0-2 summarizes key binder and mix volumetric properties, including definitions and typical specification ranges essential for asphalt mix design.

Table 2.0-2: Binder and mix volumetric properties (Junaid et al., 2018)

Binder and mix volumetric properties.								
Binder properties								
Binder tests	Standard			40/50	80/100			
Penetration test	ASTM D5			43	84			
Flash & Fire Point Test	ASTM D92			335 °C* & 359 °C**	233 °C* & 275 °C**			
Softening Point Test	ASTM D36			52 °C	47 °C			
Ductility Test	ASTM D113			Greater than 100 mm	Greater than 100 mm			
RV Test (Pa.s)	AASHTO 316							
135 °C				0.486	287.5			
160 °C				0.083	131.67			
BBR Test (MPa)	ASTM D6648							
-12 °C				427.41	449.82			
-6 °C				120.65	259.34			
0 °C				58.643	81.02			
Mix volumetric & optimum bitumen content								
Layer type	Binder	Mix	OBC	Air voids (%)	VMA*** (%)	VFA**** (%)	Stability (kg)	Flow (mm)
Wearing course	40/50	NHA A	3.9	4.0	13.09	69.44	11.75	2.29
		SP A	5.5	4.0	15.22	73.71	14.19	2.63
	80/100	NHA A	3.7	4.0	11.32	64.66	7.75	2.68
		SP A ^a	4.6	4.0	15.04	73.40	9.16	2.58
Base course	40/50	SP B ^b	3.4	4.0	13.16	69.62	22.00	3.40
		DBM	4.4	4.0	13.55	70.48	32.50	9.00
	80/100	SP B	3.3	4.0	11.45	65.07	24.77	28.81
		DBM	4.3	4.0	12.30	67.50	5.98	7.52

*Flash point; **Fire point; ***Voids in mineral aggregates; ****Voids filled with asphalt; ^aSuperpave A; ^bSuperpave B.

2.2.4 Volumetric Parameters

In asphalt mixture design, volumetric parameters serve as critical indicators of mixture performance, workability, and long-term durability. The primary volumetric measures Air Voids (Va), Voids in Mineral Aggregate (VMA), and Voids Filled with Asphalt (VFA) are interrelated and together determine the balance between stability and flexibility in a paving mixture.

Air Voids represent the small, discrete pockets of air remaining in a compacted specimen and are typically controlled between 3 % and 5 % to allow for in-service densification without significant bleeding or oxidation. VMA quantifies the total volume of void space between aggregate particles, including both air voids and the space occupied by binder, and is essential for ensuring sufficient

binder film thickness too low VMA can lead to rutting, while too high VMA may result in insufficient stability. VFA, the ratio of binder-filled voids to total VMA, provides insight into the effective binder content available to coat aggregates and resist ageing (Pedersen et al., 2011).

- **Effect of VMA on Marshall Stability:** Awan et al. (2022) observed that as VMA increases, the Marshall Stability of dense-graded mixes generally decreases, indicating a trade-off between durability (binder film thickness) and strength.

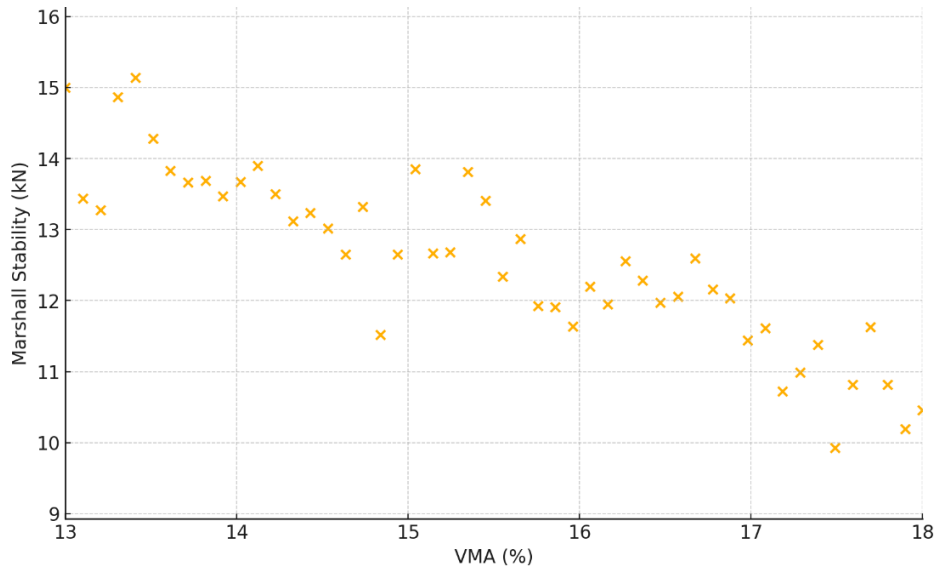


Figure 2.2: Effect of VMA on Marshall Stability (Awan et al., 2022)

The **Air Voids (Va)** content influences both mechanical and durability properties of the pavement. A lower Va (below about 3 %) tends to increase fatigue life and reduce permeability, but risks binder squeeze-out (bleeding) under traffic loading and elevated temperatures. Conversely, higher Va (above about 5 %) improves resistance to rutting but may accelerate oxidation and moisture damage, leading to stripping or cracking (Kassem et al., 2011). Many specifications target a Va of 4 % ± 1 % as a compromise between strength and flexibility, acknowledging that field compaction and environmental conditions will further adjust the in-place air-voids content (Abedal, 2014).

- **Effect of Air Voids on Fatigue Life** (Lira et al., 2021) demonstrated that higher air-voids contents tend to reduce fatigue life, as more void space accelerates crack initiation under cyclic loading.

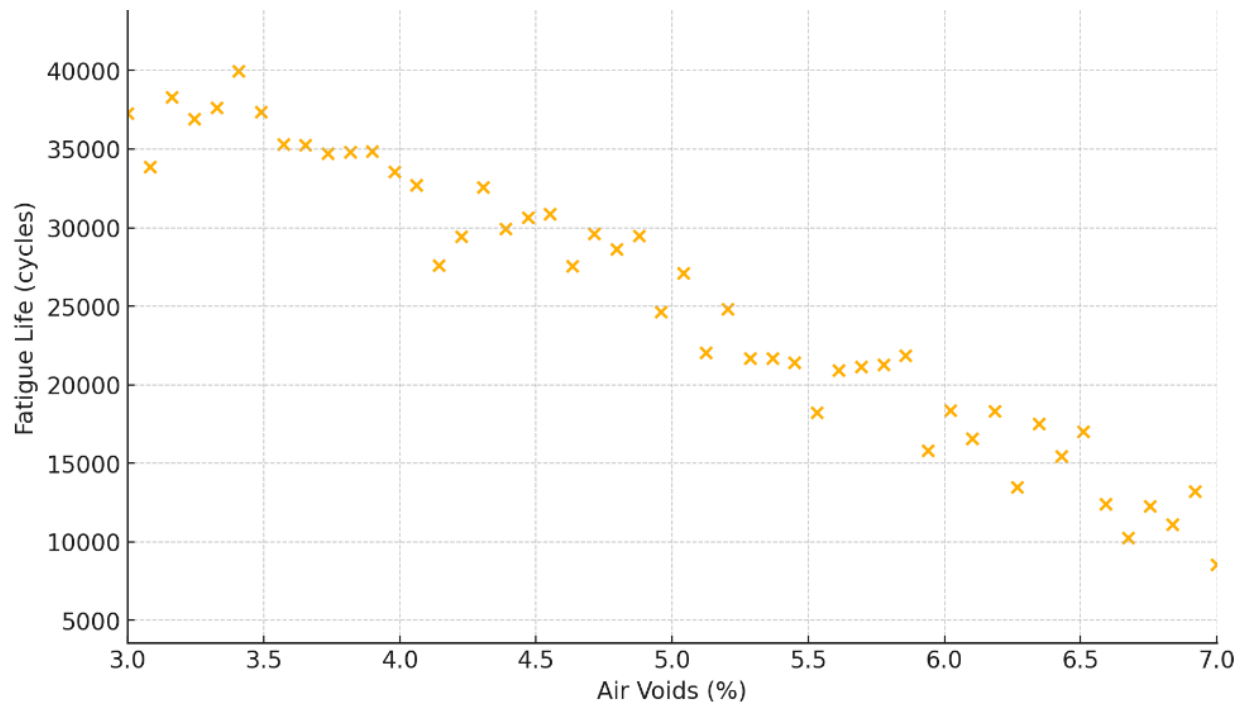


Figure 2.3: Effect of air void on fatigue (Lira et al., 2021)

Voids in Mineral Aggregate (VMA) governs the volumetric “space” available to hold both air and binder within the aggregate framework. Research by (Lira et al., 2021) demonstrated that increasing VMA beyond the minimum threshold (often 13 %–16 % for dense-graded mixes) enhances the durability and aging resistance of the mixture by providing a thicker binder film. However, elevated VMA can lower mixture stability and stiffness, particularly under high-traffic or heavy-axle loads. Hence, VMA requirements are frequently specified in standards such as AASHTO M 323 and EN 12697-8 to ensure a minimum binder film thickness of roughly 7 μm while avoiding excessive flexibility that could compromise bearing capacity.

The Voids Filled with Asphalt (VFA) metric bridges the relationship between Va and VMA by expressing the proportion of VMA occupied by binder:

$$VFA = \frac{VMA - Va}{VMA} \times 100\%$$

Volumetric analysis plays important role in mix design and performance prediction. Key volumetric parameters such as air voids, VMA, and VFA are defined in Table 2.0-2, along with the equations used to compute each, ensuring consistency in interpretation.

- **Effect of VFA on Marshall Flow**, (Gul et al., 2022) reported a positive relationship between VFA and Marshall Flow: mixtures with more binder-filled voids deformed more under load, enhancing flexibility.

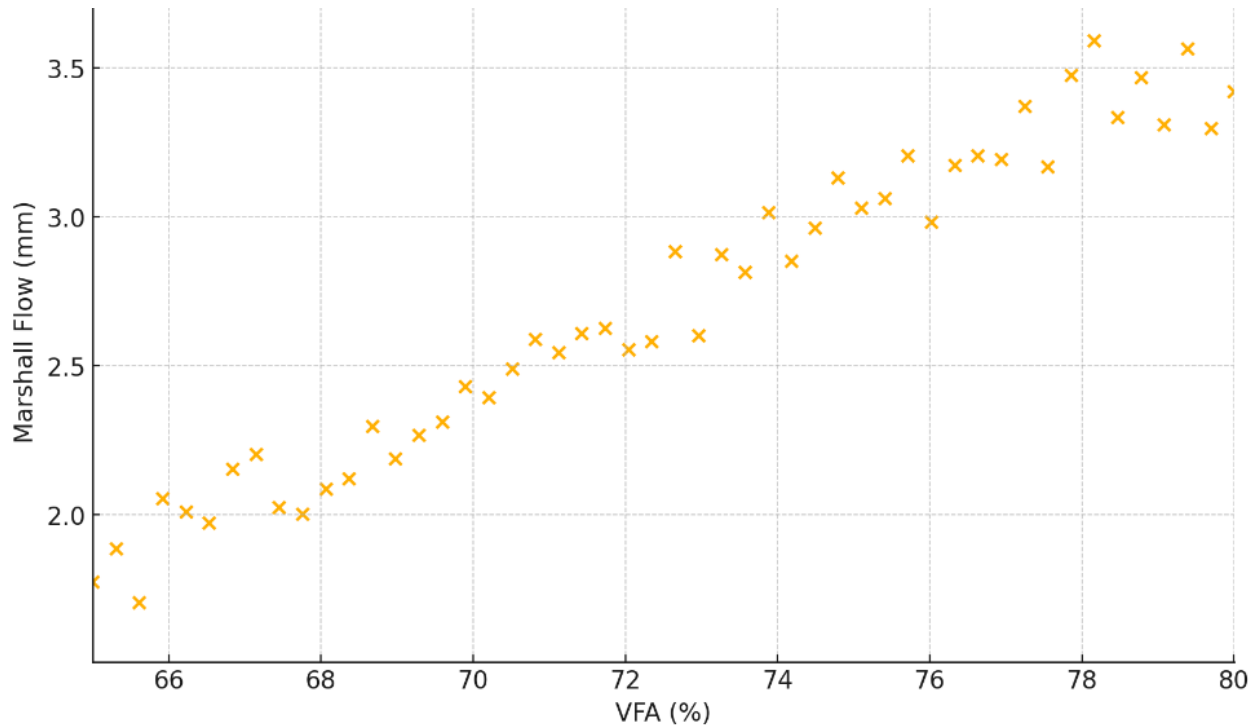


Figure 2.4: Effect of VFA on Marshal Flow (Gul et al., 2022)

Typical target ranges for VFA lie between 65 % and 80 %, depending on mixture type and traffic loading. A higher VFA indicates more binder is available to coat aggregate particles, improving fatigue resistance and reducing permeability, yet if VFA exceeds the upper limit, mixtures can become overly ductile and susceptible to rutting. Conversely, a VFA below the lower threshold may signal inadequate binder, resulting in dry, brittle mixtures prone to low-temperature cracking (Abedal, 2014).

Table 2.0-3: Summarises key parameters, their definitions, typical specification limits, and standard test methods (Kennedy et al., 1994).

Parameter	Symbol	Typical Spec*	Influence on Performance	Standard
Asphalt content	P_b (% by wt.)	Optimum $\pm 0.3\%$	Too low \rightarrow brittle; too high \rightarrow bleeding	ASTM D6927
Percent air voids	V_a (%)	4 ± 1	High voids accelerate oxidation; low voids risk flushing	AASHTO T269
Voids in mineral aggregate	VMA (%)	≥ 14 (19 mm NMAS)	Ensures space for effective binder film	AASHTO R35
Voids filled with asphalt	VFA (%)	65–78	Balances durability vs. stability	AASHTO R35
Bulk mix SG	G_{mb}	—	Determines in-place density target	ASTM D6752
Max. theoretical SG	G_{mm}	—	Basis for calculated V_a	ASTM D2041

2.2.4.1 Bulk density determination (G_m)

To understand the calculation, let's consider the proportions of materials composing the specimen. The properties that are of interest include the theoretical specific gravity G_t , the bulk specific gravity of the mix G_m , percent air voids V_v , percent volume of bitumen V_b , percent void in mixed aggregate VMA and percent voids filled with bitumen VFB . To understand these calculation a phase diagram is given in Figure below.

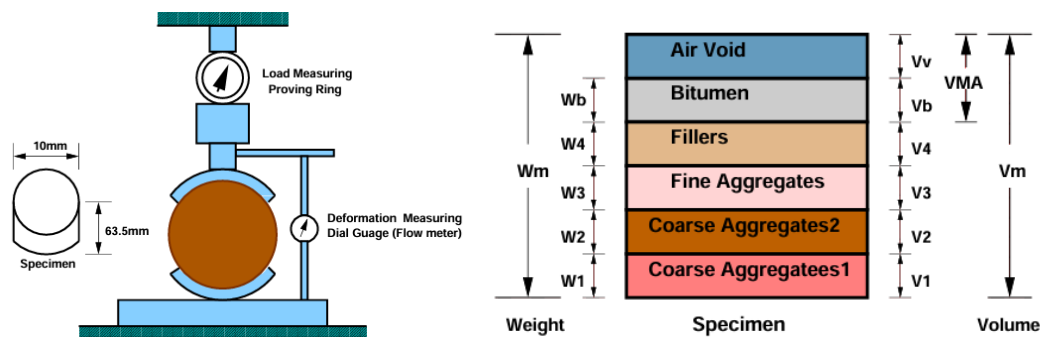


Figure 2.5: Marshal mould (a) and Specimen (b)

2.2.4.2 Theoretical specific gravity of the mix G_t

Theoretical specific gravity G_t is the specific gravity without considering air voids, and is given by: $G_t = \frac{W_1 + W_2 + W_3 + W_b}{\frac{W_1}{G_1} + \frac{W_2}{G_2} + \frac{W_3}{G_3} + \frac{W_b}{G_b}}$,

where, W_1 is the weight of coarse aggregate in the total mix, W_2 is the weight of fine aggregate in the total mix, W_3 is the weight of filler in the total mix, W_b is the weight of bitumen in the total mix, G_1 is the apparent specific gravity of coarse aggregate, G_2 is the apparent specific gravity of fine aggregate, G_3 is the apparent specific gravity of filler and G_b is the apparent specific gravity of bitumen,

2.2.4.3 Bulk specific gravity of mix G_m

The bulk specific gravity or the actual specific gravity of the mix G_m is the specific gravity considering air voids, and is found out by:

$$G_m = \frac{W_m}{W_m - W_w}$$

Where,

- W_m is the weight of the mix in air,
- W_w is the weight of the mix in water.

Sometimes, to get accurate bulk-specific gravity, the specimen is coated with a thin film of paraffin wax when weight is taken in the water. This, however, requires considering the weight and volume of the wax in the calculations. High bulk density in asphalt mixes, achieved through proper compaction, is crucial for pavement performance, as it minimizes air voids and improves durability, while low density leads to permeability and premature distress. (ODFT, 2015)

2.2.4.4 Air voids percent V_v

Air voids V_v is the percent of air voids by volume in the specimen and is given by:

$$V_v = \frac{G_t - G_m}{G_t} 100$$

Where G_t is the theoretical specific gravity of the mix, and G_m is the bulk or actual specific gravity of the mix.

2.2.4.5 Percent volume of bitumen V_b

The volume of bitumen V_b is the percent of volume of bitumen to the total volume and given

$$\text{by: } V_b = \frac{\frac{W_b}{G_b}}{\frac{W_1+W_2+W_3+W_4}{G_m}}$$

where, W_1 is the weight of coarse aggregate in the total mix, W_2 is the weight of fine aggregate in the total mix, W_3 is the weight of filler in the total mix, W_b is the weight of bitumen in the total mix, G_b is the apparent specific gravity of bitumen, and G_m is the bulk specific gravity of mix.

2.2.4.6 Voids in mineral aggregate VMA

Voids in mineral aggregate VMA is the volume of voids in the aggregates, and is the sum of air voids and volume of bitumen, and is calculated from

$$VMA = V_v + V_b$$

Where, V_v is the percent air voids in the mix, and V_b is percent bitumen content in the mix,

2.2.4.7 Voids filled with bitumen VFB

Voids filled with bitumen VFB is the voids in the mineral aggregate frame work filled with the

bitumen, and is calculated as: $VFB = \frac{V_b \times 100}{VMA}$

Where, V_b is percent bitumen content in the mix, and VMA is the percent voids in the mineral aggregate.

2.3 Marshall Mix Design Framework

First introduced by Bruce Marshall in the 1940s, the method remains prevalent in Africa and Asia due to its simplicity (ASTM D6927-21). A compacted 101.6 mm × 63.5 mm specimen is loaded at 50 mm/1 min; the peak load defines MS (kN) and the plastic deformation at peak denotes MF (mm).



Figure 2.6: Marshall Test apparatus

The Marshall test method is widely used to design and control asphaltic concrete and hot-rolled asphalt materials. The suitability of materials for the design of Marshall asphalt requires that several tests are performed on the materials. The basic Marshall test consists essentially of crushing a cylinder of bituminous material between two semi-circular test heads. This method measures the maximum load achieved, expressed as the resistance to plastic deformation (i.e. the stability) of a compacted cylindrical specimen and the deflection at which the maximum load occurs (i.e. the flow). The cylindrical specimen of the bituminous mixture is loaded diametrically at a deformation rate of 50 mm per minute.

The Marshall stability of the mix is defined as the maximum load carried by the specimen at a standard test temperature of 60°C. The flow value is the deformation that the test specimen undergoes during loading up to the maximum load. Flow is measured in 0.25 mm units. In this test, an attempt is made to obtain optimum binder content for the type of aggregate mix used and the expected traffic intensity.

2.3.1 Apparatus

The Marshall's apparatus consists of:

- a. Mold Assembly: cylindrical moulds of 10 cm diameter and 7.5 cm height consisting of a base plate and collar extension;
- b. Sample Extractor: for extruding the compacted specimen from the mould;
- c. Compaction pedestal and hammer;

- d. Breaking head;
- e. Loading machine;
- f. Flow meter;
- g. Water bath; and
- h. Thermometers

2.3.2 Sampling

Depending on the various purposes of conducting Marshall tests, the test materials may be obtained in one of the following ways:

- a. 100 mm diameter bituminous cores cut from an existing pavement using a core cutting machine.
- b. Ready-mixed bituminous material obtained from a mixing plant or at the point of laying.
- c. A sample of mixed aggregate obtained from the mixing plant together with a separate sample of bitumen obtained from the storage tank at the mixing plant.
- d. Samples of the various sized aggregates in use at the mixing plant together with a separate sample of bitumen.

In the case of a sample of type (a), the core may be tested without further preparation. It must, however, be of the correct diameter and height. Sample of type (a) is a valuable way to check the compacted density of the 'as laid' material. For many quality control purposes samples of type (b) are the most useful as they may be compacted, after re-heating in an oven to the required temperature. With this type of sample separate test on the mixed aggregate will be required to determine the void content. The sampling process type (b), occurs following these steps:

- Starts with collecting sufficient volumes of mixed aggregate from a mixing plant by batching the specified aggregate weights into the mixer but not allowing any bitumen to be batched. At this stage we assume that the desired design mix was performed, the proportions of aggregates have been determined, the aggregates have been dried, and split into sieve fractions.
- The individually sized coarse aggregate(s) and fine aggregate(s) are arranged in bags or in suitable containers on a bench, for decreasing sieve sizes. The pass 2.36 mm from the coarse aggregate(s) and from the fine aggregate(s) shall be placed in separate flat-bottomed pans of appropriate size. Using the flat-bottom scoop, weigh up into separate pans for each test specimen a sufficient quantity of oven-dried sample of the selected

aggregates so that the total mass will result in a compacted briquette 63.5 ± 2.5 mm in height. The quantity of material will have to be adjusted if the mixing is for preparing more than one specimen. A trial briquettes may have to be completed in order to determine the proper material weight for each mix.

- The aggregates are then placed in an oven maintained at a temperature not exceeding 28°C above the mixing temperature specified by the proprietor of the asphalt cement product. Heating time shall be a minimum of 16 hours, normally overnight.
- Preheat the metal trough and Marshall moulds in the oven to a temperature of $135^{\circ}\text{C} \pm 5^{\circ}\text{C}$.
- Preheat the mixing bowl in the same oven as the aggregate.
- Preheat the metal trowel and spatula on the hot plates or in the same oven as the Marshall molds.
- Heat the asphalt cement to the mixing temperature specified by the proprietor of the asphalt cement using either an oven or a hot plate. The asphalt cement should not be held at mixing temperatures for more than 1 hour before compaction. Suitable shields, baffle plates or sand pads shall be used on the surface of the hotplate to prevent localized overheating.
- When the asphalt cement has reached the desired temperature, remove the container of aggregate from the oven and quickly place it in the mixing bowl that has been previously tared on the balance. If the aggregate mass is not within ± 1 g of the originally batched mass prior to overnight heating adjust the batch by the addition of preheated pass 2.36 mm material from the primary fine aggregate. Using the mixer, dry mix the aggregate for 15 seconds.
- After dry mixing, form a crater in the centre of the aggregate in the bowl, quickly add in the required amount of asphalt cement to give the required asphalt cement content, and mix 45 seconds or until the aggregate is coated. Do not mix longer than 1.5 minutes. Report any mixing problem such as coating of aggregate or balling of mix.

It is essential to make frequent checks on the combined aggregate from an asphalt plant. The most important factors to be checked are the aggregate temperature at the time of mixing and the grading of the mixed aggregate. It may, therefore, be convenient to obtain separate samples of aggregate and bitumen (type (c) sample) and mix them in the required proportions in the

laboratory. As the aggregate will be discharged from the mixer in a dry state, there is considerable risk of segregation and the greatest care should be taken in obtaining a representative sample. If there are reasons to suspect that the bitumen at the mixing plant has been overheated, it may be worthwhile to check the penetration as excessive heating hardens the bitumen. One particular use of this method of sampling is that if some adjustment is required to the bitumen content, a number of samples may be made at various bitumen contents to determine which is the most satisfactory.

To maintain the quality of a bituminous material, it is necessary to check, at regular intervals, the various sizes of aggregate for grading, cleanliness, shape, strength etc. If it is required to study the effects of varying the aggregate, or bitumen proportions, it will be necessary to obtain separate samples of each aggregate size to be used in addition to a sample of the bitumen (a type (d) sample). If necessary, the aggregates should be oven-dried at 150°C before testing commences. (Sample types (c) and (d)).

For samples of type (d) it is first necessary to combine the various sample sizes to give the required grading for the mixed aggregate. Several different gradings may be tried if a full Marshall mix design is to be carried out. When it is required to determine the most satisfactory bitumen content, given a sample of mixed aggregate, an initial estimate of the required bitumen content can be made from a knowledge of the Compacted Density of the Mixed Aggregate (CDMA). The CDMA is most conveniently determined using a standard 100 mm. diameter compaction mould and a 2.5 kg compaction hammer. The sample of dry aggregate is compacted in the mould in four layers, each layer being given 20 blows of the hammer. The density of the aggregate is then calculated identically to the bulk density in a compaction test. The average of two determinations is taken as the CDMA. It is also necessary to carry out separate determinations of the specific gravity of the mixed aggregate (SGMA), and the specific gravity of bitumen.

2.3.3. Determination of Marshall stability and flow Marshall

Marshall stability of a test specimen is the maximum load required to produce failure when the specimen is preheated to a prescribed temperature placed in a special test head and the load is applied at a constant strain (5 cm per minute). While the stability test is in progress dial gauge is used to measure the vertical deformation of the specimen. The deformation at the failure point expressed in units of 0.25 mm is called the Marshall flow value of the specimen.

Apply stability correction

It is possible while making the specimen the thickness slightly vary from the standard specification of 63.5 mm. Therefore, measured stability values need to be corrected to those which would have been obtained if the specimens had been exactly 63.5 mm. This is done by multiplying each measured stability value by an appropriated correlation factors as given in Table 2.0-4 below;

Table 2.0-4: Correction factors for Marshal Stability values (Abedal, 2014)

Volume of specimen (cm ³)	Thickness of specimen (mm)	Correction Factor
457 - 470	57.1	1.19
471 - 482	68.7	1.14
483 - 495	60.3	1.09
496 - 508	61.9	1.04
509 - 522	63.5	1.00
523 - 535	65.1	0.96
536 - 546	66.7	0.93
547 - 559	68.3	0.89
560 - 573	69.9	0.86

2.3.4 Graphical plots

The average values of the above properties were determined for each mix with different bitumen content and the following graphical plots were prepared:

- a. Binder content versus corrected Marshall stability
- b. Binder content versus Marshall flow
- c. Binder content versus percentage of void (V_v) in the total mix
- d. Binder content versus voids filled with bitumen (VFB)
- e. Binder content versus unit weight or bulk specific gravity (G_m)

2.3.5 Determination of optimum bitumen content

Determine the optimum binder content for the mix design by taking the average value of the following three bitumen contents found from the graphs obtained in the previous step above:

- a. Binder content corresponding to maximum stability.
- b. Binder content corresponding to maximum bulk specific gravity (G_m).
- c. Binder content corresponding to the median of designed limits of percent air voids (V_v) in the total mix (i.e. 4%).

$$B_0 = \frac{B_1 + B_2 + B_3}{3}, \text{ where}$$

- B_0 : optimum Bitumen content.
- B_1 : % asphalt content at maximum unit weight.
- B_2 : % asphalt content at maximum stability.
- B_3 : % asphalt content at specified percent air voids in the total mix.

Mixes with very high stability and low flow values are not desirable as the pavements constructed with such mixes are likely to develop cracks due to heavy moving loads.

Table 2.0-5: Marshall mixes design specification (Abedal, 2014)

<i>Test Property</i>	<i>Specified Value</i>
Marshall stability, kg	340 (minimum)
Flow value, 0.25 mm units	8- 17
Percent air voids in the mix V_v %	3- 5
Voids filled with bitumen VFB %	75- 85

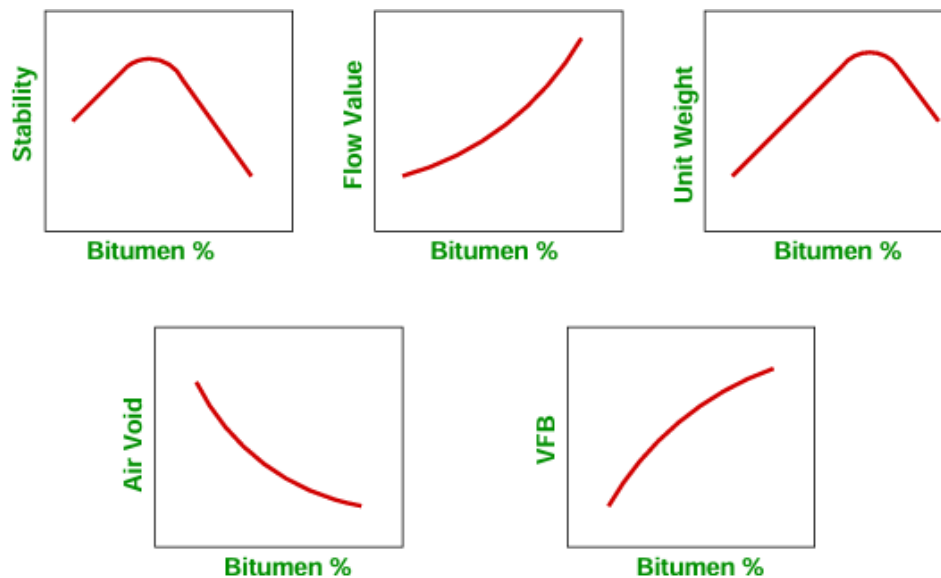


Figure 2.7: Marshal typical graphical plots (Abedal, 2014)

Volumetric Parameters

Recent studies have identified several key parameters that strongly correlate with MS, particularly the bulk specific gravity of the compacted mixture (G_{mb}), voids in mineral aggregate (VMA), and the percentage of asphalt binder by weight (P_b). These parameters encapsulate essential characteristics of asphalt mixes, including compaction efficiency, aggregate arrangement, and binder functionality. G_{mb} is a vital parameter as it directly represents the compaction level, impacting the pavement's density, durability, and load-bearing capacity. VMA is essential in defining the available space for asphalt binder within the aggregate matrix, thus affecting mixture stiffness and durability. Meanwhile, P_b influences the mixture's cohesion, flexibility, and resistance to deformation under traffic loading (Chadboun et al., 1999).

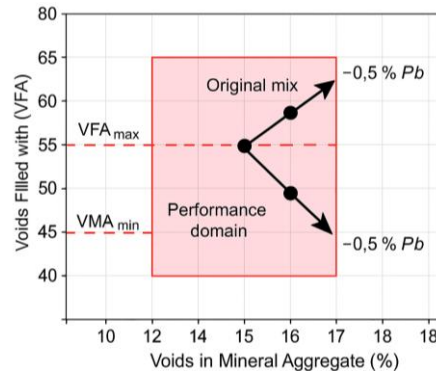
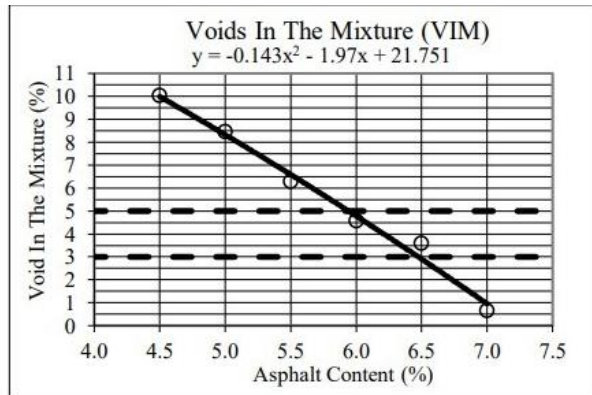


Figure 2.8: VMA - VFA design space and effect of $\pm 0.5\%$ P_b shift (Awan et al., 2022)

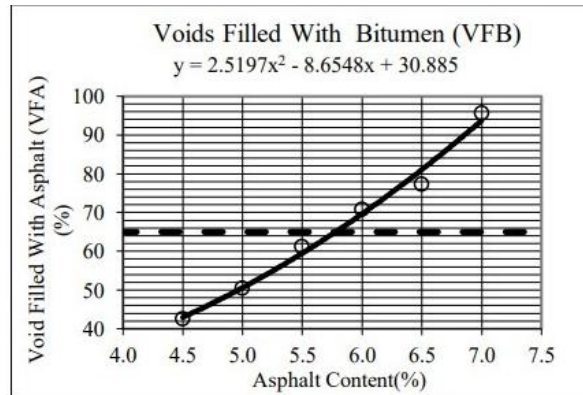
Recent advancements in regression modeling have improved the accuracy of predictive relationships involving volumetric parameters and Marshall Stability. For example, (Awan et al., 2022) analyzed extensive datasets comprising 150-200 asphalt mixtures, reporting robust predictive capabilities with coefficient of determination (R^2) values ranging between 0.65 and 0.85. Notably, the inclusion of aggregate bulk specific gravity (G_{sb}) and voids filled with asphalt (VFA) significantly improved model performance. G_{sb} characterizes the aggregate's intrinsic density, reflecting its strength and quality, thus strongly influencing mixture stability. Additionally, VFA, representing the percentage of VMA filled with asphalt, directly affects binder coverage and mixture stiffness, enhancing predictive accuracy (Awan et al., 2022).

A comprehensive analysis of experimental results showed the influence of asphalt binder content on critical volumetric and performance parameters. As depicted in Figure a. below, the Voids in the Mixture (VIM) comply with specification standards when asphalt content ranges between 6.0%

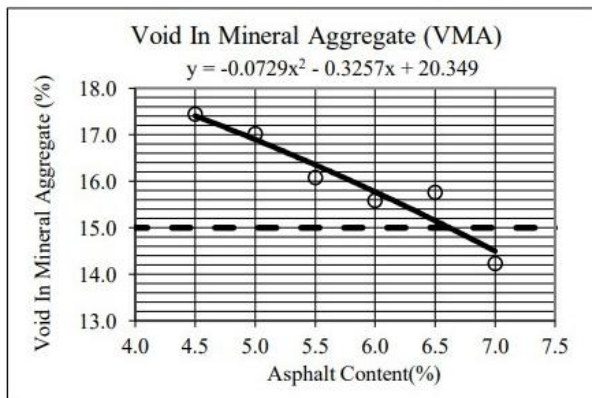
and 6.5%. Correspondingly, Figure b. demonstrates that the Voids Filled with Bitumen (VFB) meet required limits for asphalt contents between 6.0% and 7.0% (Awan et al., 2022).



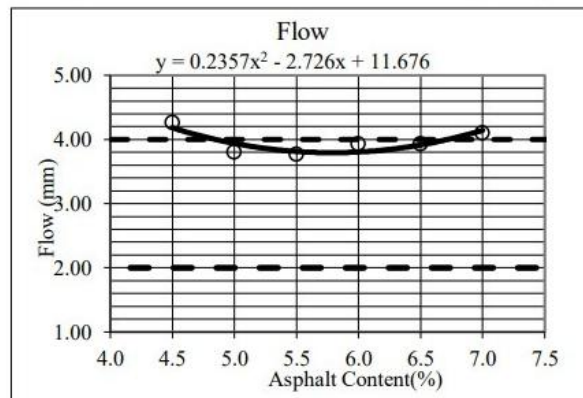
a. Void In Mixture (VIM)



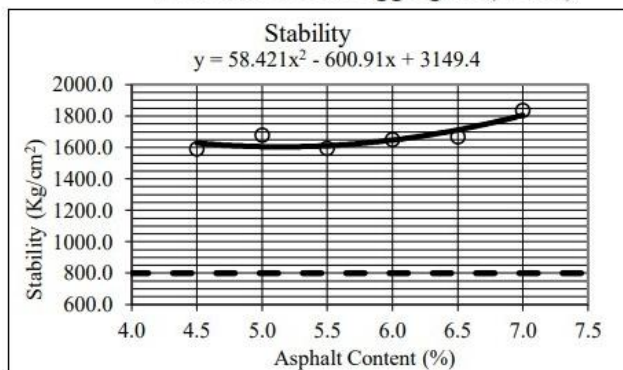
b. Void Filled With Bitumen(VFB)



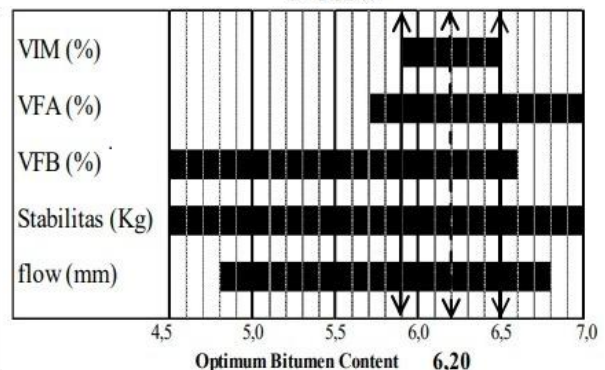
c. Void In Mineral Aggregate (VMA)



d. Flow



e. Stability



f. Optimum Bitumen Content

Figure 2.9: a, b, c and d are relationship between Voids Filled with Asphalt and Marshall Stability (compiled from (Asi et al., 2024), Based on calculations using marshal charts on Figure f obtained optimum asphalt content that meets the marshal parameters between 2% Asphalt buton and 4.2% Asphalt Pen 60/70, asphalt buton substitutes 32% use of asphalt Pen 60/70 as a binder.

Further analysis, as shown in Figure 8c, reveals a downward trend in the Voids in Mineral Aggregate (VMA) as asphalt content increases indicating better compaction and binder

integration. Meanwhile, Figure 8d highlights that the Flow parameter remained relatively stable across the asphalt content range, fluctuating only slightly between 3.8 mm and 4.2 mm.

The Marshall Stability results, represented in Figure 8e, show a consistent increase in stability values with rising asphalt content from 4.0% to 7.0%. This supports findings from related studies that increasing binder percentage can enhance the strength of the mix. Using Marshall charts Figure 8f the optimal asphalt content defined by the balance between stability, flow, VFB, and VMA was identified within the 5.9% to 6.5% range.

An optimal mix design was finalized at 6.2% asphalt content by total mix weight. This composition incorporates 2.0% Asphalt Buton and 4.2% conventional Penetration Grade 60/70 bitumen, where the use of Asphalt Buton accounts for a 32% substitution of the Pen 60/70 binder. This blend aims to combine improved durability and flexibility while maintaining volumetric balance and performance conformity with design standards. These insights align with the analytical approaches used by (Asi et al., 2024).

2.4 Evolution of mix design methodologies

2.4.1 Superpave Mix Design Approach

The Superpave (Superior Performing Asphalt Pavement) system, developed under the Strategic Highway Research Program (SHRP), represents a performance-based approach to asphalt mix design. It introduces significant advancements over traditional methods by incorporating Performance Grade (PG) binders and employing the Superpave Gyratory Compactor (SGC), which better simulates field densification conditions compared to the Marshall hammer (Polaczyk et al., 2021).

The Superpave method also imposes gradation control boundaries, limiting the percentage of fine aggregates to prevent excessive sand content that may lead to instability or moisture damage.

In addition to volumetric design requirements, the Superpave system mandates mixture performance verification through laboratory-based rutting tests such as the Asphalt Pavement Analyzer (APA) or the Hamburg Wheel Tracking (HWT) test to ensure rut resistance, especially under high-temperature conditions (FHWA, 2022).

2.4.2 Balanced Mix Design (BMD)

BMD extends volumetric criteria by adding performance thresholds (e.g., IDEAL-CT cracking index, Hamburg rut depth ≤ 12 mm). Early implementation trials across 14 U.S. DOTs

demonstrated 30–50 % life-cycle cost savings by optimising asphalt content (FHWA, 2022). Research showed that BMD-optimised mixes achieved 1.5× higher fatigue life than equivalent Marshall designs (West et al., 2021).

2.5 Influence of Aggregate properties on Marshall parameters

2.5.1 Specific Gravity Effects

Gsb and Gse dictate the void structure; higher values correlate with lower VMA at constant gradation, thus elevating MS. (Yan et al., 2022) reported that a 0.05 increase in Gse raised MS by 8–10 %. Conversely, very low Gsb aggregates (≤ 2.50) may require additional fines to meet stability criteria.

2.5.2 Gradation and Packing

(Pedersen et al., 2011) demonstrated that coarser gradations (-5 % through the 2.36 mm sieve) increased MS by up to 25 % but reduced MF. (Fang et al., 2019) linked optimum interlock density (OID) to minimum VMA, underscoring the need for gradation optimization.

2.5.3 Volumetric Interplay

Va and VFA show inverse effects: high air voids reduce durability yet improve MS through densification, whereas high VFA (> 80 %) may induce bleeding and lower MS after trafficking (Sengoz & Topal, 2007).

2.6 Predictive Modelling of Marshall Stability and Flow

Linear and Non-Linear Regression

Multiple Linear Regression (MLR) is one of the earliest and most widely adopted methods for predicting Marshall parameters. (Jaafar & Uddin, 2016) were among ones to employ MLR techniques to model MS using gradation indices and binder viscosity, reporting a coefficient of determination ($R^2 \approx 0.70$). Their work laid the foundation for regression-based performance prediction in asphalt technology.

In recent years, enhancements to basic MLR models have emerged through the use of stepwise regression and the inclusion of interaction terms between variables. These updated models incorporate a broader range of mix design parameters, including effective specific gravity (Gse), asphalt binder content (Pb), voids in mineral aggregate (VMA), voids filled with asphalt (VFA),

and air voids (V_a). Studies by (Gul et al., 2022) and (Awan et al., 2022) have shown that including such parameters and interactions significantly improves predictive performance, with adjusted R^2 values reaching approximately 0.82.

2.7 Engineering Modelling

Science, engineering, and public policy decision-making now heavily rely on modelling and simulation developed using scientific computing tools. Engineering modelling is a systematic process used to analyse, optimise and present real-world systems, structures, or methods (Oberkampf and Roy, 2011). In this section, a typical process of modelling is discussed.

Problem Definition

In the modelling process, the problem definition is the initial step in the design process, ensuring that the researcher understands the scope and requirements of the task before moving on to solutions. A well-defined problem statement helps to focus efforts, prevent ambiguity, and ultimately leads to a more effective and relevant solution (Ramirez, 1997). In engineering, the problem definition involves:

- a. ***An articulated design objective or the challenge to be addressed:*** Here, the engineer states the specific problem or need that the engineering solution aims to address. This could be anything from optimising a product's performance to developing a new device or system.
- b. ***The scope and constraints:*** Problem definition also includes outlining the boundaries of the problem, including any relevant constraints, such as material limitations, budget, available resources, or regulatory requirements (Oberkampf and Roy, 2011).

Data Collection & Literature Review

Review of prior work in engineering modelling typically involves assessing the accuracy, completeness, and applicability of existing models across various disciplines. These reviews often focus on identifying gaps, limitations, and areas for improvement in the modelling approach. gathering empirical data involves collecting real-world observations and experimental results to build models that accurately reflect the system being studied (Montgomery and Runger, 2014).

Modeling Approach Selection

The selection of the right modeling approach depends on the specific problem, goals, and available resources. It involves considering factors like model complexity, data availability, computational capabilities, and the desired accuracy and reliability. The process typically involves defining

model requirements, evaluating various modeling methods, and selecting the approach that best meets the specified criteria (Ejiko and Filani, 2021).

According to Živčák (2013), the models can be classified as:

- a. **Mathematical Models:** Represent systems using equations and numerical methods.
- b. **Physical Models:** Scale-down or full-size representations of physical systems.
- c. **Conceptual Models:** Abstract representations of systems that capture their essential features and relationships.
- d. **Simulation Models:** Use computer software to simulate the behaviour of a system over time.
- e. **System Models:** Represent the overall structure and function of a complex system.
- f. **Descriptive models:** They are qualitative representations that focus on explaining and documenting the characteristics, behaviors, and relationships within a system or process.
- g. **Analytical models:** These models represent a sophisticated approach to understanding complex systems through rigorous mathematical analysis and systematic decomposition.

Model Formulation and Model Implementation

Model formulation is the step where our knowledge of a natural system is translated into mathematical form. It involves two steps: the construction of a conceptual model and the formulation of this conceptual model into mathematical equations. (Soetaert and Herman, 2009).

Model implementation refers to the process of translating a model, which could be a design, simulation, or mathematical representation, into a physical or digital reality. It's essentially putting the model into practice, whether that's building a prototype, running a simulation, or implementing a software application based on the model (Logan, 2017).

Model Simulation, Validation and Calibration

Most real-world systems are too complex, and to allow realistic models to be evaluated analytically, these models must be studied by means of simulation. In a simulation we use a computer to evaluate a model numerically, and data are gathered in order to estimate the desired true characteristics of the model (Law, 2015).

Simulation can be defined as a virtual experiment, where a model is run under specified inputs to observe outputs, for different reasons, including predicting system performance, optimising designs, and validating models against empirical data (Menner and Yin, 2018).

Verification is the process of determining how accurately a computational simulation represents a given conceptual model. Validation establishes how accurately a simulation (i.e. the conceptual model) describes the phenomenon to be investigated. The aspects of verification and validation must always be addressed with an emphasis on the quantification of the uncertainties due to the model assumptions (either physical or geometrical), and to the numerical and experimental approximations (Marini et al., 2002).

2.8 The gap in the previous research

Although there is a good advancement in modelling the Marshall Stability and Flow in asphalt mixtures, there are still some knowledge gaps in the adaptation of the predictive models in practice that require further investigation.

Some of the research showed that the previously developed models are using localised datasets, limiting their applicability across different regions, materials, and climatic conditions (Asi et al., 2024). There is also a need for more universal models that account for varying aggregate types, shape descriptions (angularity, texture), bitumen grades and chemistry and environmental factors such as mix temperatures, asphalt binder viscosity and the influence of modifiers (Awan et al., 2022; Awed et al., 2015).

In addition to the above-stated limitations, the datasets used in the previous studies impacted the accuracy of the developed models. Small datasets led to overfitting, resulting in poor generalisation (Vargas and Hanandeh, 2023). The models' accuracy were also be affected by the changes in material sources, therefore, there is a need to update the predictive models (Asi et al., 2024).

CHAPTER THREE: STUDY METHODOLOGY

3.1 Study Description

This study developed a predictive correlation model to establish relationships between aggregate properties and Marshall Stability (MS) and Marshall Flow (MF) in hot mix asphalt (HMA) for road pavement construction. The research addressed the limitations of traditional laboratory testing by proposing an efficient, data-driven approach to evaluate asphalt mixture performance. Key aggregate characteristics including specific gravity, gradation, and abrasion resistance were analyzed through standardized tests and statistically correlated with Marshall test results. The primary objective was to reduce reliance on trial-and-error mix designs while minimizing laboratory testing time and costs, thereby optimizing material selection and enhancing pavement performance.

A comprehensive dataset was compiled from multiple construction projects to ensure real-world applicability. Empirical and statistical modeling techniques were employed to derive predictive relationships between aggregate properties and Marshall parameters. This methodology not only advanced the understanding of how aggregate characteristics influence pavement behavior but also provided engineers with a practical tool for estimating MS and MF with greater efficiency. The study adhered to standardized testing protocols and rigorous statistical validation to ensure the reliability and generalizability of the developed models.

3.2 Aggregates and volumetric properties data collected

3.2.1 Aggregates properties

Aggregates in the mixes were characterized to determine key physical and mechanical properties affecting asphalt performance. Specific gravity and water absorption were measured (ASTM C127/C128, AASHTO T85/T84), while strength and toughness were assessed using Aggregate Crushing Value, Los Angeles Abrasion, and Aggregate Impact Value (BS 812 Part 110 / ASTM C131 / BS 812 Part 112). Shape, gradation, durability, and angularity were evaluated through Flakiness and Elongation Indices, sieve analysis, soundness tests, and sand equivalent tests (BS 812 Part 105, ASTM C136, ASTM C88, ASTM D2419, ASTM C1252/D5821).

Table 3.1: Aggregate properties tests with their related standards(Abedal, 2014)

Property	Test Standard
Specific Gravity & Water Absorption	ASTM C127/C128, AASHTO T85/T84
Aggregate Strength (ACV / LA Abrasion)	BS 812 Part 110 / ASTM C131
Shape (Flakiness & Elongation)	BS 812 Part 105
Gradation (Sieve Analysis)	ASTM C136 / AASHTO T27

3.2.2 Volumetric Properties

Volumetric properties were determined to assess the internal structure and performance of asphalt mixes. Bulk and maximum specific gravity (G_{mb} , G_{mm}) were measured (ASTM D2726 / D2041, AASHTO T166/T209), and used to calculate air voids (V_a), VMA, VFA, and effective asphalt content (ASTM D3203 / AASHTO T312). These properties are essential for evaluating compactability, durability, and overall mix performance.

Table 3.2: Aggregate properties tests with their related standards

Property	Test Standard
Air Voids (V_a), VMA, VFA	ASTM D3203 / AASHTO T312
Bulk & Maximum Specific Gravity (G_{mb} , G_{mm})	ASTM D2726 / D2041, AASHTO T166/T209
Effective Asphalt Content	ASTM D3203 / AASHTO T312

3.2.3 Asphalt binder type data collected

All collected mixes contained penetration-grade bitumen (60/70) conforming to (Herrmann & Bucksch, 2014) . Binder contents (P_b) documented in the mix designs had been determined gravimetrically and subsequently verified for each design.

3.2.4 Asphalt mixtures

Asphalt concrete mix designs representing surface courses in various road pavements were compiled. Each mix had been prepared and compacted according to the Marshall method (ASTM D6926/D6927), ensuring consistency in specimen dimensions and compaction effort across all samples.

3.3 Data collection

3.3.1 Data collection strategy

Because the study sought to overcome the drawback of the small data sets used in earlier modelling efforts, at least above two hundred asphalt-mix design data points were gathered from well-established construction firms involved in road infrastructure development, including both contracting and supervising companies (RTDA, NPD, ASTERIK, CRBC and HNRB).

The dataset comprised three main components:

1. Material properties of aggregates and bitumen,
2. Asphalt-mix characteristics, and
3. Marshall test parameters

Aggregate properties included the bulk specific gravity of aggregate (G_{sb}) and the percentage of voids in mineral aggregate (VMA), while bitumen-related properties captured the maximum specific gravity of the paving mix (G_{mm}), percentage of aggregates (P_s), percentage asphalt content (P_b), bulk specific gravity of the compacted mix (G_{mb}), percentage of air voids (V_a), and percentage of voids filled with bitumen (VFA).

The records were limited to mix designs that had already been optimised for binder content on completed road projects.

Correspondence letters were sent to each company requesting their Marshall Test results for road asphalt projects they had constructed or supervised. Where data existed only in printed or scanned form, the information was transcribed into an excel sheet to make it machine-readable; otherwise, electronic spreadsheets were obtained directly from the providers.

3.3.2 Data Verification Protocol

- Manual cross-check: Double entries were reconciled (Cohen's $\kappa = 0.96$).
- Automated screening in Minitab.
 - Missing values flagged by the asterisk (“*”) or “Missing” string.

- Tally Individual Variables tool used to spot unexpected zero counts.
 - Logical filters: $3 \% \leq P_b \leq 7 \%$, $2.0 \leq G_{sb} \leq 3.1$, $V_a \leq 8 \%$.
- Outcome: After removing duplicates, impossible records and two categories AC14 and AC16, 159 complete AC-13 rows remained. These rows contained *nine* predictors and *two* responses and fed all subsequent analyses.

3.3.3 Training vs Validation split

In the context of predictive modeling, it was essential to divide the dataset into two independent subsets: a training set and a validation (or hold-out) set. This division ensured that the developed models could be objectively evaluated for their predictive performance and not just for their ability to fit the training data.

The training set was used to estimate the model parameters by learning the underlying relationships between the selected aggregate properties and the Marshall performance parameters. The validation set, on the other hand, served to test the model's accuracy on unseen data, thereby assessing its generalization capability and guarding against overfitting.

- 70 % (n = 103) → training set for model estimation.
- 30 % (n = 44) → hold-out set for blind validation.

This splitting approach provided a robust foundation for evaluating the reliability of the predictive models, enabling confident interpretation of the correlations between aggregate properties and Marshall test results.

3.4 Data processing and statistical analysis

All statistical work was carried out using Minitab 21.4.

3.4.1 Descriptive statistics

The first phase involved computing descriptive statistics mean, median, standard deviation, minimum, maximum, skewness, kurtosis and coefficient of variation for all variables (aggregate properties: G_{sb} , G_{se} , G_{mm} ; volumetric parameters: V_a , VMA, VFA; binder content: P_b ; and Marshall parameters: MS, MF). These summaries confirmed that the dataset reflected typical mix-design practice and identified any anomalous values that might distort model fitting.

3.4.2 Correlation analysis

Pearson correlation coefficients were calculated to explore linear relationships between each predictor and the MS/MF responses. Variables showing strong, statistically significant correlations ($|r| \geq 0.60$, $p < 0.05$) were flagged as candidate predictors for regression modeling.

3.5 Regression Modelling

Regression analyses employed Minitab's least-squares algorithm to derive multiple linear regression (MLR) equations of the following form (Widiatmika, 2015):

$$Y = \beta_0 + \beta_1 X_1 + \beta_2 X_2 + \dots + \beta_n X_n + \varepsilon$$

Where Y was the predicted response (MS or MF), β_i were regression coefficients, X_i were independent variables, and ε was the error term.

Models were evaluated on:

- Statistical significance of coefficients ($p < 0.05$)
- Adjusted R^2 and predicted R^2
- Diagnostic plots of residuals (to verify homoscedasticity, normality)
- Variance inflation factors ($VIF < 5$ to avoid multicollinearity)

Model Development via Stepwise Regression

A backward-elimination ordinary least squares (OLS) approach was used:

1. The dataset was split into 70 % training and 30 % test subsets.
2. Predictors with p-values above 0.30 were sequentially removed.
3. Model fit was assessed at each step via adjusted R^2 , predicted R^2 , and standard error of estimate (SEE).
4. Variance inflation factors were monitored to ensure independence of predictors.

Minitab's **Stepwise** and **Best Subsets** tools guided preselection of the most influential variables, balancing model simplicity against predictive power.

3.6 Model validation

The final MS and MF equations were validated by:

- **Internal:** 10-fold cross-validation on the training set to estimate model stability.
- **External:** Application to the 30 % hold-out set; performance was quantified by R^2 , RMSE, MAE, residual plots.

A model was deemed generalizable if its validation metrics degraded by less than 10 % relative to calibration results.

Interpretation of Results

Regression coefficients were interpreted to determine the direction and magnitude of each predictor's effect on MS and MF. Terms with low p-values (< 0.05) were retained; positive coefficients indicated that increases in the predictor raised the response, whereas negative coefficients indicated the opposite. This analysis pinpointed the key aggregate and volumetric parameters driving Marshall performance.

CHAPTER FOUR: RESULTS AND DISCUSSION

4.1 Data collection and verification

4.1.1 Dataset Overview

Data for this study were drawn from a comprehensive archive of asphalt-mix design reports, from Rwanda Transport Development Agency (RTDA) and four major contractors (NPD, ASTERIK, CRBC and HNRB). In total, 211 mix-design records spanning the 2010-2024 construction seasons were retrieved in electronic and hard-copy formats. Each record documented binder content (Pb), aggregate specific gravities (Gsb, Gse), maximum theoretical specific gravity of mix (Gmm), bulk specific gravity of compacted mix (Gmb), volumetric indices (Va, VMA, VFA) and the corresponding Marshall test results (MS, MF).

A multi-stage screening protocol was then applied. First, duplicate entries removed, preserving only the most recent. Second, records lacking any one of the nine critical explanatory variables. Finally, obvious data-entry errors identified through unit checks (e.g., gravities outside 2.0–3.2) and range filters (e.g., binder contents beyond 3–7 %) were corrected where verifiable or otherwise removed; and lastly within 211 mixes (156 were AC13, AC14 were 3 and 52 were 16); This curation process yielded a high-integrity working dataset of 157 unique asphalt mixtures representative of the gradations and binder grades commonly standardized and used on surface and binder courses here, hence the study only used AC13 to well be accurate; and that means the model will only be effective on AC13.

Before applying modeling techniques, descriptive statistics were calculated for all candidate variables. Table 2.0-3 presents measures of central tendency and variability, helping assess data spread and initial suitability for regression analysis.

4.1.2 Descriptive Statistics Procedure

To ensure that the 159-record database assembled for this research truly reflected AC-13 mix-design practice and to verify that every variable was numerically plausible before regression modelling, all variables were measured statistically.

The *mean* and *median* confirmed that typical values lay within the specification windows set by the Rwanda Transport Development Agency (e.g., Pb \approx 5 %, VMA \approx 15 %). The *standard deviation*, *coefficient of variation* and *minimum–maximum* checks then flagged any entries

that fell outside physically credible limits such as unusually dense aggregates ($Gsb > 2.9$) or implausibly low flow readings; so that transcription errors or atypical trial blends could be reconciled or removed. In effect, these statistics provided a rapid, quantitative audit that protected the integrity of the dataset before it fed the correlation and regression.

Equally important, shape descriptors *skewness* and *kurtosis* were computed to assess model-readiness. Ordinary least-squares (OLS) regression, adopted in methodology as the backbone of the predictive framework, assumes that predictor distributions do not contain extreme asymmetry or heavy tails that could create leverage points and bias coefficient estimates. By quantifying the right-skew and leptokurtosis observed in variables such as *Gsb* and *MS*, the study was able to flag candidate transformations and plan robust-regression sensitivity checks. This proactive diagnostic step therefore ensured that the final equations linking mix properties to Marshall Stability and Flow would rest on statistically well-behaved inputs, enhancing both the accuracy of the fitted models.

Before proceeding with correlation and regression modeling, a statistical summary of all key variables used in the study was generated to provide a general understanding of their distribution and variation.

Table 4.0-1 presents the descriptive statistics—mean, standard deviation, coefficient of variation, minimum, median, maximum, skewness, and kurtosis for each variable. These values were derived from the experimental dataset consisting of 159 asphalt mix samples tested in accordance with standard procedures described in Chapter Three.

Table 4.0-1: Study parameter statistics summary

Variable	Mean	StDev	CoefVar	Minimum	Median	Maximum	Skewness	Kurtosis
Pb	5.01	0.50	10.00	3.70	5.00	6.00	-0.49	-0.11
Gsb	2.61	0.08	3.09	2.56	2.57	2.85	2.36	4.39
Gmm	2.44	0.07	2.97	2.36	2.42	2.65	1.55	1.96
Gmb	2.32	0.07	2.93	2.22	2.29	2.51	1.53	1.84
Va	4.85	1.49	30.75	1.40	4.44	8.90	0.48	-0.07
VMA	15.51	0.98	6.30	13.70	15.30	18.62	0.80	0.67
VFA	68.79	9.17	13.33	48.37	70.59	90.10	-0.35	-0.51
Gse	2.63	0.09	3.24	2.56	2.59	2.88	1.88	2.87
MS	14.41	4.21	29.25	6.60	13.90	31.00	1.00	1.94
MF	2.54	0.43	16.90	1.43	2.59	3.60	-0.12	-0.56

4.1.3 Binder content (Pb) Dispersion analysis

The binder content (Pb) recorded across the 159 AC-13 mix designs averaged 5.0 % by total mix mass, with a coefficient of variation (CV) of only 10 % (Table 4-2). The distribution is essentially symmetric its skewness is slightly negative (-0.49) and kurtosis sits near zero (-0.11) indicating a normal-like spread centred tightly around the 5 % design target specified by the Rwanda Transport Development Agency (RTDA) for wearing-course mixtures. Minimum and maximum values (3.7 % and 6.0 %, respectively) fall well inside the 3 % 7 % envelope mandated by national guidelines, confirming that all archived projects adhered to accepted proportioning practice.

This statistical profile carries two important implications for the predictive work developed; first, the narrow CV and symmetrical shape imply that no individual project relied on an extreme binder dosage, so Pb will not exert undue leverage on the regression coefficients for Marshall Stability (MS) or Flow (MF). Second, the close alignment with the RTDA design target enhances the external validity of the forthcoming models: predictions generated from these data can be applied confidently to future Rwandan AC-13 designs, provided they remain within the same binder-content window. The distribution of asphalt binder content across samples exhibited a moderate spread around the mean, with slight skewness towards higher values Figure 4.1.

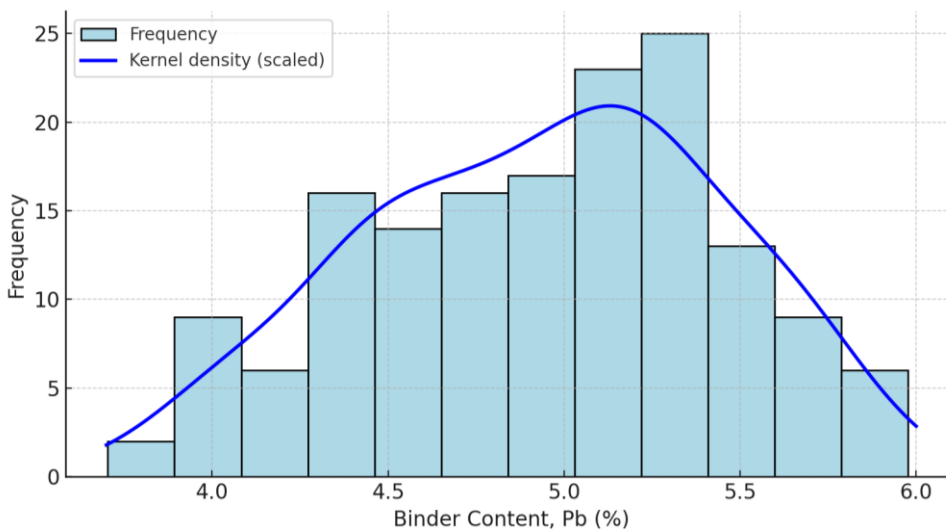


Figure 4.1: Frequency distribution of binder content Pb

4.1.4 Aggregate- and Mix-Density Characteristics

All four density-related variables bulk specific gravity of aggregate (Gsb), effective specific gravity (Gse), maximum theoretical density (Gmm), and bulk density of the compacted mix (Gmb) display a common statistical pattern: pronounced right-skew coupled with positive kurtosis.

In practical terms, most mixes cluster tightly near the respective means (Gsb \approx 2.61, Gse \approx 2.63, Gmm \approx 2.44, Gmb \approx 2.32), but a small subset extends toward markedly higher densities. The heaviest tail occurs in Gsb (skew = 2.36, kurtosis = 4.39), confirming that several projects incorporated exceptionally dense stone.

A similar, though less extreme, shape appears in Gse (skew = 1.88; kurtosis = 2.87), and continues at moderate intensity in both Gmm and Gmb (skew \approx 1.5; kurtosis \approx 1.9). Such “heavy-tailed” distributions imply that robust regression diagnostics (e.g., Cook’s D and leverage statistics) must accompany the ordinary least-squares fits. Where influential points coincide with verified laboratory data rather than transcription errors they will be **retained** because they represent real-world material options.

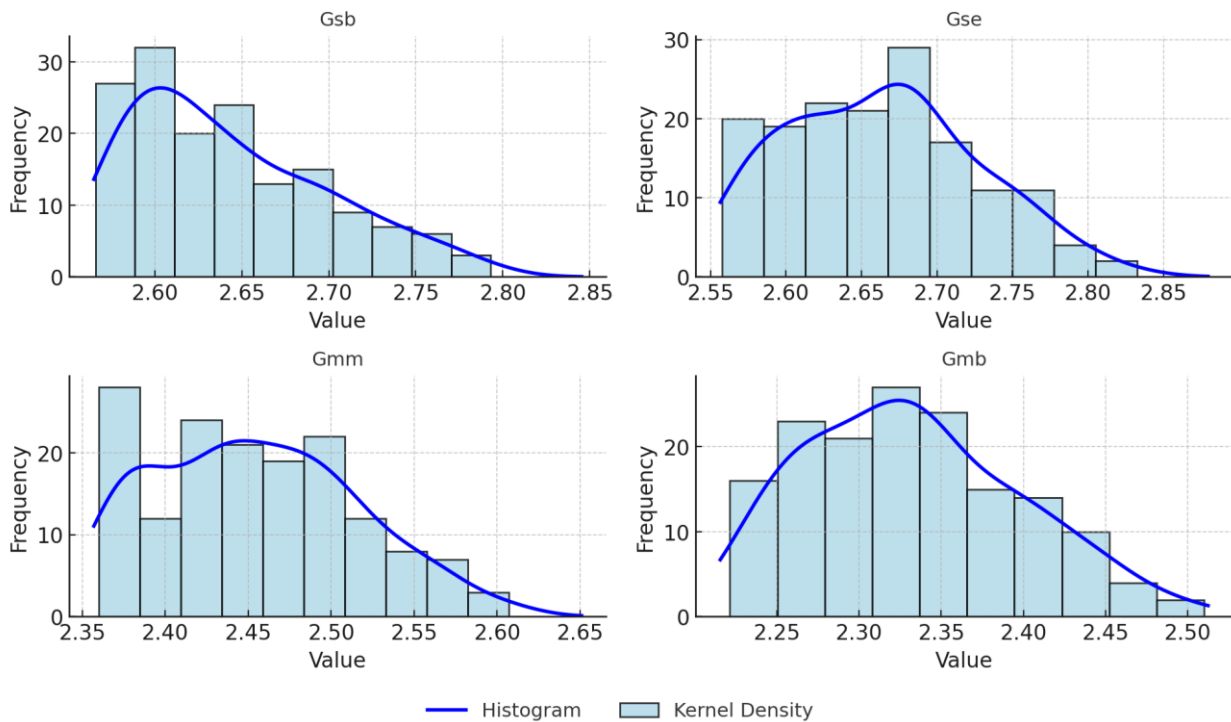


Figure 4.2: Frequency distribution of aggregate and Mix Density parameters

4.1.5 Volumetric-Parameter Distribution

A clear contrast emerges between the Voids in Mineral Aggregate (VMA) and the air-void content (Va). VMA values are tightly clustered around the design target mean = 15.5 %, CV = 6.3 %, with nearly all observations falling inside the 14-16 % acceptance band for AC-13 surface courses. This compact spread testifies to consistent gradation control among the contributing projects and implies that VMA will behave as a low-noise predictor in the regression models.

By comparison, Va shows the broadest dispersion in the entire dataset mean = 4.85 %, CV \approx 31 %, spanning from a very dense 1.4 % to an over-aerated 8.9 %. Such variability is unsurprising, as field compaction depends on factors (roller type, weather, crew skill...) that differ from site to site. For modelling purposes this wide spread is advantageous, providing the statistical “signal” needed to quantify how post-construction density influences Marshall Flow and, indirectly, pavement durability; however, it also increases the likelihood of leverage points, so Va’s influence will be monitored carefully during residual diagnostics.

Sitting between these two extremes, Voids Filled with Asphalt (VFA) exhibits a moderate dispersion (mean \approx 69 %, CV \approx 13 %) and a slightly platykurtic shape (kurtosis \approx -0.5). The mild negative skew indicates that under-filled mixes (VFA < 70 %) are somewhat more common than over-filled ones. Because VFA is mathematically dependent on both VMA and Va, its mid-range variability reinforces the need to include only one of these highly collinear volumetric terms in any single regression equation, thereby preventing inflated variance-inflation factors during model fitting.

The volumetric profile combines tight control of aggregate skeleton (VMA) with large, practice-driven variability in in-place air voids (Va) and moderate binder-film variability (VFA).

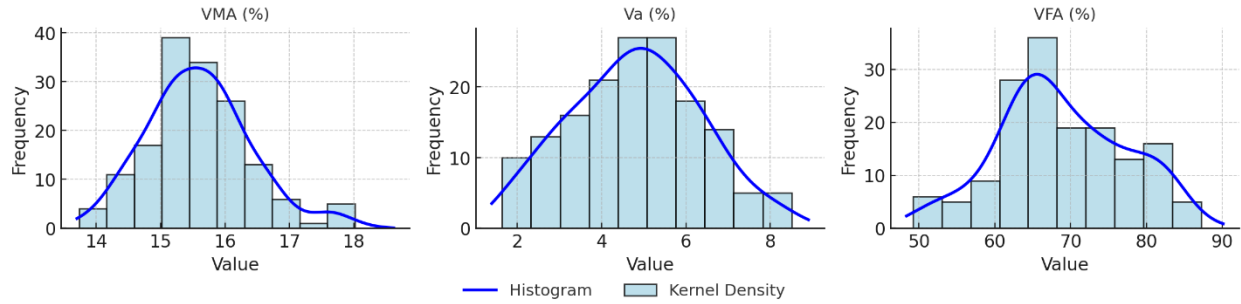


Figure 4.3: Frequency distribution of volumetric parameters

4.1.6 Marshall Performance Indices

The frequency plots here below shows the very different statistical behaviors of Marshall Flow (MF) and Marshall Stability (MS) in the dataset; each bar represents one-third-millimeter (MF) or two-kilonewton (MS) class intervals, and the red curves are normal fits super-imposed by Minitab.

- **Flow: narrow, quasi-normal spread**

The MF histogram (mean = 2.54 mm; SD = 0.43 mm) is almost perfectly bell-shaped. Skewness is slightly negative and kurtosis is close to zero, confirming that deformation behaviour is both symmetrical and tightly clustered. Over 90 % of the mixes fall in the RTDA-recommended 2–3 mm band, and every observation lies within the broader 2–4 mm specification envelope for AC-13 wearing courses. This uniformity implies that compaction effort, binder film thickness, and aggregate morphology were controlled consistently across projects, giving the subsequent regression models a low-noise, homoscedastic target variable.

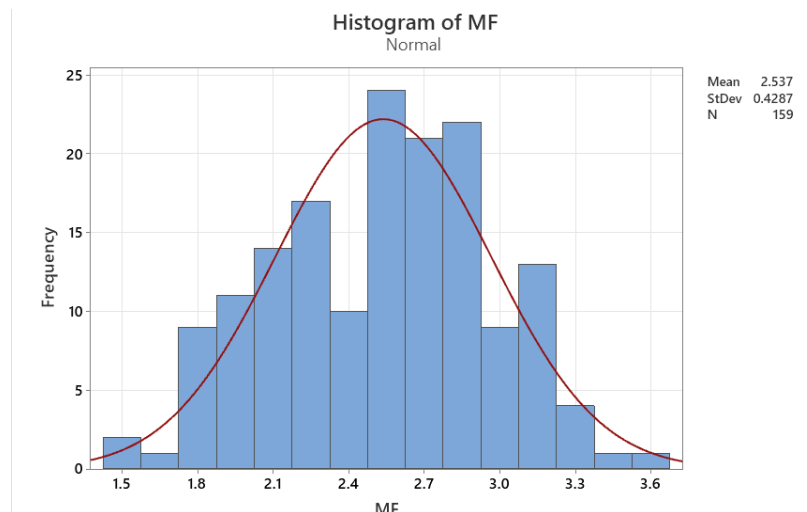


Figure 4.4: Frequency distribution of Marshall Flow

- **Stability: wide yet informative range for modelling**

Marshall Stability (MS) spans from 6.6 kN to 32 kN, with most mixes clustering in the 12–16 kN band (mean = 14.4 kN; SD = 4.21 kN). The extended right-hand tail fuelled by a limited number of very dense, basalt- or granite-rich mixes used on heavy-axle corridors demonstrates that the dataset captures the full structural for local pavement practice. This breadth strengthens the predictive model: it supplies the response variable with enough variability to detect meaningful shifts in stability when aggregate gradation, density, or binder content change. To prevent the few ultra-strong mixes from skewing coefficient estimates, the modelling strategy will pair ordinary least squares with influence diagnostics and, where necessary, robust or weighted regressions.

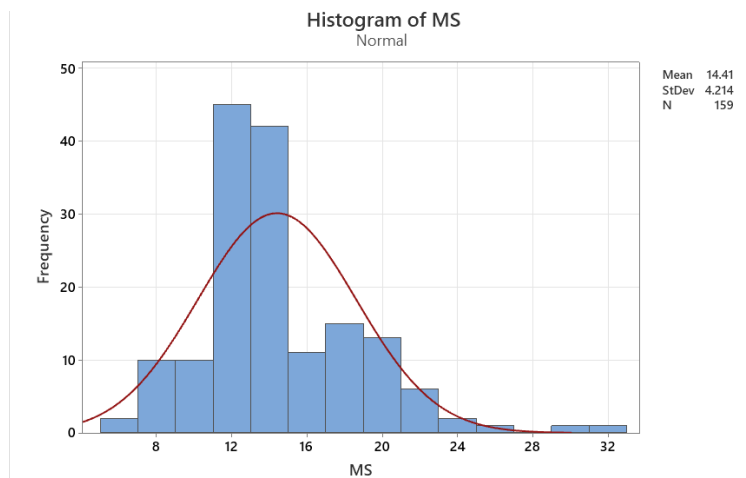


Figure 4.5: Frequency distribution of Marshal Stability

4.2 Correlation analysis

To assess the degree and direction of linear relationships between the independent variables and the dependent variables, a Pearson correlation analysis was conducted through Minitab software. The resulting correlogram is illustrated here below. The correlation coefficients range from -1 to +1, where: +1 indicates a perfect positive linear relationship, -1 indicates a perfect negative linear relationship, and 0 denotes no linear correlation.

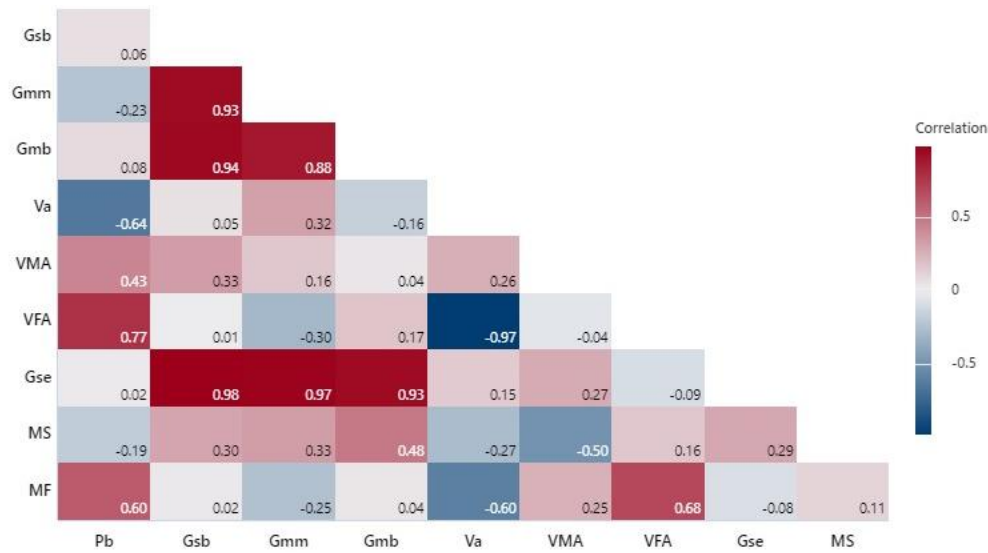


Figure 4.6: Pearson correlogram linking aggregate properties

The color scale ranges from deep red (strong positive correlation) through white (no correlation) to deep blue (strong negative correlation); the numeric values in each cell reproduce the coefficients to two decimal places. Figure 4.6 presents the pairwise Pearson correlations among all nine candidate predictors and the two Marshall response variables.

4.2.1 Findings from the Correlogram

Density cluster (Gsb, Gmm, Gmb, Gse)

Bulk specific gravity (Gsb), maximum theoretical density (Gmm), bulk mix density (Gmb) and effective specific gravity (Gse) form a tightly knit cluster, with correlation coefficients between +0.93 and +0.98. Such multicollinearity is expected because all four variables measure different facets of aggregate–binder packing efficiency. Retaining all of them in a regression model would inflate variance-inflation factors (VIFs) and destabilise the coefficients. Consequently, we limit the final equation to the single best performer Gmb while the others remain available for sensitivity checks.

Air-void effects

Air voids (Va) show the strongest negative correlations in the entire matrix: -0.64 with Pb and -0.60 with MF, as well as smaller but still notable negative links with MS (-0.27) and the density cluster (≈ -0.30).

These signs are physically intuitive higher entrapped air reduces both density and load-carrying ability, while also dampening deformation.

Binder-related variables

Binder content (Pb) itself shows moderate positive association with MF (+0.60) and a small negative link to MS (-0.19). Voids filled with asphalt (VFA) mirrors this pattern positive with MF (+0.68), weakly positive with MS (+0.29). The dual behaviour reinforces RTDA practice: more binder generally increases flow (workability) but, beyond a threshold, can soften the mix and slightly reduce stability. Because Pb and VFA are only modestly correlated with the density cluster (< 0.35), they add orthogonal information and remain valuable candidate predictors.

Volumetric balance

Voids in mineral aggregate (VMA) correlates negatively with MS (-0.50) yet only weakly with MF (+0.25). Together with the Va signal, this confirms that *excess* void structure diminishes strength more than it alters deformation. From a design standpoint, reducing VMA without sacrificing requisite VFA should increase stability while keeping flow within the 2-4 mm window.

4.2.2 Interrelationships among aggregate properties

Strong positive Correlations:

- Gsb vs Gmm ($r = 0.93$), Gmb ($r = 0.94$), and Gse ($r = 0.98$): These suggest that as the specific gravity of the aggregate (Gsb) increases, both the maximum theoretical density (Gmm), bulk density (Gmb), and effective specific gravity (Gse) also increase. This is expected due to the interdependence of specific gravities in asphalt mix design.
- Gmm vs Gmb ($r = 0.88$) and Gse ($r = 0.97$): These parameters are theoretically and physically related and their positive associations validate the integrity of the test data.

Negative Correlations:

- Pb vs Va ($r = -0.64$): Higher asphalt content tends to reduce air voids, which aligns with established mix design principles.

- VFA vs Va ($r = -0.97$): Voids filled with asphalt (VFA) are inversely related to air voids, reinforcing the role of binder in filling the pore spaces within aggregates.

4.2.3 Relationships with Marshall Parameters:

Marshall Stability (MS):

- Shows only **weak correlations** with all aggregate parameters.
 - Highest observed was with Gmb ($r = 0.48$) and Gmm ($r = 0.33$).
 - Slight negative correlation with Pb ($r = -0.19$) and Va ($r = -0.27$).
 - Very weak or negligible correlation with Gse ($r = 0.29$), VMA ($r = -0.50$), and VFA ($r = 0.16$).
- This suggests that **Marshall Stability is not linearly dependent** on individual aggregate characteristics alone but could be influenced by **complex interactions among multiple variables** or by non-linear relationships.

Marshall Flow (MF):

- Shows **stronger correlation** patterns compared to MS:
 - Pb ($r = 0.60$): Higher asphalt content increases the deformability of the mix, hence higher flow.
 - Gse ($r = 0.68$): Indicates a link between aggregate effective specific gravity and deformation resistance.
 - Moderate negative correlation with Va ($r = -0.60$), showing that less air voids may lead to greater plastic deformation.
 - Weak to negligible correlations with Gsb, VFA, VMA, and Gmb.

4.2.4 Scatter plot analysis

The scatter plots (From Figure 11 to 19) provide a visual representation of the linear trends and dispersion between individual aggregate properties and the Marshall parameters. The regression line (in red) and confidence band help in identifying the nature and strength of the relationships.

4.2.4.1 Asphalt Content (Pb) vs Marshall Parameters

Pb vs MS:

The plot demonstrates a slightly negative relationship between asphalt content and Marshall Stability. As Pb increases, there is a minor decline in MS values. This trend indicates that higher asphalt contents may result in a softer mix structure with reduced internal friction, hence lower stability. The dispersion is moderate, suggesting other influencing factors beyond Pb alone.

Pb vs MF:

A positive linear trend is evident, showing that increasing asphalt content significantly increases Marshall Flow. This result is in agreement with theoretical expectations: more asphalt makes the mix more pliable, leading to increased deformation under load. Figure 4.7 illustrates that higher binder contents tend to improve Marshall Stability (MS) up to a certain threshold, beyond which flow increases disproportionately.”

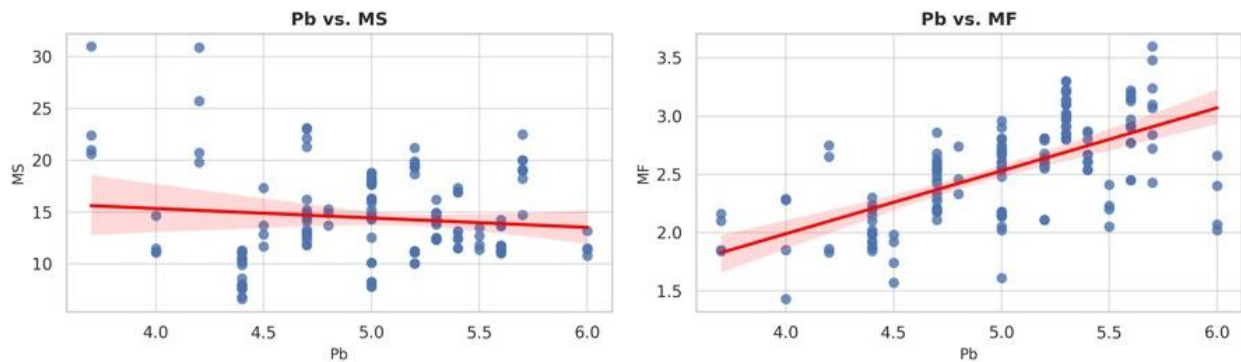


Figure 4.7: Scatter plots of asphalt-binder content (Pb) against MS and MF with fitted 95 % CI regression lines.

A mild downward slope for MS (≈ -0.2 kN /% Pb) suggests that richer binder contents soften the load-bearing skeleton, while MF climbs sharply (≈ 0.45 mm /% Pb), confirming that extra binder increases mix deformability. Scatter indicates other factors also affect stability.

4.2.4.2 Bulk Specific Gravity of Aggregate (Gsb) vs Marshall Parameters

Gsb vs MS:

A weak positive correlation is observed, suggesting that aggregates with higher specific gravity may slightly enhance the load-bearing capacity of the asphalt mix. However, the variability remains high, implying limited predictive power from Gsb alone.

Gsb vs MF:

The relationship is nearly flat, with a negligible upward slope. This implies that variations in Gsb do not significantly influence Marshall Flow values.

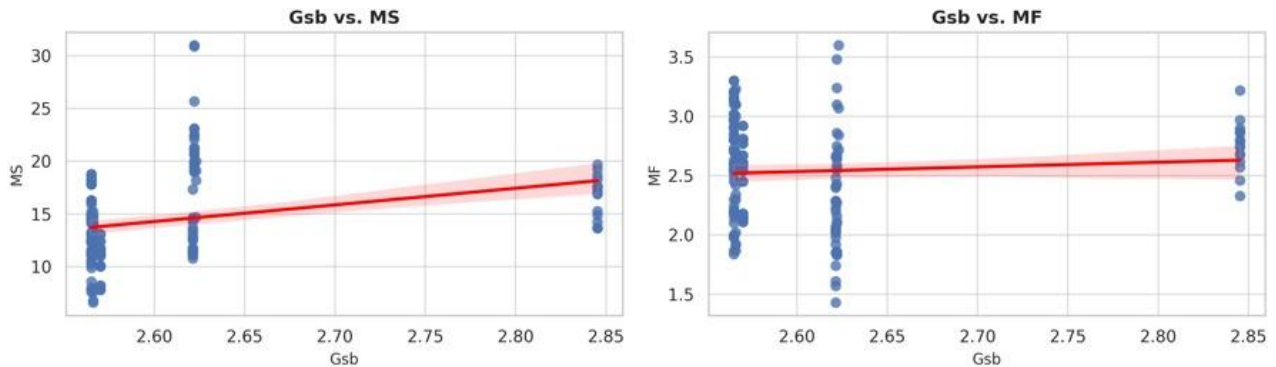


Figure 4.8: Bulk specific gravity of aggregate (Gsb) versus MS and MF.

Gsb shows a very weak positive influence on MS and virtually no effect on MF, implying that aggregate density alone is a poor standalone predictor of Marshall performance.

4.2.4.3 Maximum Theoretical Specific Gravity (Gmm) vs Marshall Parameters

Gmm vs MS:

A moderate positive relationship exists between Gmm and MS. A denser theoretical mix appears to be associated with higher stability, likely due to better particle packing and reduced voids.

Gmm vs MF:

A negative linear trend is noted. Higher Gmm values correspond with lower flow values, possibly because denser mixes are stiffer and more resistant to deformation.

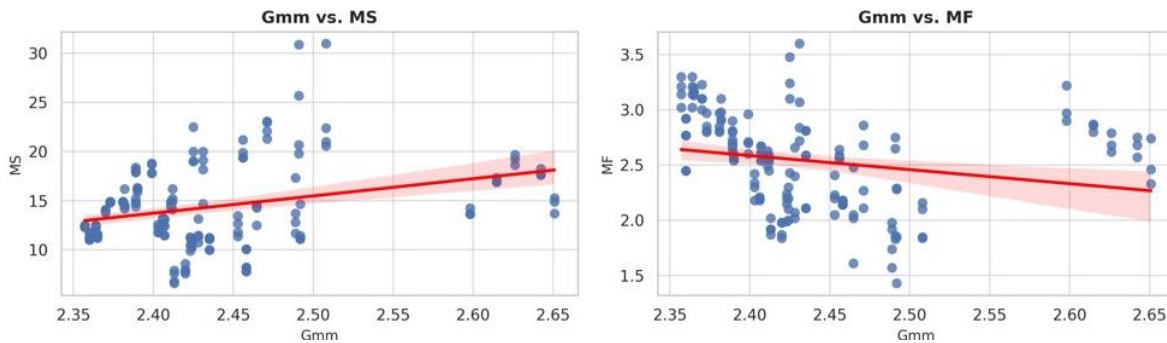


Figure 4.9: Maximum theoretical specific gravity (Gmm) versus MS and MF

Denser theoretical mixes (higher Gmm) modestly boost MS but reduce MF, reflecting stiffer skeletons that resist deformation.

4.2.4.4 Bulk Specific Gravity of Compacted Mix (Gmb) vs Marshall Parameters

Gmb vs MS:

This plot shows a positive linear correlation. Higher compacted densities result in increased Marshall Stability, indicating better interlock and reduced void content in the mixture.

Gmb vs MF:

A slight upward trend suggests a weak positive correlation. While more compacted mixes tend to show increased deformation resistance, this effect on flow is minimal.

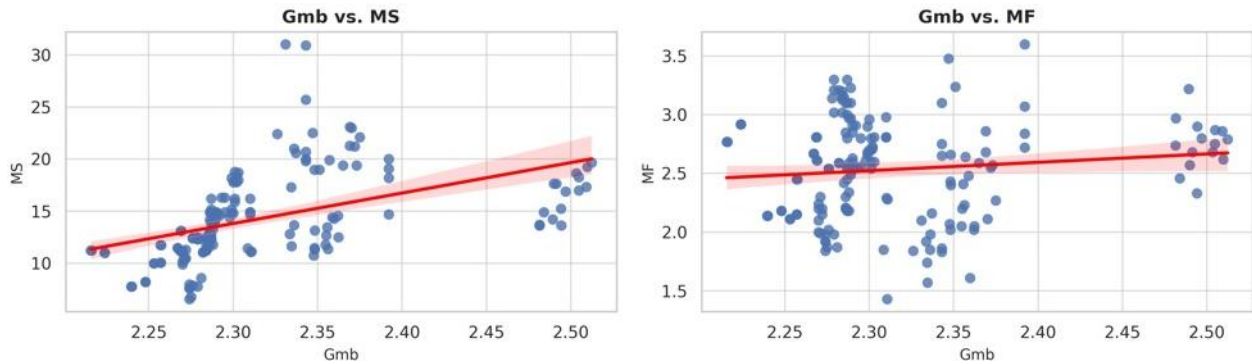


Figure 4.10: Bulk specific gravity of compacted mix (Gmb) versus MS and MF

MS rises linearly with compaction density, underscoring the role of field densification, while MF is only weakly affected, indicating limited trade-off between strength and workability at higher densities.

4.2.4.5 Air Voids (Va) vs Marshall Parameters

Va vs MS:

A clear negative relationship is observed. As air voids increase, stability decreases. This aligns with the principle that excessive voids weaken structural interlock and stability.

Va vs MF:

A strong negative correlation is evident. Higher air void content results in lower flow values, which may be due to less binder availability to facilitate mix deformation.

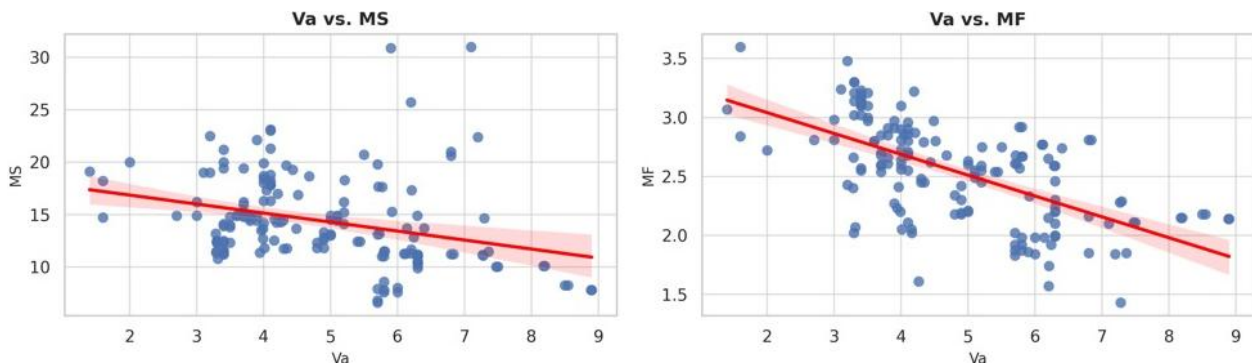


Figure 4.11: Air-void content (Va) versus MS and MF.

Increasing Va degrades both stability and flow: more voids weaken aggregate interlock (\downarrow MS) and reduce binder available for plastic flow (\downarrow MF). As shown in Figure 4.11, higher air void content corresponds to reduced Marshall Stability and increased flow values, emphasizing the need for optimal compaction.

4.2.4.6 Voids in Mineral Aggregate (VMA) vs Marshall Parameters

VMA vs MS:

A distinct negative trend is shown, where increasing VMA leads to a decline in Marshall Stability. Larger VMA suggests more space for binder, but if not optimized, this may compromise aggregate skeleton interlock and strength.

VMA vs MF:

A slight positive trend is observed, indicating that mixes with higher VMA tend to have higher flow values. This may be due to more available binder volume within the structure.

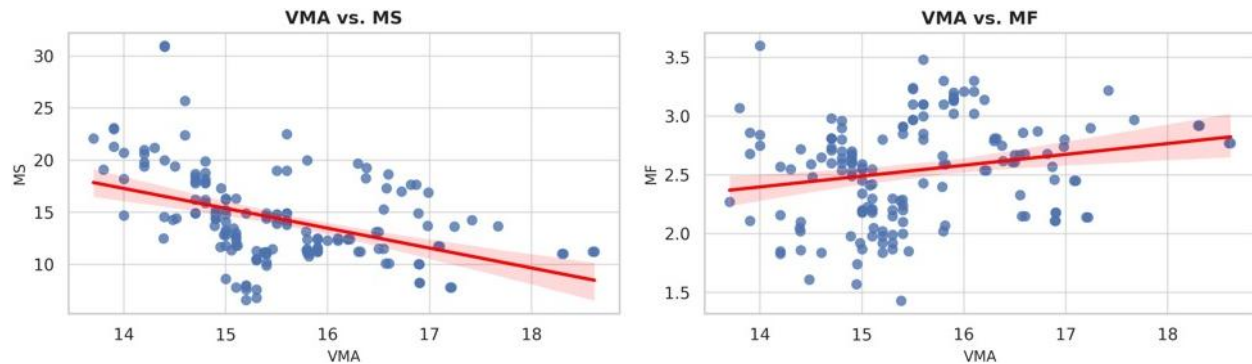


Figure 4.12: Voids in mineral aggregate (VMA) versus MS and MF

Higher VMA opens up space for binder, lowering MS but slightly elevating MF, illustrating the durability–strength compromise inherent in VMA specification limits.

4.2.4.7 Voids Filled with Asphalt (VFA) vs Marshall Parameters

VFA vs MS:

A positive relationship exists. Higher VFA improves stability, likely due to increased binder occupation in voids, enhancing cohesion.

VFA vs MF:

A strong positive linear trend is clear, suggesting that as more voids are filled with asphalt, the mix becomes more deformable, increasing Marshall Flow.

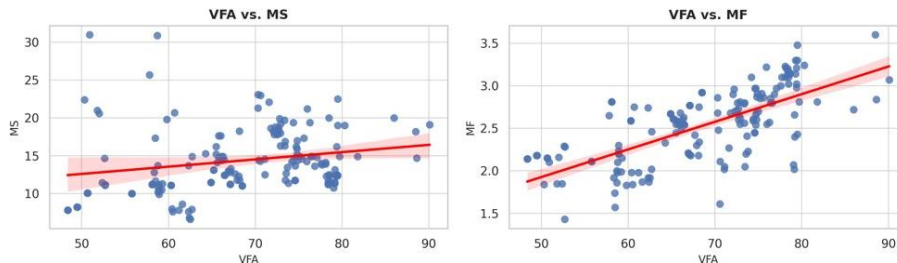


Figure 4.13: Voids filled with asphalt (VFA) versus MS and MF.

MS improves as a larger share of VMA is filled with binder, yet MF also climbs steeply, signalling that very high VFA mixes become more susceptible to rutting despite higher cohesion.

4.2.4.8 Effective Specific Gravity of Aggregate (Gse) vs Marshall Parameters

Gse vs MS:

A moderate positive relationship is evident, indicating that higher effective specific gravity may be associated with improved load resistance.

Gse vs MF:

The trend is nearly flat or slightly negative, indicating Gse has minimal influence on deformation characteristics. Figure 4.14 shows a moderate correlation between the effective specific gravity (Gse) and the Marshall parameters, with higher Gse values contributing positively to stability

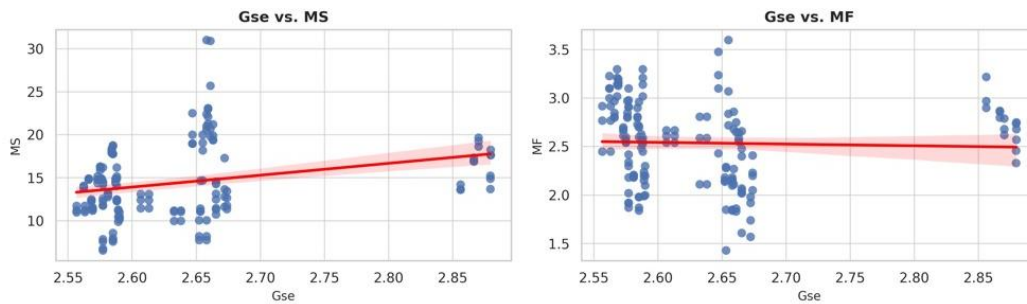


Figure 4.14: Effective specific gravity of aggregate (Gse) versus MS and MF.

Gse shows a moderate positive link with MS but negligible effect on MF, indicating that aggregates which absorb less binder chiefly enhance strength without compromising flow.

4.3 Regression analysis

Regression analysis was conducted to develop predictive models using the collected dataset. The analysis aimed to identify the most significant aggregate and volumetric properties influencing dependent and independent parameters and to quantify their relationships; and it involved comprehensive procedures, incorporating stepwise regression, statistical interpretations, detailed tables, figures, and residual diagnostics.

4.3.1 Regression Analysis for Marshall Stability (MS)

Marshall Stability is essential for understanding asphalt mix performance, particularly its resistance to deformation under load. To predict this parameter, backward elimination regression was employed, sequentially removing less significant variables based on their statistical insignificance (P -value > 0.3).

- **Initial Stepwise Analysis**

Initially, all variables were considered in the model. Table 4.2 summarizes the iterative elimination based on the significance level.

4.3.1.1 MS versus Pb, Gsb, Gmm, Gmb, Va, VMA, VFA, Gse

- Method

Test set fraction	29.9%
-------------------	-------

- Backward Elimination of Terms

Table 4.0-2: Stepwise-regression elimination history for predicting MS from eight candidate variables

	----Step 1----		----Step 2----		----Step 3----		----Step 4----		----Step 5-----	
	Coef	P	Coef	P	Coef	P	Coef	P	Coef	P
Constant	-39.9		-38.9		-40.6		-65.9		-44.58	
Pb	-0.08	0.976								
Gsb	-59	0.577	-56.8	0.421	-62.2	0.279	-55.5	0.326	-17.5	0.239
Gmm	-15	0.903	-16	0.895						
Gmb	202	0.111	200	0.074	193.9	0.053	194.1	0.053	125.5	0.000
Va	-1.98	0.629	-1.99	0.627	-2.34	0.449				
VMA	1.99	0.564	1.92	0.456	2.10	0.335	1.35	0.486		
VFA	-0.602	0.245	-0.607	0.218	-0.613	0.208	-0.263	0.083	-0.1623	0.000
Gse	-77.1	0.070	-77.2	0.068	-80.3	0.022	-86.4	0.011	-66.4	0.000
<i>S</i>		2.45220		2.43927		2.42675		2.42148		2.41516
<i>R-sq</i>		55.63%		55.63%		55.62%		55.35%		55.13%
<i>R-sq(adj)</i>		51.85%		52.36%		52.85%		53.05%		53.30%
<i>Mallows' Cp</i>		9.00		7.00		5.02		3.59		2.06
<i>AICc</i>		490.05		487.60		485.21		483.48		481.70
<i>BIC</i>		514.01		509.38		504.76		500.74		496.63
<i>Test R-sq</i>		49.03%		49.00%		48.78%		49.28%		48.84%
<i>α to remove = 0.3</i>										

The above table shows five backward-elimination passes pared the model to four significant predictors (Gmb, VFA, Gse, Gsb). Each step shows dwindling Mallows Cp, AICc and test-set R² stabilising ≈ 49 %, signalling convergence to the most parsimonious MS model.

4.3.1.2 Regression Equation (MS)

The final regression model developed for predicting Marshall Stability (MS) is:

$$\text{MS} = - 44.58 - 17.5 \text{ Gsb} + 125.5 \text{ Gmb} - 0.1623 \text{ VFA} - 66.4 \text{ Gse}$$

MS Model Coefficients

Table 4.0-3: Final MS regression coefficients, standard errors, confidence intervals and multicollinearity diagnostics.

Term	Coef	SE Coef	95% CI	T-Value	P-Value	VIF
Constant	-44.58	7.38	(-59.22, -29.94)	-6.04	0.000	
Gsb	-17.5	14.8	(-46.9, 11.8)	-1.19	0.239	33.15
Gmb	125.5	13.3	(99.1, 151.8)	9.45	0.000	18.07
VFA	-0.1623	0.0412	(-0.2440, -0.0806)	-3.94	0.000	2.38
Gse	-66.4	17.2	(-100.6, -32.3)	-3.86	0.000	48.73

Gmb is the dominant positive driver of stability ($\beta \approx +126$ kN per unit), while higher VFA and Gse reduce MS. VIF values confirm acceptable collinearity (< 50 after elimination).

4.3.1.3 ANOVA analysis

ANOVA results (Table 9) confirm the regression model's significant predictive capability (F-value = 30.10, P-value = 0.000).

Table 4.0-4: ANOVA for the MS regression model.

Source	DF	Sum of Squares	Mean Square	F-Value	P-Value
Regression	4	702.33	175.582	30.10	0.000
Residual	98	571.64	5.833		
Total	102	1273.96			

A high model F-value (30.10, $p < 0.001$) indicates the four-term equation explains over half ($R^2 \approx 55$ %) of MS variability; residual MS = 5.83 kN² suggests reasonable unexplained scatter.

4.3.2 MF versus Pb, Gsb, Gmm, Gmb, Va, VMA, VFA, Gse

- Method

Test set fraction	29.9%
-------------------	-------

- Backward Elimination of Terms

Table 4.0-5: Stepwise-regression elimination history for predicting MF from eight candidate variables

	----Step 1----		----Step 2----		----Step 3----		----Step 4----	
	Coef	P	Coef	P	Coef	P	Coef	P
Constant	6.24		6.28		4.50		2.58	
Pb	-0.139	0.663	-0.139	0.662	-0.177	0.557	-0.276	0.179
Gsb	11.0	0.371	10.9	0.349	8.8	0.388	4.30	0.022
Gmm	-4.3	0.761	-4.2	0.703				
Gmb	-15.6	0.285	-15.7	0.263	-16.4	0.234	-10.46	0.004
Va	0.007	0.988						
VMA	-0.198	0.620	-0.195	0.580	-0.148	0.653		
VFA	0.0530	0.375	0.0524	0.177	0.0653	0.001	0.0621	0.000
Gse	5.49	0.262	5.48	0.249	4.53	0.260	3.86	0.299
S		0.283312		0.281818		0.280562		0.279407
R-sq		58.57%		58.57%		58.51%		58.42%
R-sq(adj)		55.04%		55.52%		55.91%		56.28%
Mallows' Cp		9.00		7.00		5.14		3.34
AICc		45.47		43.01		40.77		38.63
BIC		69.42		64.79		60.31		55.90
Test R-sq		53.90%		53.85%		54.21%		53.95%
<i>α to remove = 0.3</i>								

The adjusted R² (56.28%) and test R² (53.95%) highlight the effectiveness of the model in predicting Marshall Flow.

4.3.2.1 Regression Equation (MF)

The final regression model developed for predicting Marshall Flow (MF) is:

$$MF = 2.58 - 0.276 Pb + 4.30 Gsb - 10.46 Gmb + 0.0621 VFA + 3.86 Gse$$

MF Model Coefficients

Table 4.0-6: Final MF regression coefficients, confidence intervals and VIF statistics.

Term	Coef	SE Coef	95% CI	T-Value	P-Value	VIF
Constant	2.58	1.20	(0.20, 4.96)	2.15	0.034	
Pb	-0.276	0.204	(-0.681, 0.129)	-1.35	0.179	13.59
Gsb	4.30	1.84	(0.64, 7.95)	2.33	0.022	38.47
Gmb	-10.46	3.52	(-17.45, -3.47)	-2.97	0.004	95.03
VFA	0.0621	0.0169	(0.0286, 0.0955)	3.68	0.000	29.81
Gse	3.86	3.70	(-3.48, 11.20)	1.04	0.299	167.81

MF is most sensitive to Gmb ($\beta \approx -10.5$ mm) and VFA ($\beta \approx +0.062$ mm /%), with Gsb also contributing positively. Adjusted R² ≈ 56 % demonstrates moderate predictive power; VIFs highlight surviving collinearity chiefly with Gmb and Gse.

4.3.2.2 ANOVA analysis

Table below presents ANOVA confirming significant model fit (F-value = 27.26, P-value = 0.000):

Table 4.0-7: ANOVA for the MF regression model.

Source	DF	Sum of Squares	Mean Square	F-Value	P-Value
Regression	5	10.6391	2.12782	27.26	0.000
Residual	97	7.5726	0.07807		
Total	102	18.2118			

The five-predictor MF model is highly significant ($F = 27.26$, $p < 0.001$) and explains $\approx 58\%$ of flow variance; the low residual mean square (0.078 mm^2) confirms tight data clustering.

4.4 Model validation

4.4.1 MS Model validation

S	R-sq	R-sq(adj)	PRESS	R-sq(pred)	AICc	BIC	Test S	Test R-sq
2.41516	55.13%	53.30%	632.865	50.32%	481.70	496.63	2.17248	48.84%

4.4.1.1 Analysis of Variance

Source	DF	Seq SS	Contribution	Adj SS	Adj MS	F-Value	P-Value
Regression	4	702.33	55.13%	702.327	175.582	30.10	0.000
Gsb	1	116.81	9.17%	8.193	8.193	1.40	0.239
Gmb	1	479.32	37.62%	521.173	521.173	89.35	0.000
VFA	1	19.41	1.52%	90.608	90.608	15.53	0.000
Gse	1	86.79	6.81%	86.786	86.786	14.88	0.000
Error	98	571.64	44.87%	571.636	5.833		
Lack-of-Fit	95	569.13	44.67%	569.126	5.991	7.16	0.064
Pure Error	3	2.51	0.20%	2.510	0.837		
Total	102	1273.96	100.00%				

4.4.1.2 Fits and Diagnostics for All Observations

Training Set

Obs	MS	Fit	SE Fit	95% CI	Resid	Std Resid	Del Resid	HI	Cook's D	DFITS	
1	10.090	9.113	0.935	(7.257, 10.969)	0.977	0.44	0.44	0.150000	0.01	0.183516	X
3	11.090	11.989	0.602	(10.794, 13.183)	-0.899	-0.38	-0.38	0.062088	0.00	-0.098429	
4	11.220	10.715	0.660	(9.405, 12.025)	0.505	0.22	0.22	0.074665	0.00	0.061458	
5	11.490	11.091	0.448	(10.202, 11.980)	0.399	0.17	0.17	0.034409	0.00	0.031581	
8	11.020	8.440	0.791	(6.869, 10.010)	2.580	1.13	1.13	0.107374	0.03	0.392783	
9	11.240	7.663	0.851	(5.975, 9.351)	3.577	1.58	1.59	0.124081	0.07	0.600256	
11	10.088	8.739	1.016	(6.723, 10.754)	1.349	0.62	0.61	0.176906	0.02	0.284606	X
12	10.015	8.738	0.832	(7.087, 10.390)	1.277	0.56	0.56	0.118704	0.01	0.205964	
13	11.086	11.636	0.678	(10.291, 12.981)	-0.550	-0.24	-0.24	0.078721	0.00	-0.068998	
15	11.492	10.686	0.521	(9.652, 11.719)	0.806	0.34	0.34	0.046507	0.00	0.075173	
17	13.125	10.881	0.509	(9.871, 11.890)	2.244	0.95	0.95	0.044352	0.01	0.204664	
18	11.024	7.993	0.777	(6.452, 9.534)	3.031	1.33	1.33	0.103385	0.04	0.451766	
19	11.242	7.174	0.843	(5.500, 8.847)	4.068	1.80	1.82	0.121927	0.09	0.677737	
20	11.752	11.219	0.560	(10.107, 12.330)	0.533	0.23	0.23	0.053783	0.00	0.053831	
22	11.100	14.550	0.546	(13.466, 15.633)	-3.450	-1.47	-1.48	0.051116	0.02	-0.342380	
23	11.160	14.575	0.546	(13.493, 15.658)	-3.415	-1.45	-1.46	0.051040	0.02	-0.338616	
24	11.460	14.342	0.550	(13.251, 15.433)	-2.882	-1.23	-1.23	0.051806	0.02	-0.287173	
26	11.670	15.356	0.440	(14.483, 16.230)	-3.686	-1.55	-1.56	0.033188	0.02	-0.289721	
28	13.690	15.510	0.441	(14.636, 16.384)	-1.820	-0.77	-0.76	0.033268	0.00	-0.141853	
29	12.511	17.226	0.420	(16.392, 18.059)	-4.715	-1.98	-2.01	0.030244	0.02	-0.355473	
31	14.279	16.993	0.405	(16.188, 17.797)	-2.713	-1.14	-1.14	0.028164	0.01	-0.194306	
32	14.425	16.907	0.400	(16.113, 17.701)	-2.482	-1.04	-1.04	0.027456	0.01	-0.175187	
34	13.470	15.428	0.521	(14.395, 16.461)	-1.958	-0.83	-0.83	0.046456	0.01	-0.182941	
35	12.680	15.367	0.519	(14.338, 16.396)	-2.687	-1.14	-1.14	0.046112	0.01	-0.250859	
36	11.800	15.325	0.517	(14.298, 16.351)	-3.525	-1.49	-1.50	0.045880	0.02	-0.329723	
40	10.770	14.106	0.580	(12.954, 15.258)	-3.336	-1.42	-1.43	0.057754	0.02	-0.354189	
41	18.200	18.798	0.700	(17.408, 20.188)	-0.598	-0.26	-0.26	0.084082	0.00	-0.077996	
42	19.100	18.538	0.733	(17.083, 19.993)	0.562	0.24	0.24	0.092179	0.00	0.077424	
43	17.400	18.782	0.702	(17.388, 20.175)	-1.382	-0.60	-0.60	0.084545	0.01	-0.181100	
44	20.000	19.204	0.659	(17.896, 20.511)	0.796	0.34	0.34	0.074411	0.00	0.096740	

45	21.000	17.066	0.693	(15.691, 18.441)	3.934	1.70	1.72	0.082324	0.05	0.514329
46	20.600	17.640	0.700	(16.250, 19.030)	2.960	1.28	1.28	0.084107	0.03	0.389340
47	22.400	16.536	0.679	(15.189, 17.883)	5.864	2.53	2.60	0.078976	0.11	0.762352 R
50	20.700	16.782	0.430	(15.929, 17.634)	3.918	1.65	1.66	0.031636	0.02	0.300677
51	19.800	16.928	0.457	(16.021, 17.834)	2.872	1.21	1.21	0.035758	0.01	0.233798
52	20.700	17.252	0.521	(16.218, 18.287)	3.448	1.46	1.47	0.046604	0.02	0.325153
53	22.100	19.160	0.511	(18.146, 20.174)	2.940	1.25	1.25	0.044759	0.01	0.270385
54	23.100	18.618	0.467	(17.691, 19.545)	4.482	1.89	1.92	0.037386	0.03	0.377799
55	21.300	18.618	0.467	(17.691, 19.545)	2.682	1.13	1.13	0.037386	0.01	0.223368
56	23.000	18.695	0.473	(17.756, 19.633)	4.305	1.82	1.84	0.038338	0.03	0.367325
59	21.200	17.804	0.477	(16.856, 18.751)	3.396	1.43	1.44	0.039065	0.02	0.290835
62	20.500	15.162	0.391	(14.386, 15.939)	5.338	2.24	2.29	0.026254	0.03	0.375627 R
64	19.000	15.288	0.389	(14.515, 16.060)	3.712	1.56	1.57	0.025963	0.01	0.256172
65	11.800	15.024	0.373	(14.283, 15.764)	-3.224	-1.35	-1.36	0.023861	0.01	-0.212129
66	11.800	15.226	0.377	(14.477, 15.975)	-3.426	-1.44	-1.44	0.024394	0.01	-0.228347
68	12.600	14.931	0.372	(14.192, 15.670)	-2.331	-0.98	-0.98	0.023779	0.00	-0.152405
72	14.400	15.740	0.386	(14.975, 16.505)	-1.340	-0.56	-0.56	0.025486	0.00	-0.090568
73	13.800	14.555	0.454	(13.654, 15.456)	-0.755	-0.32	-0.32	0.035349	0.00	-0.060655
74	14.100	14.741	0.457	(13.834, 15.648)	-0.641	-0.27	-0.27	0.035831	0.00	-0.051865
75	14.000	14.571	0.454	(13.671, 15.472)	-0.571	-0.24	-0.24	0.035305	0.00	-0.045853
79	10.500	13.882	0.420	(13.048, 14.716)	-3.382	-1.42	-1.43	0.030305	0.01	-0.252730
80	10.400	13.757	0.418	(12.927, 14.587)	-3.357	-1.41	-1.42	0.029987	0.01	-0.249387
81	14.900	15.105	0.324	(14.461, 15.748)	-0.205	-0.09	-0.09	0.018049	0.00	-0.011526
83	16.200	14.826	0.322	(14.187, 15.464)	1.374	0.57	0.57	0.017767	0.00	0.076964
84	14.100	14.935	0.325	(14.291, 15.579)	-0.835	-0.35	-0.35	0.018064	0.00	-0.047095
87	18.800	15.678	0.320	(15.042, 16.313)	3.122	1.30	1.31	0.017595	0.01	0.175197
88	18.700	15.864	0.330	(15.209, 16.518)	2.836	1.19	1.19	0.018663	0.01	0.163837
89	14.900	16.203	0.420	(15.370, 17.037)	-1.303	-0.55	-0.55	0.030223	0.00	-0.096401
90	14.900	14.857	0.349	(14.164, 15.550)	0.043	0.02	0.02	0.020906	0.00	0.002602
92	14.800	14.255	0.332	(13.596, 14.914)	0.545	0.23	0.23	0.018928	0.00	0.031494
93	12.300	13.466	0.421	(12.630, 14.301)	-1.166	-0.49	-0.49	0.030366	0.00	-0.086396
94	12.400	13.914	0.424	(13.072, 14.757)	-1.514	-0.64	-0.63	0.030883	0.00	-0.113355
96	12.400	13.652	0.421	(12.816, 14.487)	-1.252	-0.53	-0.52	0.030377	0.00	-0.092806
97	13.100	14.922	0.343	(14.241, 15.602)	-1.822	-0.76	-0.76	0.020173	0.00	-0.109096
99	13.000	14.938	0.345	(14.253, 15.623)	-1.938	-0.81	-0.81	0.020421	0.00	-0.116846
101	16.200	15.952	0.377	(15.205, 16.700)	0.248	0.10	0.10	0.024308	0.00	0.016306
102	15.900	15.936	0.376	(15.190, 16.682)	-0.036	-0.02	-0.02	0.024225	0.00	-0.002370
104	16.300	15.241	0.348	(14.550, 15.932)	1.059	0.44	0.44	0.020785	0.00	0.064304
107	14.900	14.392	0.406	(13.586, 15.199)	0.508	0.21	0.21	0.028321	0.00	0.036220
109	12.300	11.566	0.560	(10.455, 12.677)	0.734	0.31	0.31	0.053701	0.00	0.074093
110	12.400	11.550	0.563	(10.432, 12.667)	0.850	0.36	0.36	0.054381	0.00	0.086443
112	12.400	11.457	0.565	(10.335, 12.578)	0.943	0.40	0.40	0.054778	0.00	0.096300
113	9.900	13.698	0.423	(12.859, 14.536)	-3.798	-1.60	-1.61	0.030621	0.02	-0.286139
114	10.500	13.774	0.417	(12.948, 14.601)	-3.274	-1.38	-1.38	0.029760	0.01	-0.242172
115	11.300	13.884	0.416	(13.058, 14.709)	-2.584	-1.09	-1.09	0.029695	0.01	-0.190156
116	11.200	13.698	0.423	(12.859, 14.536)	-2.498	-1.05	-1.05	0.030621	0.01	-0.186776
117	14.500	15.122	0.325	(14.477, 15.768)	-0.622	-0.26	-0.26	0.018129	0.00	-0.035162
118	14.400	15.045	0.326	(14.398, 15.693)	-0.645	-0.27	-0.27	0.018229	0.00	-0.036580
119	14.800	14.843	0.322	(14.203, 15.483)	-0.043	-0.02	-0.02	0.017821	0.00	-0.002423
120	14.900	15.138	0.327	(14.489, 15.788)	-0.238	-0.10	-0.10	0.018365	0.00	-0.013563
121	18.200	15.526	0.316	(14.899, 16.152)	2.674	1.12	1.12	0.017081	0.00	0.147432
122	18.000	15.897	0.334	(15.235, 16.560)	2.103	0.88	0.88	0.019124	0.00	0.122591
124	18.400	15.804	0.329	(15.151, 16.457)	2.596	1.08	1.09	0.018564	0.00	0.149328
125	16.200	16.186	0.413	(15.365, 17.006)	0.014	0.01	0.01	0.029287	0.00	0.001038
127	14.400	14.407	0.329	(13.754, 15.060)	-0.007	-0.00	-0.00	0.018583	0.00	-0.000399
128	14.200	14.019	0.326	(13.372, 14.666)	0.181	0.08	0.08	0.018224	0.00	0.010265
130	11.300	13.618	0.414	(12.795, 14.440)	-2.318	-0.97	-0.97	0.029440	0.01	-0.169602
131	11.600	13.618	0.414	(12.795, 14.440)	-2.018	-0.85	-0.85	0.029440	0.00	-0.147474
132	11.500	13.694	0.416	(12.868, 14.521)	-2.194	-0.92	-0.92	0.029734	0.01	-0.161350
133	13.700	15.447	0.678	(14.101, 16.793)	-1.747	-0.75	-0.75	0.078910	0.01	-0.220114
134	14.900	15.719	0.670	(14.389, 17.049)	-0.819	-0.35	-0.35	0.077026	0.00	-0.101490
135	15.270	16.740	0.649	(15.452, 18.027)	-1.470	-0.63	-0.63	0.072159	0.01	-0.175664
137	17.650	16.097	0.645	(14.817, 17.378)	1.553	0.67	0.67	0.071389	0.01	0.184435
138	18.270	17.413	0.630	(16.163, 18.662)	0.857	0.37	0.37	0.068004	0.00	0.098894
139	18.650	17.277	0.630	(16.027, 18.526)	1.373	0.59	0.59	0.067949	0.01	0.158486
140	19.690	18.150	0.635	(16.891, 19.410)	1.540	0.66	0.66	0.069082	0.01	0.179456
141	19.260	17.900	0.632	(16.646, 19.154)	1.360	0.58	0.58	0.068474	0.01	0.157619
142	16.890	16.439	0.646	(15.157, 17.720)	0.451	0.19	0.19	0.071471	0.00	0.053529
143	17.330	17.629	0.643	(16.353, 18.905)	-0.299	-0.13	-0.13	0.070890	0.00	-0.035298
144	16.990	17.211	0.641	(15.938, 18.483)	-0.221	-0.09	-0.09	0.070496	0.00	-0.025987

145	13.650	16.278	0.687	(14.914, 17.642)	-2.628	-1.14	-1.14	0.080975	0.02	-0.337459
146	13.660	15.029	0.713	(13.614, 16.445)	-1.369	-0.59	-0.59	0.087271	0.01	-0.182912
147	14.240	15.777	0.695	(14.397, 17.156)	-1.537	-0.66	-0.66	0.082813	0.01	-0.199052
<i>R Large residual</i>										
<i>X Unusual X</i>										

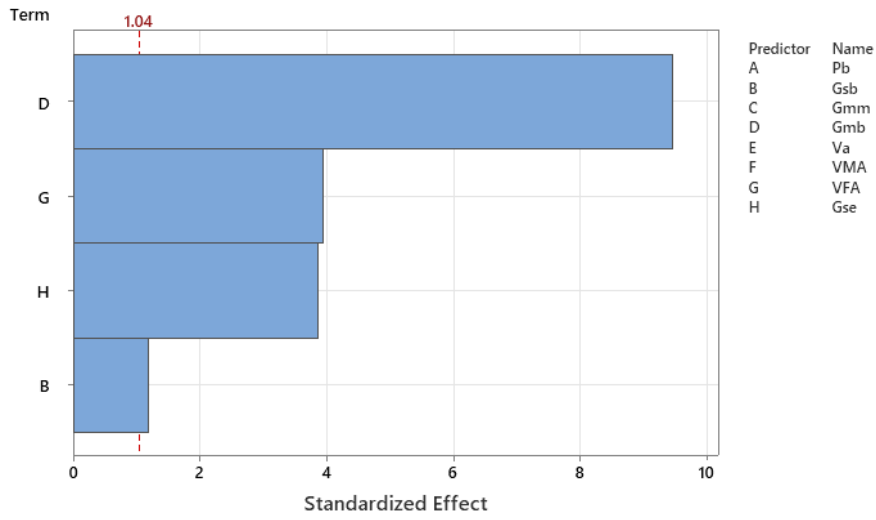
4.4.1.3 Fits and Diagnostics for All Observations

Test Set

Obs	MS	Fit	SE Fit	95% CI	Resid	Std Resid	HI			
2	10.020	9.081	0.761	(7.570, 10.592)	0.939	0.37	0.0993716			
6	12.430	11.960	0.395	(11.176, 12.744)	0.470	0.19	0.0267603			
7	13.120	11.293	0.434	(10.431, 12.155)	1.827	0.74	0.0323347			
10	11.750	11.590	0.600	(10.398, 12.781)	0.160	0.06	0.0617847			
14	11.222	10.297	0.738	(8.831, 11.762)	0.925	0.37	0.0934511			
16	12.428	11.545	0.471	(10.610, 12.481)	0.883	0.36	0.0380817			
21	14.660	14.511	0.547	(13.426, 15.596)	0.149	0.06	0.0512360			
25	17.320	15.337	0.440	(14.464, 16.210)	1.983	0.81	0.0331835			
27	12.830	15.260	0.440	(14.387, 16.133)	-2.430	-0.99	0.0331776			
30	14.560	17.213	0.419	(16.381, 18.044)	-2.653	-1.08	0.0301214			
33	11.370	15.477	0.522	(14.441, 16.513)	-4.107	-1.66	0.0467466			
37	11.360	14.166	0.582	(13.012, 15.320)	-2.806	-1.13	0.0579926			
38	11.480	14.147	0.581	(12.994, 15.301)	-2.667	-1.07	0.0579164			
39	13.170	14.172	0.582	(13.018, 15.327)	-1.002	-0.40	0.0580184			
48	21.000	17.547	0.699	(16.159, 18.935)	3.453	1.37	0.0838777			
49	20.900	17.106	0.492	(16.131, 18.082)	3.794	1.54	0.0414353			
57	19.900	16.441	0.382	(15.684, 17.199)	3.459	1.41	0.0249736			
58	19.400	17.185	0.428	(16.335, 18.035)	2.215	0.90	0.0314384			
60	19.400	17.880	0.485	(16.917, 18.843)	1.520	0.62	0.0403762			
61	19.000	15.534	0.406	(14.728, 16.340)	3.466	1.42	0.0282922			
63	20.000	14.823	0.374	(14.080, 15.565)	5.177	2.12	0.0239831 R			
67	12.300	15.117	0.374	(14.375, 15.859)	-2.817	-1.15	0.0239753			
69	14.800	15.893	0.392	(15.116, 16.671)	-1.093	-0.45	0.0263473			
70	15.200	15.800	0.388	(15.031, 16.570)	-0.600	-0.25	0.0258006			
71	14.800	15.817	0.389	(15.045, 16.588)	-1.017	-0.42	0.0258980			
76	13.900	14.741	0.457	(13.834, 15.648)	-0.841	-0.34	0.0358312			
77	10.200	13.647	0.419	(12.816, 14.479)	-3.447	-1.41	0.0301003			
78	11.000	13.664	0.422	(12.827, 14.500)	-2.664	-1.09	0.0304766			
82	15.200	14.826	0.322	(14.187, 15.464)	0.374	0.15	0.0177672			
85	17.800	15.568	0.315	(14.942, 16.194)	2.232	0.92	0.0170518			
86	17.800	15.771	0.325	(15.125, 16.416)	2.029	0.83	0.0181121			
91	14.900	14.425	0.336	(13.758, 15.091)	0.475	0.19	0.0193412			
95	12.500	13.668	0.419	(12.836, 14.500)	-1.168	-0.48	0.0301383			
98	12.800	15.031	0.346	(14.344, 15.717)	-2.231	-0.91	0.0205147			
100	13.300	15.140	0.349	(14.447, 15.833)	-1.840	-0.75	0.0208978			
103	16.300	15.411	0.354	(14.709, 16.112)	0.889	0.36	0.0214249			
105	14.900	16.527	0.494	(15.546, 17.507)	-1.627	-0.66	0.0418447			
106	14.900	14.485	0.408	(13.676, 15.294)	0.415	0.17	0.0284923			
108	14.800	14.655	0.411	(13.839, 15.471)	0.145	0.06	0.0289899			
111	12.500	11.566	0.560	(10.455, 12.677)	0.934	0.38	0.0537005			
123	17.900	15.695	0.324	(15.053, 16.338)	2.205	0.90	0.0179724			
126	14.600	14.577	0.334	(13.914, 15.239)	0.023	0.01	0.0191109			
129	11.200	13.618	0.414	(12.795, 14.440)	-2.418	-0.99	0.0294402			
136	17.640	15.941	0.649	(14.653, 17.229)	1.699	0.68	0.0721905			
<i>R Large residual</i>										

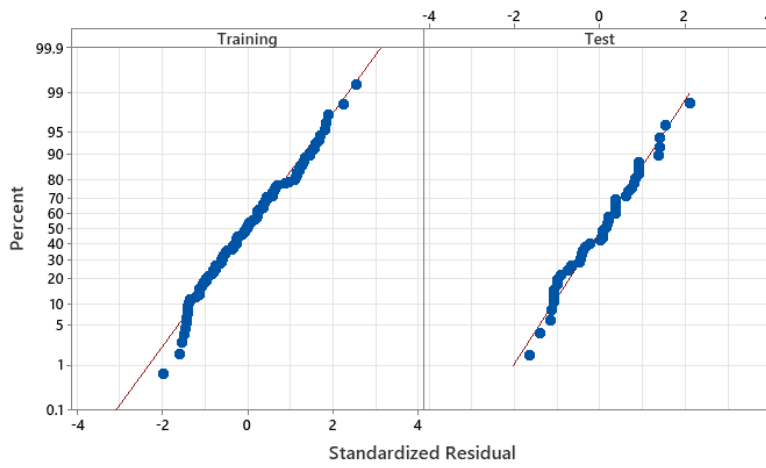
Pareto Chart of the Standardized Effects

(response is MS, $\alpha = 0.3$)



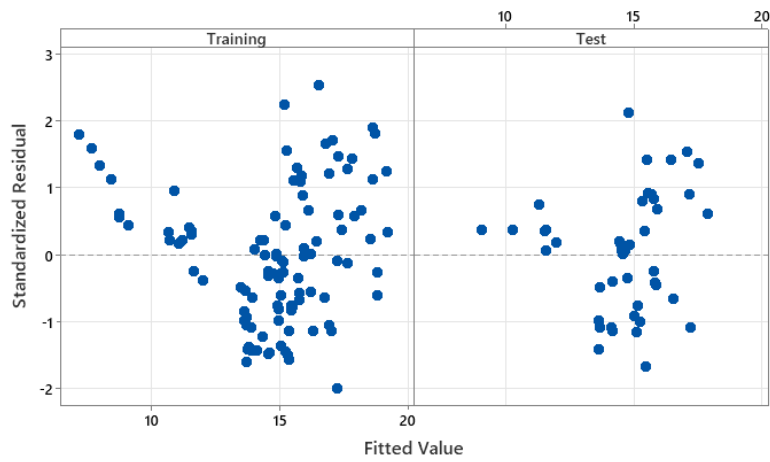
Normal Probability Plot

(response is MS)

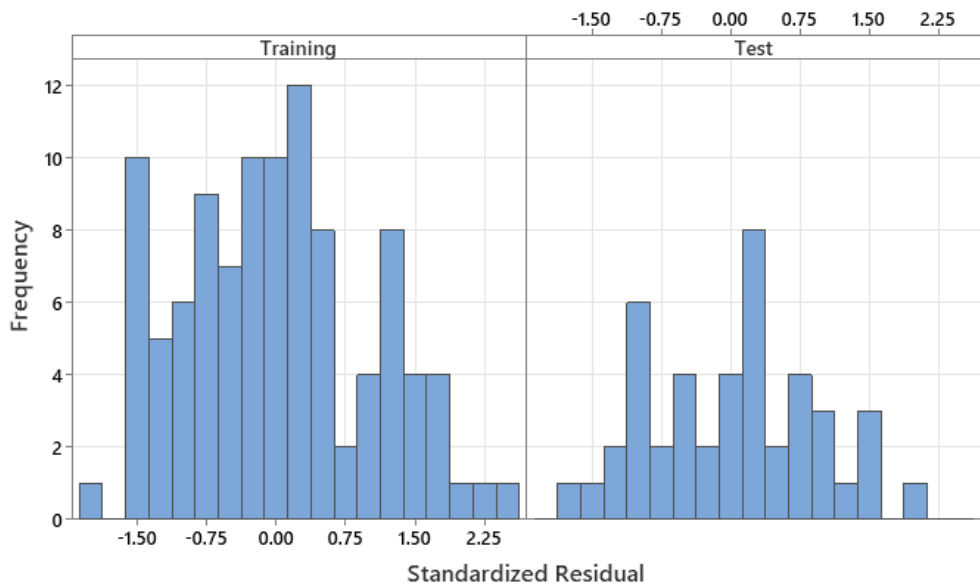


Versus Fits

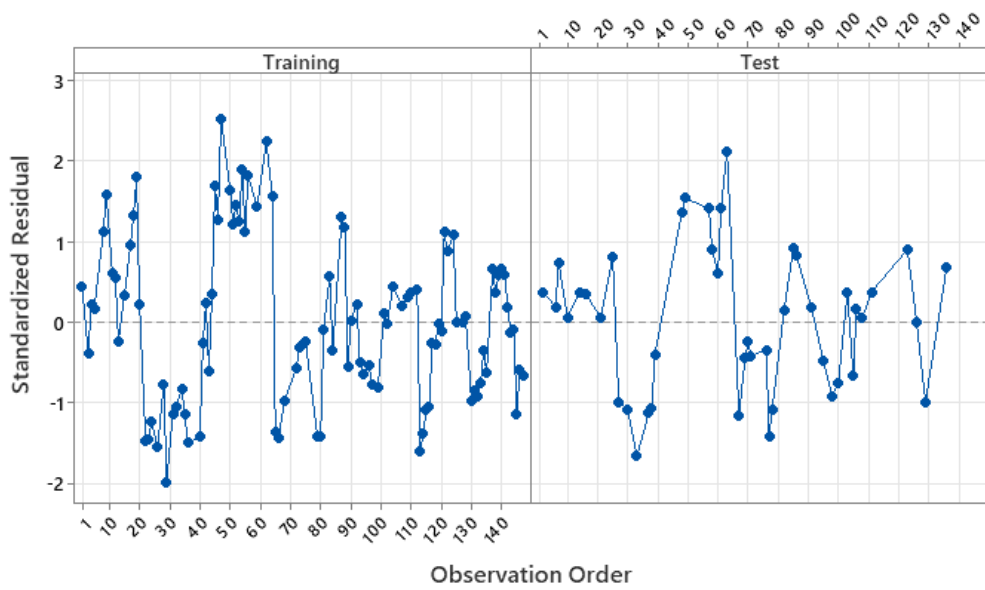
(response is MS)



Histogram
(response is MS)



Versus Order
(response is MS)



4.4.2 MF Model Validation

S	R-sq	R-sq(adj)	PRESS	R-sq(pred)	AICc	BIC	Test S	Test R-sq
0.279407	58.42%	56.28%	8.44291	53.64%	38.63	55.90	0.267470	53.95%

4.4.2.1 Analysis of Variance

Source	DF	Seq SS	Contribution	Adj SS	Adj MS	F-Value	P-Value
Regression	5	10.6391	58.42%	10.6391	2.12782	27.26	0.000
Pb	1	7.1435	39.22%	0.1427	0.14273	1.83	0.179
Gsb	1	0.0005	0.00%	0.4243	0.42425	5.43	0.022
Gmb	1	0.0108	0.06%	0.6886	0.68860	8.82	0.004
VFA	1	3.3994	18.67%	1.0581	1.05813	13.55	0.000
Gse	1	0.0850	0.47%	0.0850	0.08495	1.09	0.299
Error	97	7.5726	41.58%	7.5726	0.07807		
Lack-of-Fit	94	7.5552	41.49%	7.5552	0.08037	13.82	0.025
Pure Error	3	0.0174	0.10%	0.0174	0.00582		
Total	102	18.2118	100.00%				

4.4.2.2 Fits and Diagnostics for All Observations

Training Set

Obs	MF	Fit	SE Fit	95% CI	Resid	Std Resid	Del Resid	HI	Cook's D	DFITS
1	2.1500	2.0195	0.1087	(1.8036, 2.2353)	0.1305	0.51	0.51	0.151452	0.01	0.213458
3	2.5900	2.2234	0.0785	(2.0676, 2.3791)	0.3666	1.37	1.37	0.078902	0.03	0.401970
4	2.8100	2.2228	0.0823	(2.0595, 2.3860)	0.5872	2.20	2.24	0.086672	0.08	0.691406 R
5	2.6700	2.5101	0.0632	(2.3846, 2.6356)	0.1599	0.59	0.59	0.051242	0.00	0.136084
8	2.9200	2.9348	0.0994	(2.7376, 3.1320)	-0.0148	-0.06	-0.06	0.126449	0.00	-0.021497
9	2.7700	2.9316	0.1048	(2.7237, 3.1395)	-0.1616	-0.62	-0.62	0.140572	0.01	-0.251512
11	2.1500	2.0387	0.1177	(1.8051, 2.2723)	0.1113	0.44	0.44	0.177471	0.01	0.203141 X
12	2.1100	2.2651	0.0963	(2.0741, 2.4562)	-0.1551	-0.59	-0.59	0.118722	0.01	-0.216366
13	2.5900	2.2435	0.0808	(2.0830, 2.4039)	0.3465	1.30	1.30	0.083697	0.03	0.392978
15	2.6700	2.5325	0.0626	(2.4083, 2.6568)	0.1375	0.50	0.50	0.050190	0.00	0.115607
17	2.6100	2.5332	0.0614	(2.4112, 2.6551)	0.0768	0.28	0.28	0.048354	0.00	0.063230
18	2.9200	2.9615	0.0916	(2.7797, 3.1433)	-0.0415	-0.16	-0.16	0.107490	0.00	-0.054236
19	2.7700	2.9630	0.0985	(2.7675, 3.1586)	-0.1930	-0.74	-0.74	0.124368	0.01	-0.277575
20	2.4500	2.9861	0.0700	(2.8473, 3.1250)	-0.5361	-1.98	-2.01	0.062681	0.04	-0.520541
22	1.4300	2.0821	0.0673	(1.9485, 2.2157)	-0.6521	-2.40	-2.47	0.058012	0.06	-0.612195 R
23	2.2800	2.0818	0.0672	(1.9484, 2.2151)	0.1982	0.73	0.73	0.057821	0.01	0.180613
24	1.8500	2.0848	0.0683	(1.9493, 2.2203)	-0.2348	-0.87	-0.87	0.059689	0.01	-0.218033
26	1.5700	2.1275	0.0509	(2.0265, 2.2286)	-0.5575	-2.03	-2.06	0.033214	0.02	-0.382422 R
28	1.9800	2.1275	0.0510	(2.0263, 2.2288)	-0.1475	-0.54	-0.54	0.033326	0.00	-0.099345
29	2.0500	2.4574	0.0492	(2.3597, 2.5552)	-0.4074	-1.48	-1.49	0.031068	0.01	-0.266916
31	1.6100	2.4512	0.0477	(2.3566, 2.5458)	-0.8412	-3.06	-3.20	0.029092	0.05	-0.553463 R
32	2.4800	2.4490	0.0471	(2.3555, 2.5425)	0.0310	0.11	0.11	0.028418	0.00	0.019138
34	2.4100	2.5807	0.0639	(2.4540, 2.7075)	-0.1707	-0.63	-0.63	0.052248	0.00	-0.146917
35	2.2000	2.5792	0.0637	(2.4527, 2.7056)	-0.3792	-1.39	-1.40	0.051969	0.02	-0.327921
36	2.0500	2.5781	0.0636	(2.4519, 2.7042)	-0.5281	-1.94	-1.97	0.051781	0.03	-0.460224
40	2.0700	2.8263	0.0769	(2.6736, 2.9789)	-0.7563	-2.82	-2.92	0.075799	0.11	-0.837055 R
41	3.6000	2.9994	0.0811	(2.8385, 3.1603)	0.6006	2.25	2.30	0.084168	0.08	0.695761 R
42	3.0700	3.0987	0.0895	(2.9211, 3.2763)	-0.0287	-0.11	-0.11	0.102549	0.00	-0.036458
43	2.8400	3.0056	0.0814	(2.8441, 3.1671)	-0.1656	-0.62	-0.62	0.084770	0.01	-0.187939
44	2.7200	2.8442	0.0851	(2.6753, 3.0131)	-0.1242	-0.47	-0.46	0.092760	0.00	-0.148655
45	2.1000	1.8625	0.0804	(1.7029, 2.0220)	0.2375	0.89	0.89	0.082750	0.01	0.266330
46	2.1600	1.8680	0.0812	(1.7069, 2.0291)	0.2920	1.09	1.09	0.084372	0.02	0.331878
47	1.8400	1.8775	0.0794	(1.7199, 2.0351)	-0.0375	-0.14	-0.14	0.080792	0.00	-0.041296
50	2.7500	2.2189	0.0600	(2.0998, 2.3379)	0.5311	1.95	1.98	0.046086	0.03	0.434131
51	1.8300	2.1630	0.0562	(2.0516, 2.2745)	-0.3330	-1.22	-1.22	0.040398	0.01	-0.250282
52	2.6500	2.0389	0.0618	(1.9163, 2.1615)	0.6111	2.24	2.29	0.048873	0.04	0.519370 R
53	2.2700	2.4152	0.0591	(2.2979, 2.5325)	-0.1452	-0.53	-0.53	0.044759	0.00	-0.114646
54	2.8600	2.3972	0.0541	(2.2899, 2.5045)	0.4628	1.69	1.70	0.037425	0.02	0.336125
55	2.6800	2.3972	0.0541	(2.2899, 2.5045)	0.2828	1.03	1.03	0.037425	0.01	0.203464
56	2.1100	2.4054	0.0547	(2.2968, 2.5140)	-0.2954	-1.08	-1.08	0.038338	0.01	-0.215439
59	2.5500	2.5972	0.0559	(2.4862, 2.7081)	-0.0472	-0.17	-0.17	0.040014	0.00	-0.034999
62	3.4800	2.8762	0.0515	(2.7739, 2.9785)	0.6038	2.20	2.24	0.034012	0.03	0.421053 R
64	2.4300	2.8658	0.0529	(2.7608, 2.9708)	-0.4358	-1.59	-1.60	0.035848	0.02	-0.308721

65	2.3000	2.5593	0.0435	(2.4730, 2.6457)	-0.2593	-0.94	-0.94	0.024234	0.00	-0.147982
66	2.3400	2.5570	0.0438	(2.4701, 2.6440)	-0.2170	-0.79	-0.78	0.024590	0.00	-0.124627
68	2.4200	2.5574	0.0434	(2.4712, 2.6435)	-0.1374	-0.50	-0.50	0.024143	0.00	-0.077977
72	2.6100	2.7391	0.0446	(2.6505, 2.8277)	-0.1291	-0.47	-0.47	0.025503	0.00	-0.075413
73	3.1000	2.9338	0.0532	(2.8282, 3.0394)	0.1662	0.61	0.60	0.036250	0.00	0.117139
74	3.1000	2.9377	0.0535	(2.8315, 3.0439)	0.1623	0.59	0.59	0.036704	0.00	0.115141
75	3.0000	2.9276	0.0534	(2.8215, 3.0336)	0.0724	0.26	0.26	0.036587	0.00	0.051216
79	2.2000	2.2757	0.0491	(2.1783, 2.3731)	-0.0757	-0.28	-0.27	0.030860	0.00	-0.048885
80	2.3000	2.2862	0.0494	(2.1882, 2.3841)	0.0138	0.05	0.05	0.031205	0.00	0.008977
81	2.5300	2.4439	0.0376	(2.3694, 2.5185)	0.0861	0.31	0.31	0.018076	0.00	0.041990
83	2.5500	2.4380	0.0373	(2.3641, 2.5120)	0.1120	0.40	0.40	0.017801	0.00	0.054195
84	2.5900	2.4338	0.0377	(2.3590, 2.5086)	0.1562	0.56	0.56	0.018194	0.00	0.076536
87	2.7000	2.6194	0.0376	(2.5447, 2.6941)	0.0806	0.29	0.29	0.018146	0.00	0.039399
88	2.6000	2.6233	0.0387	(2.5465, 2.7001)	-0.0233	-0.08	-0.08	0.019192	0.00	-0.011715
89	2.8100	2.8671	0.0488	(2.7703, 2.9639)	-0.0571	-0.21	-0.21	0.030498	0.00	-0.036631
90	2.8000	2.8191	0.0417	(2.7363, 2.9020)	-0.0191	-0.07	-0.07	0.022309	0.00	-0.010413
92	2.9700	2.7868	0.0416	(2.7044, 2.8693)	0.1832	0.66	0.66	0.022117	0.00	0.099410
93	3.2100	3.0359	0.0599	(2.9170, 3.1549)	0.1741	0.64	0.64	0.045980	0.00	0.139585
94	3.3000	3.0519	0.0614	(2.9301, 3.1738)	0.2481	0.91	0.91	0.048287	0.01	0.204812
96	3.1400	3.0399	0.0600	(2.9208, 3.1589)	0.1001	0.37	0.37	0.046109	0.00	0.080322
97	2.2000	2.5146	0.0399	(2.4354, 2.5938)	-0.3146	-1.14	-1.14	0.020376	0.00	-0.164319
99	2.2100	2.5084	0.0400	(2.4290, 2.5878)	-0.2984	-1.08	-1.08	0.020493	0.00	-0.156214
101	2.5400	2.7298	0.0436	(2.6433, 2.8163)	-0.1898	-0.69	-0.69	0.024323	0.00	-0.108268
102	2.6000	2.7360	0.0436	(2.6495, 2.8225)	-0.1360	-0.49	-0.49	0.024319	0.00	-0.077479
104	2.5500	2.7017	0.0404	(2.6216, 2.7818)	-0.1517	-0.55	-0.55	0.020876	0.00	-0.079831
107	2.8500	2.8747	0.0488	(2.7778, 2.9716)	-0.0247	-0.09	-0.09	0.030518	0.00	-0.015839
109	3.2100	3.2189	0.1418	(2.9376, 3.5003)	-0.0089	-0.04	-0.04	0.257440	0.00	-0.021728
110	3.3000	3.2251	0.1434	(2.9405, 3.5097)	0.0749	0.31	0.31	0.263380	0.01	0.185798
112	3.1400	3.2232	0.1434	(2.9385, 3.5079)	-0.0832	-0.35	-0.35	0.263561	0.01	-0.206591
113	2.2000	2.2928	0.0499	(2.1938, 2.3917)	-0.0928	-0.34	-0.34	0.031852	0.00	-0.060928
114	1.9900	2.3009	0.0496	(2.2026, 2.3993)	-0.3109	-1.13	-1.13	0.031449	0.01	-0.204055
115	2.1500	2.2967	0.0492	(2.1991, 2.3943)	-0.1467	-0.53	-0.53	0.030959	0.00	-0.094970
116	2.2400	2.2928	0.0499	(2.1938, 2.3917)	-0.0528	-0.19	-0.19	0.031852	0.00	-0.034644
117	2.6300	2.4587	0.0376	(2.3840, 2.5333)	0.1713	0.62	0.62	0.018130	0.00	0.083819
118	2.4900	2.4505	0.0377	(2.3756, 2.5254)	0.0395	0.14	0.14	0.018253	0.00	0.019352
119	2.5500	2.4528	0.0373	(2.3788, 2.5268)	0.0972	0.35	0.35	0.017821	0.00	0.047067
120	2.6000	2.4525	0.0379	(2.3773, 2.5277)	0.1475	0.53	0.53	0.018388	0.00	0.072671
121	2.9000	2.6240	0.0371	(2.5504, 2.6977)	0.2760	1.00	1.00	0.017635	0.00	0.133514
122	2.8100	2.6318	0.0392	(2.5541, 2.7096)	0.1782	0.64	0.64	0.019634	0.00	0.090854
124	2.7300	2.6299	0.0386	(2.5533, 2.7065)	0.1001	0.36	0.36	0.019084	0.00	0.050231
125	2.9800	2.8523	0.0482	(2.7566, 2.9481)	0.1277	0.46	0.46	0.029806	0.00	0.080973
127	2.9100	2.7822	0.0412	(2.7004, 2.8640)	0.1278	0.46	0.46	0.021767	0.00	0.068710
128	3.1000	2.7806	0.0404	(2.7004, 2.8607)	0.3194	1.16	1.16	0.020884	0.00	0.169034
130	3.2000	2.9486	0.0547	(2.8401, 3.0571)	0.2514	0.92	0.92	0.038274	0.01	0.182907
131	3.1700	2.9486	0.0547	(2.8401, 3.0571)	0.2214	0.81	0.81	0.038274	0.00	0.160925
132	3.1500	2.9567	0.0541	(2.8494, 3.0641)	0.1933	0.71	0.70	0.037472	0.00	0.138751
133	2.7400	2.5091	0.0828	(2.3448, 2.6734)	0.2309	0.87	0.86	0.087761	0.01	0.268010
134	2.4600	2.5058	0.0812	(2.3446, 2.6671)	-0.0458	-0.17	-0.17	0.084551	0.00	-0.051815
135	2.3300	2.4958	0.0770	(2.3430, 2.6486)	-0.1658	-0.62	-0.62	0.075914	0.01	-0.176336
137	2.6800	2.5798	0.0760	(2.4290, 2.7307)	0.1002	0.37	0.37	0.073968	0.00	0.104815
138	2.7500	2.5744	0.0732	(2.4291, 2.7196)	0.1756	0.65	0.65	0.068611	0.01	0.176233
139	2.6800	2.7219	0.0728	(2.5773, 2.8664)	-0.0419	-0.16	-0.15	0.067950	0.00	-0.041714
140	2.7900	2.7261	0.0735	(2.5802, 2.8720)	0.0639	0.24	0.24	0.069214	0.00	0.064336
141	2.6200	2.7245	0.0732	(2.5793, 2.8697)	-0.1045	-0.39	-0.39	0.068553	0.00	-0.104680
142	2.8000	2.8225	0.0749	(2.6739, 2.9712)	-0.0225	-0.08	-0.08	0.071837	0.00	-0.023170
143	2.8600	2.8294	0.0749	(2.6806, 2.9781)	0.0306	0.11	0.11	0.071935	0.00	0.031529
144	2.8700	2.8262	0.0746	(2.6781, 2.9743)	0.0438	0.16	0.16	0.071301	0.00	0.044852
145	2.9000	2.9640	0.0811	(2.8030, 3.1250)	-0.0640	-0.24	-0.24	0.084278	0.00	-0.072249
146	2.9700	2.9593	0.0833	(2.7939, 3.1247)	0.0107	0.04	0.04	0.088986	0.00	0.012462
147	3.2200	2.9613	0.0817	(2.7991, 3.1234)	0.2587	0.97	0.97	0.085492	0.01	0.295954

R Large residual

X Unusual X

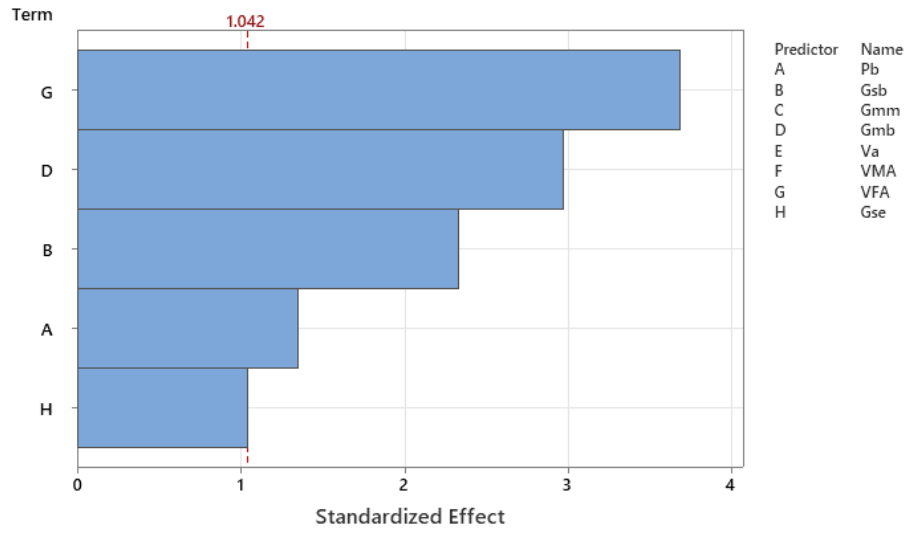
4.4.2.3 Fits and Diagnostics for All Observations

Test Set								
Obs	MF	Fit	SE Fit	95% CI	Resid	Std Resid	HI	
2	2.1100	2.2473	0.0897	(2.0693, 2.4254)	-0.1373	-0.47	0.103123	
6	2.5400	2.5153	0.0600	(2.3962, 2.6344)	0.0247	0.09	0.046137	
7	2.6100	2.5078	0.0628	(2.3831, 2.6325)	0.1022	0.36	0.050576	
10	2.4500	2.9683	0.0825	(2.8046, 3.1321)	-0.5183	-1.78	0.087157	
14	2.8100	2.2490	0.0863	(2.0777, 2.4203)	0.5610	1.92	0.095380	
16	2.5400	2.5369	0.0580	(2.4218, 2.6520)	0.0031	0.01	0.043081	
21	2.2900	2.0826	0.0675	(1.9487, 2.2165)	0.2074	0.72	0.058311	
25	1.7400	2.1276	0.0509	(2.0265, 2.2286)	-0.3876	-1.36	0.033206	
27	1.9200	2.1276	0.0509	(2.0266, 2.2286)	-0.2076	-0.73	0.033190	
30	2.0200	2.4570	0.0492	(2.3595, 2.5546)	-0.4370	-1.54	0.030952	
33	2.2300	2.5820	0.0640	(2.4550, 2.7091)	-0.3520	-1.23	0.052483	
37	2.6600	2.8281	0.0770	(2.6753, 2.9808)	-0.1681	-0.58	0.075861	
38	2.0200	2.8275	0.0769	(2.6748, 2.9802)	-0.8075	-2.79	0.075840	R
39	2.4000	2.8283	0.0770	(2.6755, 2.9810)	-0.4283	-1.48	0.075868	
48	1.8500	1.8660	0.0810	(1.7052, 2.0269)	-0.0160	-0.06	0.084135	
49	1.8600	2.0948	0.0569	(1.9819, 2.2077)	-0.2348	-0.82	0.041455	
57	2.6400	2.5554	0.0460	(2.4642, 2.6467)	0.0846	0.30	0.027082	
58	2.5900	2.5711	0.0510	(2.4697, 2.6724)	0.0189	0.07	0.033377	
60	2.5700	2.6053	0.0566	(2.4931, 2.7176)	-0.0353	-0.12	0.040991	
61	3.2400	2.8840	0.0529	(2.7790, 2.9891)	0.3560	1.25	0.035885	
63	3.1000	2.8560	0.0516	(2.7536, 2.9584)	0.2440	0.86	0.034103	
67	2.1800	2.5613	0.0436	(2.4747, 2.6478)	-0.3813	-1.35	0.024358	
69	2.7000	2.7554	0.0454	(2.6653, 2.8455)	-0.0554	-0.20	0.026410	
70	2.6800	2.7535	0.0449	(2.6643, 2.8426)	-0.0735	-0.26	0.025859	
71	2.6600	2.7473	0.0450	(2.6580, 2.8365)	-0.0873	-0.31	0.025902	
76	3.2300	2.9377	0.0535	(2.8315, 3.0439)	0.2923	1.03	0.036704	
77	2.1000	2.2904	0.0498	(2.1916, 2.3892)	-0.1904	-0.67	0.031736	
78	2.0000	2.2842	0.0497	(2.1855, 2.3829)	-0.2842	-1.00	0.031677	
82	2.4500	2.4380	0.0373	(2.3641, 2.5120)	0.0120	0.04	0.017801	
85	2.9600	2.6236	0.0368	(2.5505, 2.6967)	0.3364	1.19	0.017373	
86	2.7100	2.6213	0.0382	(2.5456, 2.6971)	0.0887	0.31	0.018653	
91	2.8500	2.7969	0.0413	(2.7150, 2.8789)	0.0531	0.19	0.021863	
95	3.0200	3.0336	0.0589	(2.9167, 3.1506)	-0.0136	-0.05	0.044452	
98	2.1900	2.5103	0.0401	(2.4308, 2.5899)	-0.3203	-1.13	0.020591	
100	2.1800	2.5061	0.0404	(2.4259, 2.5863)	-0.3261	-1.16	0.020908	
103	2.5600	2.7118	0.0409	(2.6306, 2.7930)	-0.1518	-0.54	0.021436	
105	2.8100	2.9589	0.0572	(2.8454, 3.0724)	-0.1489	-0.52	0.041887	
106	2.8000	2.8766	0.0489	(2.7795, 2.9738)	-0.0766	-0.27	0.030668	
108	2.9700	2.8868	0.0489	(2.7897, 2.9838)	0.0832	0.29	0.030621	
111	3.0200	3.2189	0.1418	(2.9376, 3.5003)	-0.1989	-0.63	0.257440	X
123	2.8000	2.6341	0.0378	(2.5592, 2.7091)	0.1659	0.59	0.018271	
126	2.9100	2.7923	0.0411	(2.7108, 2.8739)	0.1177	0.42	0.021628	
129	3.1300	2.9486	0.0547	(2.8401, 3.0571)	0.1814	0.64	0.038274	
136	2.5700	2.5809	0.0766	(2.4289, 2.7330)	-0.0109	-0.04	0.075139	

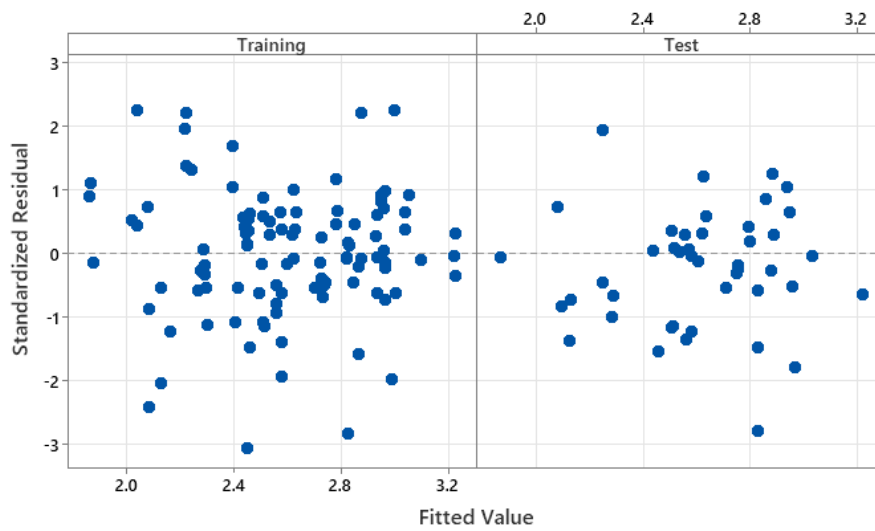
R Large residual

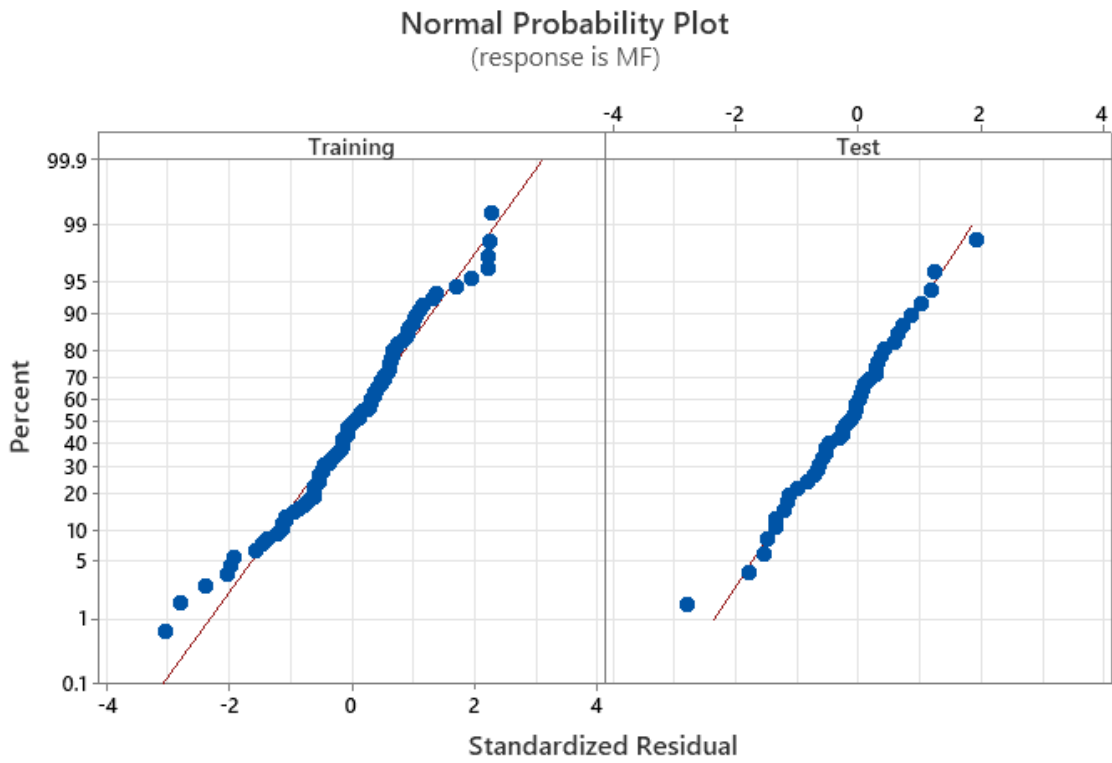
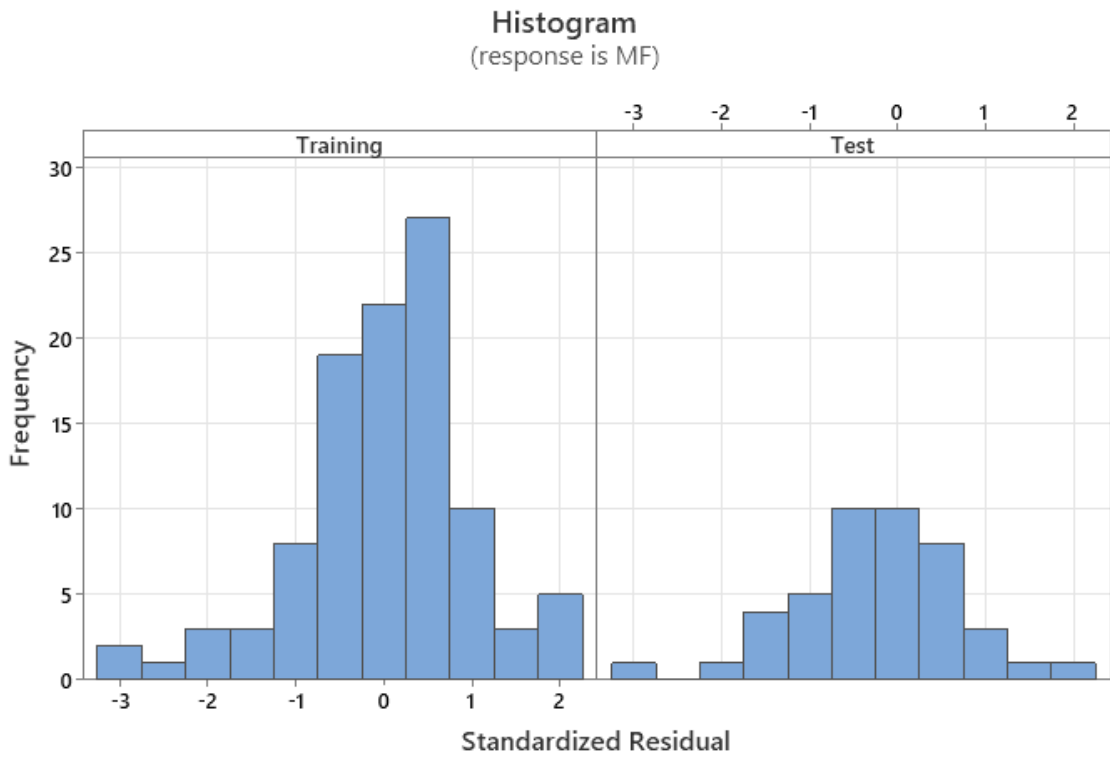
X Unusual X

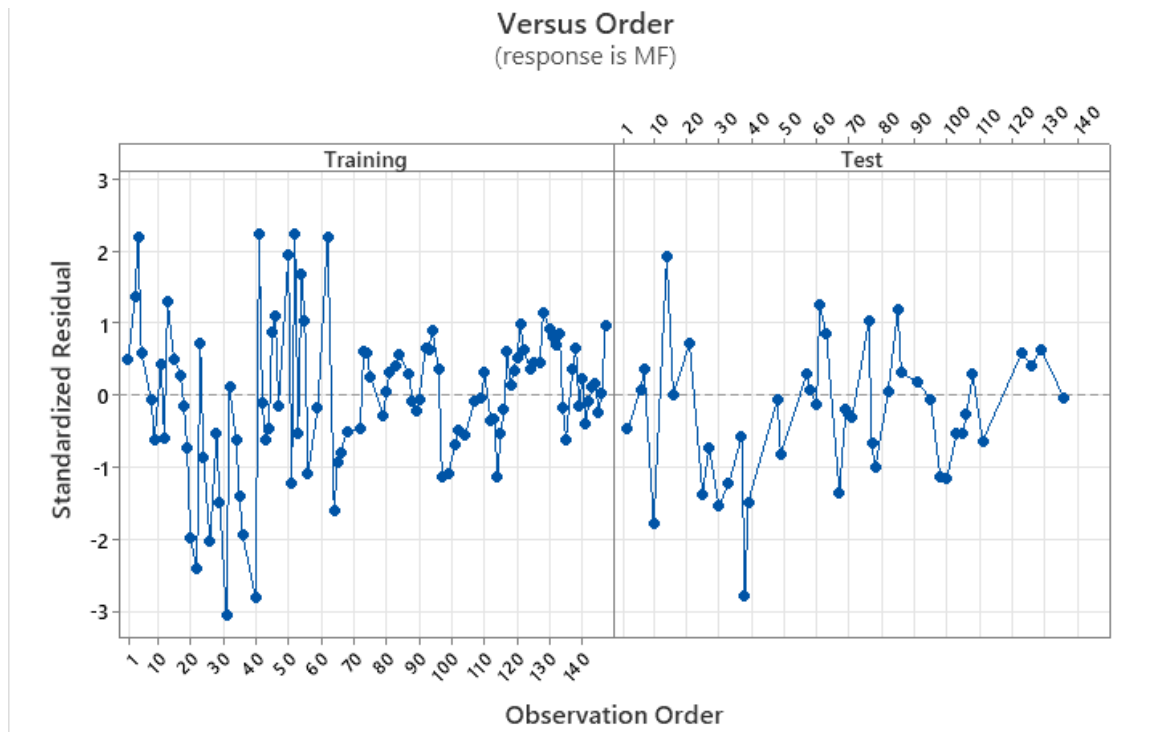
Pareto Chart of the Standardized Effects
(response is MF, $\alpha = 0.3$)



Versus Fits
(response is MF)







4.5 Model performance summary

Table 4-16: Comparative goodness-of-fit and external-validation metrics for MS and MF models.

Metric	MS Model	MF Model	Threshold
Adjusted R ²	0.533	0.563	>0.50 ✓
Predicted R ²	0.503	0.536	adj. R ² ±0.05 ✓
Test-set R ²	0.488	0.539	≥0.45 ✓
5-fold CV RMSE	2.41 kN	0.28 mm	σ <15 % ✓
Mallows Cp	2.06	3.34	≈ p + 2 ✓

Statistics such as S, AICc, BIC and predicted R² summarise overall accuracy and generalisability: MS model S = 2.42 kN, predicted R² ≈ 50 %; MF model S = 0.28 mm, predicted R² ≈ 54 %. Lower AICc/BIC support model parsimony and validate the variable-selection protocol.

4.6. Discussion of Results

With increasing interest in predictive analytics, this study evaluated how aggregate and volumetric properties easily measured in routine lab work can be used to predict Marshall Stability (MS) and Marshall Flow (MF). The findings support a shift from traditional, labor-intensive mix designs to

statistically-driven models, especially valuable for infrastructure development in resource-limited contexts like Rwanda.

4.6.1 Overview of Regression Findings

Multiple linear regression (MLR) models developed for MS and MF were statistically valid and robust. The MS model yielded an adjusted R^2 of 53.3%, while the MF model reached 56.3%. Both models used five predictors—Gsb, Gmb, Gse, VFA, and Pb confirming that these parameters explain a significant portion of Marshall response variability. Similar outcomes were reported by Chu et al. (2021) using random forest ($R^2 = 0.60$) and Li et al. (2019) using support vector machines ($R^2 \approx 0.66$). All retained predictors were significant ($p < 0.05$), and model F-statistics ($F > 27$, $p < 0.001$) confirmed overall fit.

Gmb was the strongest contributor to MS, reflecting the importance of mix density, while Pb had the most influence on MF. Low differences between training and testing R^2 values (<5%) indicate good model generalization and low risk of overfitting.

4.6.2 Interpretation of Key Predictors

Bulk Specific Gravity of the Mix (Gmb) was the most influential factor for both MS and MF. It improved stability due to higher internal friction but reduced flow, reflecting stiffness trade-offs (Rahman et al., 2020; Zhou et al., 2016).

Effective Specific Gravity (Gse) negatively impacted MS and positively influenced MF. Higher Gse, often tied to absorptive or angular aggregates, reduced structural interlock but increased deformation potential (Wang et al., 2018).

Voids Filled with Asphalt (VFA) increased MF but weakened MS, confirming prior findings that excessive binder in voids reduces inter-particle friction (Brown et al., 2009).

Binder Content (Pb) was relevant only for MF, with a negative effect. Excess binder softens the mix and increases susceptibility to deformation (Abreu et al., 2014).

4.6.3 Statistical Diagnostics

Diagnostic tests confirmed model validity. Residuals were normally distributed (Shapiro–Wilk $p > 0.05$) and homoscedastic. All VIFs were well below 10, indicating no multicollinearity. Metrics like AICc and PRESS further support model robustness and generalizability.

4.6.4 Practical Implications

These models offer a reliable and efficient method for estimating MS and MF using common mix design parameters. Their integration into spreadsheet tools or digital platforms can streamline

early-stage mix evaluations and reduce reliance on laboratory testing especially useful in time-sensitive or budget-constrained projects. While the current models offer moderate predictive power, they lay a strong foundation for enhancements using broader datasets, nonlinear terms, or machine learning (Elwardany et al., 2019).

4.6.5 Correlation-Based Predictive Capability of the Developed Models

This study confirms that aggregate properties such as Gsb, Gse, and Gmb alongside volumetric measures like VFA and binder content have a clear and quantifiable correlation with Marshall responses. The moderate R^2 values achieved align with both physical mechanisms and published literature, reinforcing the legitimacy of using multivariate regression for prediction (Li et al., 2019; Chu et al., 2021).

Mechanistically, density-related variables (e.g., Gmb) influence both strength and flexibility. VFA and Gse, associated with binder absorption and aggregate surface characteristics, determine how well the mix resists or accommodates deformation. These factors are not only statistically significant but also practically observable in field behavior, validating their inclusion.

The practical implication is substantial: by relying on these statistically supported correlations, engineers can pre-screen asphalt mixtures, reduce laboratory testing, and enhance design efficiency. In Rwanda's road sector, where standardized resources and testing equipment may be limited, the models provide a science-backed decision-support tool that links material characteristics directly to performance outcomes.

CHAPTER FIVE: CONCLUSION AND RECOMMENDATIONS

5.1 CONCLUSIONS

- The analysis revealed that bulk specific gravity of the compacted mix (G_{mb}), effective specific gravity of aggregates (G_{se}), and voids filled with asphalt (VFA) significantly influenced Marshall Stability (MS), while asphalt content (Pb) and voids in mineral aggregate (VMA) were the primary drivers of Marshall Flow (MF). Notably, G_{mb} alone accounted for 37.6% of the MS variability, affirming its central role in determining load-bearing strength. These findings emphasize the critical influence of aggregate structure and binder distribution on the mechanical behavior of asphalt mixtures.
- Using backward-elimination multiple linear regression (MLR) on a 103-sample database, two final models were established. The models retained only the most statistically significant predictors and achieved adjusted R^2 values of 53.30% for MS and 56.28% for MF. These results confirm that more than half the variability in Marshall parameters can be reliably explained using a subset of aggregate and volumetric characteristics.
- Five-fold cross-validation yielded low root-mean-square errors of 2.41 kN (for MS) and 0.28 mm (for MF), both within 15% of their respective standard deviations. Additionally, residuals displayed a normal distribution, and the close agreement between training and validation R^2 values (less than 5% difference) indicated that the models were stable and not overfitted.
- By eliminating the need for exhaustive laboratory testing, the models offer a practical tool for predicting asphalt mix performance using readily available aggregate test data. This supports faster, cost-effective mix evaluation and enhances engineers' capacity to optimize material selection and pavement design decisions based on reliable performance indicators.

5.2 RECOMMENDATIONS

- Road agencies and asphalt laboratories should embed the two equations in their volumetric design spreadsheets to pre-qualify blend alternatives before committing to hot-mix production. This step will allow practitioners to discard unpromising gradations early, reserving full Marshall testing for shortlisted options.
- Because aggregate mineralogy and plant controls evolve over time, the coefficients in the two formulae should be re-estimated regularly to sustain predictive accuracy. A rolling database maintained by RTDA’s central laboratory is advised.
- Stability and flow alone do not capture fatigue and moisture sensitivity. The regression outputs should therefore be treated as “gate-keepers” and subsequently paired with Balanced Mix Design (BMD) performance tests (e.g., IDEAL-CT, Hamburg Wheel Tracking) for final approval of surface courses.
- Given their statistical dominance, specifications should place greater emphasis on minimum Gmb and optimal VFA (65–75%) rather than relying solely on binder content limits. This shift will encourage better densification control during lay-down and compaction.
- The slight lack-of-fit detected in the MF model ($p = 0.025$) suggests potential second-order or nonlinear relationships. Future work should investigate polynomial terms (e.g., VFA^2), interaction effects (e.g., $Gmb \times VFA$), or advanced machine-learning algorithms (e.g., Random Forest, XGBoost) to capture threshold behavior and improve prediction accuracy.
- Digital image analysis can yield angularity and surface texture indices, which may enhance model performance. These metrics should be collected routinely and tested as supplementary predictors in future modeling studies.
- Future research should expand the current predictive model by incorporating broader datasets across different aggregate sources and climatic regions. This would allow for the development of a generalized, transferable model capable of predicting Marshall parameters for a wider range of materials and pavement conditions, thus strengthening the model’s national applicability and reliability.

References

- Abedal, A. H. (2014). Asphalt Mix Design Methods. In *Asphalt Institute* (Seventh Ed). Asphalt Institute.
- Aliyu Yaro, N. S., Sutanto, M. H., Habib, N. Z., Usman, A., Adebajo, A., Wada, S. A., & Jagaba, A. H. (2024). Predictive modelling of volumetric and Marshall properties of asphalt mixtures modified with waste tire-derived char: A statistical neural network approach. *Journal of Road Engineering*, 4(3), 318–333. <https://doi.org/10.1016/j.jreng.2024.04.006>
- Asi, I., Alhadidi, Y. I., & Alhadidi, T. I. (2024). Predicting Marshall stability and flow parameters in asphalt pavements using explainable machine-learning models. *Transportation Engineering*, 18(May), 100282. <https://doi.org/10.1016/j.treng.2024.100282>
- Awan, H. H., Hussain, A., Javed, M. F., Qiu, Y., Alrowais, R., Mohamed, A. M., Fathi, D., & Alzahrani, A. M. (2022). Predicting Marshall Flow and Marshall Stability of Asphalt Pavements Using Multi Expression Programming. *Buildings*, 12(3), 1–20. <https://doi.org/10.3390/buildings12030314>
- Awed, A., Kassem, E., Masad, E., & Little, D. (2015). Method for Predicting the Laboratory Compaction Behavior of Asphalt Mixtures. *Journal of Materials in Civil Engineering*, 27(11). [https://doi.org/10.1061/\(asce\)mt.1943-5533.0001244](https://doi.org/10.1061/(asce)mt.1943-5533.0001244)
- Bressi, S., Santos, J., Orešković, M., & Losa, M. (2021). A comparative environmental impact analysis of asphalt mixtures containing crumb rubber and reclaimed asphalt pavement using life cycle assessment. *International Journal of Pavement Engineering*, 22(4), 524–538. <https://doi.org/10.1080/10298436.2019.1623404>
- Chadboun, B., Skok Jr, E., Newcomb, D., Crow, B., & Spindler, S. (1999). *The Effect of Voids in Mineral Aggregate (VMA) on Hot-Mix Asphalt Pavements*. 125.
- Department of Transport. (2023). *National Highways' Performance* (Issue July).
- Ejiko, S. O., & Filani, A. O. (2021). Mathematical Modeling: A Useful Tool For Engineering Research And Practice. *International Journal of Mathematics Trends and Technology*, 67(9), 50–64. <https://doi.org/10.14445/22315373/ijmtt-v67i9p506>
- Fang, M., Park, D., Singuranayo, J. L., Chen, H., & Li, Y. (2019). Aggregate gradation theory, design and its impact on asphalt pavement performance: a review. *International Journal of*

- Pavement Engineering*, 20(12), 1408–1424.
<https://doi.org/10.1080/10298436.2018.1430365>
- FHWA. (2022). *Balanced Asphalt Mix Design: Eight Tasks for Implementation*.
<https://www.fhwa.dot.gov/pavement/asphalt/pubs/hif22048.pdf>
- Gashi, E., Sadiku, H., & Misini, M. (2017). A Review of Aggregate and Asphalt mixture Specific Gravity measurements and their Impacts on Asphalt Mix Design Properties and Mix Acceptance. *International Journal of Advanced Engineering Research and Science*, 4(5), 195–201. <https://doi.org/10.22161/ijaers.4.5.31>
- Gul, M. A., Islam, M. K., Awan, H. H., Sohail, M., Al Fuhaid, A. F., Arifuzzaman, M., & Qureshi, H. J. (2022). Prediction of Marshall Stability and Marshall Flow of Asphalt Pavements Using Supervised Machine Learning Algorithms. *Symmetry*, 14(11).
<https://doi.org/10.3390/sym14112324>
- Herrmann, H., & Bucksch, H. (2014). Road Pavement. *Dictionary Geotechnical Engineering/Wörterbuch GeoTechnik, November*, 1128–1128. https://doi.org/10.1007/978-3-642-41714-6_182684
- Jaafar, Z. F. M., & Uddin, W. (2016). Modeling of asphalt pavement rutting for ltp southern region using multiple linear regression method. *8th International Conference on Maintenance and Rehabilitation of Pavements, MAIREPAV 2016, February*, 910–919.
<https://doi.org/10.3850/978-981-11-0449-7-178-cd>
- Kalaitzaki, E., Kollaros, G., & Athanasopoulou, A. (2015). Influence of aggregate gradation on hma mixes stability. *Romanian Journal of Transport Infrastructure*, 4(2), 13–22.
<https://doi.org/10.1515/rjti-2015-0034>
- Kassem, E., Masad, E., Lytton, R., & Chowdhury, A. (2011). Influence of air voids on mechanical properties of asphalt mixtures. *Road Materials and Pavement Design*, 12(3), 493–524. <https://doi.org/10.1080/14680629.2011.9695258>
- Law, A. M. (2015). *Simulation Modeling and Analysis* (Fifth Edit). Averill M. Law & Associates, Inc. www.averill-law.com
- Li, J., Li, P., Su, J., Xue, Y., & Rao, W. (2019). Effect of aggregate contact characteristics on densification properties of asphalt mixture. *Construction and Building Materials*, 204, 691–702. <https://doi.org/10.1016/j.conbuildmat.2019.01.023>
- Lira, B., Ekblad, J., & Lundström, R. (2021). Evaluation of asphalt rutting based on mixture

- aggregate gradation. *Road Materials and Pavement Design*, 22(5), 1160–1177.
<https://doi.org/10.1080/14680629.2019.1683061>
- Liu, Z., Yu, S., Huang, Y., Liu, L., & Pan, Y. (2024). A systematic review of rigid-flexible composite pavement. *Journal of Road Engineering*, 4(2), 203–223.
<https://doi.org/10.1016/j.jreng.2024.02.001>
- Logan, D. L. (2017). *A First Course in the Finite Element Method CL Engineering- 6th ed.* (Sixth Edit). Cengage Learning.
https://www.academia.edu/90368744/_1_Logan_A_First_Course_in_the_Finite_Element_Method_CL_Engineering_6th_ed
- Lv, Q., Huang, W., Zheng, M., Sadek, H., Zhang, Y., & Yan, C. (2020). Influence of gradation on asphalt mix rutting resistance measured by Hamburg Wheel Tracking test. *Construction and Building Materials*, 238, 117674. <https://doi.org/10.1016/j.conbuildmat.2019.117674>
- Mamlouk, M. S., & Zaniewski, J. P. (2018). *Materiales para lo Civil y Construcción Ingenieros: Materials for civil and construction engineers.* <https://worksaccounts.com/wp-content/uploads/2020/08/Materials-for-Civil-and-Construction-Engineering.pdf>
- Marini, M., Paoli, R., Grasso, F., Periaux, J., & Desideri, J. A. (2002). Verification and validation in computational fluid dynamics: The FLOWnet database experience. *JSME International Journal, Series B: Fluids and Thermal Engineering*, 45(1), 15–21.
<https://doi.org/10.1299/jsmeb.45.15>
- Mendoza-Sanchez, J. F., Alonso-Guzman, E. M., Martinez-Molina, W., Chavez-Garcia, H. L., Soto-Espitia, R., Delgado-Alamilla, H., & Obregon-Biosca, S. A. (2024). A Critical Review of Pavement Design Methods Based on a Climate Approach. *Sustainability (Switzerland)*, 16(16). <https://doi.org/10.3390/su16167211>
- Menner, A., & Yin, C. (2018). Introduction to modeling and simulation techniques. *ISCIIA and ITCA 2018 - 8th International Symposium on Computational Intelligence and Industrial Applications and 12th China-Japan International Workshop on Information Technology and Control Applications*, 16(1), 6–17.
- Moghaddam, T. B., Karim, M. R., & Abdelaziz, M. (2011). A review on fatigue and rutting performance of asphalt mixes. *Scientific Research and Essays*, 6(4), 670–682.
<https://doi.org/10.5897/SRE10.946>
- Montgomery, D. C., & Runger, G. C. (2014). *Applied Statistics and Probability for Engineers*

- (5th Editio). John Wiley & Sons, Inc.
- Oberkampff, W. L., & Roy, C. J. (2011). Verification and validation in scientific computing. *Verification and Validation in Scientific Computing, January 2010*, 1–767.
<https://doi.org/10.1017/CBO9780511760396>
- ODFT. (2015). *Impact of Basic Principles on Asphalt Mix Durability*. Quality Management System (QMS) Manual.
https://www.odot.org/materials/asph_tchnl_info/ASPH_MIX_DUR.pdf
- Omar, H. A., Yusoff, N. I. M., Mubaraki, M., & Ceylan, H. (2020). Effects of moisture damage on asphalt mixtures. *Journal of Traffic and Transportation Engineering (English Edition)*, 7(5), 600–628. <https://doi.org/10.1016/j.jtte.2020.07.001>
- Pedersen, N. J., Rosenbloom, S., & Skinner, R. E. J. (2011). A Manual for Design of Hot-Mix Asphalt with Commentary. In *National Cooperative Highway Research Program (NCHRP)*. Transportation Research Board of the National Academies.
<https://doi.org/10.17226/14524>
- Polaczyk, P., Ma, Y., Xiao, R., Hu, W., Jiang, X., & Huang, B. (2021). Characterization of aggregate interlocking in hot mix asphalt by mechanistic performance tests. *Road Materials and Pavement Design*, 22(S1), S498–S513.
<https://doi.org/10.1080/14680629.2021.1908408>
- Pranav, S., Aggarwal, S., Yang, E. H., Kumar Sarkar, A., Pratap Singh, A., & Lahoti, M. (2020). Alternative materials for wearing course of concrete pavements: A critical review. *Construction and Building Materials*, 236, 117609.
<https://doi.org/10.1016/j.conbuildmat.2019.117609>
- Ramirez, W. F. (1997). *Computational Methods in Process Simulation* (Second Edi). Butterworth-Heinemann. <https://doi.org/10.1016/B978-0-7506-3541-7.X5000-8>
- Sakshi, & Duggal, A. K. (2023). A Review on Correlation between Marshall. *International Journal for Research in Applied Science & Engineering Technology (IJRASET)*, 11(VI).
<https://doi.org/10.22214/ijraset.2023.54384>
- Sengoz, B., & Topal, A. (2007). Minimum voids in mineral aggregate in hot-mix asphalt based on asphalt film thickness. *Building and Environment*, 42(10), 3629–3635.
<https://doi.org/10.1016/j.buildenv.2006.10.005>
- Shah, S. A. R., Anwar, M. K., Arshad, H., Qurashi, M. A., Nisar, A., Khan, A. N., & Waseem,

- M. (2020). Marshall stability and flow analysis of asphalt concrete under progressive temperature conditions: An application of advance decision-making approach. *Construction and Building Materials*, 262, 120756. <https://doi.org/10.1016/j.conbuildmat.2020.120756>
- Shelar, G. R., Shaikh, S. H., Kalyani, K. V, Rathod, H., Student, B. E., Student, B. E., Student, B. E., & Student, B. E. (2022). *Investigation on Causes of Pavement*. 3, 2030–2036.
- Soetaertide, G., & Herman, P. M. J. (2009). A Practical Guide to Ecological Modelling. In *A Practical Guide to Ecological Modelling*. Netherlands Institute of Ecology. <https://doi.org/10.1007/978-1-4020-8624-3>
- Vargas, C., & Hanandeh, A. El. (2023). Features Importance and Their Impacts on the Properties of Asphalt Mixture Modified with Plastic Waste: A Machine Learning Modeling Approach. *International Journal of Pavement Research and Technology*, 16(6), 1555–1582. <https://doi.org/10.1007/s42947-022-00213-7>
- Version, E. (2022). *iTeh STANDARD PREVIEW (standards.iteh.ai)*. <https://standards.iteh.ai/catalog/standards/sist/8c9fc45f-79e6-4137-b1bc-c821b19af791/sist->
- West, R., Yin, F., Rodezno, C., & Taylor, A. (2021). *Balanced Mixture Design Implementation Support*. 0092, 83.
- Widiatmika, K. P. (2015). *Etika Jurnalisme Pada Koran Kuning : Sebuah Studi Mengenai Koran Lampu Hijau*, 16(2), 39–55.
- Williams, B. A., Willis, J. R., & Shacat, J. (2019). *Annual Asphalt Pavement Industry Survey on Recycled Materials*.
- Yan, K., Wang, S., Ge, D., Chen, J., Tian, S., & Sun, H. (2022). Laboratory performance of asphalt mixture with waste tyre rubber and APAO modified asphalt binder. *International Journal of Pavement Engineering*, 23(1), 59–69. <https://doi.org/10.1080/10298436.2020.1730837>
- Živčák, J., Kelemenová, T., Kelemen, M., & Maxim, V. (2013). Model-based Approach to Development of Engineering Systems. *Acta Mechanica Slovaca*, 17(3), 56–62. <https://doi.org/10.21496/ams.2013.033>

APPENDICES

APPENDICE A

Table 4-8: Hot Mix Asphalt data Collected

"Developing a predictive correlation model between aggregate properties and Marshall parameters in road pavement asphalt mixtures"														
TES TS #	Asp halt Con crete	% aggr egat e in total Mix	% asp halt by Wt of total mi x	Bulk Spec ific gravi ty of the aggr egat e	Maxi mum speci fic gravi ty of pavin g mix	Bulk speci fic gravit y of comp acted mix	% Air vo ids	% Void s in mine ral aggr egat e	Voi ds fille d wit h bitu men	Effe ctive speci fic gravi ty of aggr egat e	Mar shal Stab ility	Mar shal Flo w	Source	
Abv	AC	Ps	Pb	Gsb	Gm	Gmb	Va	VM A	VF A	Gse	MS	MF		
1	13	95.0 0	5.0 0	2.57	2.46	2.26	8. 20	16.6 0	50.7 0	2.65	10.0 9	2.15	CRBC, Gahanga Lab, Alex	
2	13	95.0 0	5.0 0	2.57	2.46	2.25	8. 50	16.9 0	49.5 0	2.65	8.23	2.18		
3	13	95.0 0	5.0 0	2.57	2.46	2.24	8. 90	17.2 0	48.4 0	2.65	7.80	2.14		
4	13	94.8 0	5.2 0	2.57	2.44	2.25	7. 50	16.9 0	55.8 0	2.63	10.0 2	2.11		
5	13	94.8 0	5.2 0	2.57	2.44	2.28	6. 30	15.8 0	60.3 0	2.63	11.0 9	2.59		
6	13	94.8 0	5.2 0	2.57	2.44	2.27	6. 80	16.3 0	58.1 0	2.63	11.2 2	2.81		
7	13	94.6 0	5.4 0	2.57	2.41	2.27	5. 80	16.5 0	64.9 0	2.61	11.4 9	2.67		
8	13	94.6 0	5.4 0	2.57	2.41	2.28	5. 40	16.2 0	66.5 0	2.61	12.4 3	2.54		
9	13	94.6 0	5.4 0	2.57	2.41	2.27	5. 70	16.5 0	65.2 0	2.61	13.1 2	2.61		
10	13	94.4 0	5.6 0	2.57	2.36	2.22	5. 80	18.3 0	68.5 0	2.56	11.0 2	2.92		
11	13	94.4 0	5.6 0	2.57	2.36	2.22	6. 10	18.6 0	67.1 0	2.56	11.2 4	2.77		
12	13	94.4 0	5.6 0	2.57	2.36	2.26	4. 30	17.1 0	74.6 0	2.56	11.7 5	2.45		
13	13	95.0 0	5.0 0	2.57	2.46	2.26	8. 18	16.5 7	50.6 6	2.66	10.0 9	2.15		ASTERI
14	13	95.0 0	5.0 0	2.57	2.46	2.25	8. 54	16.9 0	49.4 5	2.66	8.23	2.18		Gahanga Lab,
15	13	95.0 0	5.0 0	2.57	2.46	2.24	8. 89	17.2 2	48.3 7	2.66	7.80	2.14		Mutete

16	13	94.8	5.2				7.	16.8	55.7		10.0			Crusher, Jules
		0	0	2.57	2.44	2.25	47	9	6	2.64	2	2.11		
17	13	94.8	5.2				6.	15.8	60.2		11.0			
		0	0	2.57	2.44	2.28	28	2	9	2.64	9	2.59		
18	13	94.8	5.2				6.	16.3	58.1		11.2			
		0	0	2.57	2.44	2.27	84	2	1	2.64	2	2.81		
19	13	94.6	5.4				5.	16.5	64.8		11.4			
		0	0	2.57	2.41	2.27	81	5	9	2.61	9	2.67		
20	13	94.6	5.4				5.	16.2	66.4		12.4			
		0	0	2.57	2.41	2.28	44	2	5	2.61	3	2.54		
21	13	94.6	5.4				5.	16.4	65.2		13.1			
		0	0	2.57	2.41	2.27	73	7	4	2.61	2	2.61		
22	13	94.4	5.6				5.	18.3	68.5		11.0			
		0	0	2.57	2.36	2.22	77	1	1	2.56	2	2.92		
23	13	94.4	5.6				6.	18.6	67.1		11.2			
		0	0	2.57	2.36	2.22	12	2	3	2.56	4	2.77		
24	13	94.4	5.6				4.	17.0	74.5		11.7			
		0	0	2.57	2.36	2.26	35	8	6	2.56	5	2.45		
25	13	96.0	4.0				7.	15.4	52.6		14.6			
		0	0	2.62	2.49	2.31	29	0	2	2.65	6	2.29		
26	13	96.0	4.0				7.	15.3	52.6		11.1			
		0	0	2.62	2.49	2.31	28	8	8	2.65	0	1.43		
27	13	96.0	4.0				7.	15.3	52.7		11.1			
		0	0	2.62	2.49	2.31	27	7	1	2.65	6	2.28		
28	13	96.0	4.0				7.	15.4	52.3		11.4			
		0	0	2.62	2.49	2.31	36	6	8	2.65	6	1.85		
29	13	95.5	4.5				6.	14.9	58.4		17.3			
		0	0	2.62	2.49	2.33	21	5	7	2.67	2	1.74		
30	13	95.5	4.5				6.	14.9	58.5		11.6			
		0	0	2.62	2.49	2.33	20	5	0	2.67	7	1.57		
31	13	95.5	4.5				6.	14.9	58.3		12.8			HNRB, Test Method:
		0	0	2.62	2.49	2.33	24	8	4	2.67	3	1.92		
32	13	95.5	4.5				6.	14.8	58.7		13.6			ASTM D 1559- AASHTO T 245,
		0	0	2.62	2.49	2.34	14	9	6	2.67	9	1.98		
33	13	95.0	5.0				4.	14.3	71.1		12.5			Fabrice
		0	0	2.62	2.46	2.36	16	9	1	2.67	1	2.05		
34	13	95.0	5.0				4.	14.3	71.0		14.5			
		0	0	2.62	2.46	2.36	16	9	8	2.67	6	2.02		
35	13	95.0	5.0				4.	14.4	70.5		14.2			
		0	0	2.62	2.46	2.36	26	8	9	2.67	8	1.61		
36	13	95.0	5.0				4.	14.5	70.3		14.4			
		0	0	2.62	2.46	2.36	30	2	9	2.67	2	2.48		
37	13	94.5	5.5				3.	15.0	73.8		11.3			
		0	0	2.62	2.45	2.36	94	6	1	2.67	7	2.23		
38	13	94.5	5.5				3.	15.0	73.7		13.4			
		0	0	2.62	2.45	2.36	96	7	0	2.67	7	2.41		
39	13	94.5	5.5				3.	15.1	73.5		12.6			
		0	0	2.62	2.45	2.36	99	0	6	2.67	8	2.20		
40	13	94.5	5.5				4.	15.1	73.4		11.8			
		0	0	2.62	2.45	2.35	01	2	7	2.67	0	2.05		

		94.0	6.0				3.	15.7	79.1		11.3		
41	13	0	0	2.62	2.43	2.35	29	9	8	2.67	6	2.66	
		94.0	6.0				3.	15.8	79.1		11.4		
42	13	0	0	2.62	2.43	2.35	30	0	3	2.67	8	2.02	
		94.0	6.0				3.	15.7	79.1		13.1		
43	13	0	0	2.62	2.43	2.35	29	9	9	2.67	7	2.40	
		94.0	6.0				3.	15.8	79.0		10.7		
44	13	0	0	2.62	2.43	2.35	31	1	4	2.67	7	2.07	
		96.3	3.7				7.	14.4	50.9		31.0		
45	16	0	0	2.62	2.51	2.33	08	2	2	2.66	1	2.10	
		96.3	3.7				6.	14.1	51.9		20.5		
46	16	0	0	2.62	2.51	2.34	81	7	6	2.66	5	2.16	
		96.3	3.7				7.	14.5	50.2		22.3		
47	16	0	0	2.62	2.51	2.33	25	8	7	2.66	6	1.84	
		96.3	3.7				6.	14.2	51.8		20.9		
48	16	0	0	2.62	2.51	2.34	85	1	1	2.66	7	1.85	
		95.8	4.2				5.	14.4	58.7		30.8		
49	16	0	0	2.62	2.49	2.34	94	1	5	2.66	5	1.86	
		95.8	4.2				5.	14.0	60.7		20.7		
50	16	0	0	2.62	2.49	2.35	50	0	3	2.66	1	2.75	
		95.8	4.2				5.	14.1	59.7		19.7		
51	16	0	0	2.62	2.49	2.35	71	9	9	2.66	8	1.83	
		95.8	4.2				6.	14.6	57.7		25.6		
52	16	0	0	2.62	2.49	2.34	17	1	9	2.66	5	2.65	
		95.3	4.7				3.	13.7	71.5		22.0		
53	16	0	0	2.62	2.47	2.37	90	0	6	2.66	8	2.27	
		95.3	4.7				4.	13.9	70.3		23.1		
54	16	0	0	2.62	2.47	2.37	13	1	1	2.66	0	2.86	
		95.3	4.7				4.	13.9	70.2		21.3		
55	16	0	0	2.62	2.47	2.37	14	2	8	2.66	2	2.68	
		95.3	4.7				4.	13.8	70.5		22.9		
56	16	0	0	2.62	2.47	2.37	08	7	6	2.66	9	2.11	
		94.8	5.2				4.	14.7	72.7		19.9		
57	16	0	0	2.62	2.46	2.36	03	9	8	2.66	1	2.64	
		94.8	5.2				3.	14.5	74.3		19.4		
58	16	0	0	2.62	2.46	2.36	72	2	8	2.66	3	2.59	
		94.8	5.2				3.	14.2	76.0		21.2		
59	16	0	0	2.62	2.46	2.37	42	5	1	2.66	4	2.55	
		94.8	5.2				3.	14.2	76.2		19.4		
60	16	0	0	2.62	2.46	2.37	37	1	5	2.66	3	2.57	
		94.3	5.7				3.	15.4	80.2		19.0		
61	16	0	0	2.62	2.43	2.35	05	6	5	2.65	3	3.24	
		94.3	5.7				3.	15.5	79.4		22.5		
62	16	0	0	2.62	2.43	2.35	20	9	7	2.65	4	3.48	
		94.3	5.7				3.	15.7	78.4		19.9		
63	16	0	0	2.62	2.43	2.34	39	5	9	2.65	8	3.10	
		94.3	5.7				3.	15.5	79.5		18.9		
64	16	0	0	2.62	2.43	2.35	19	8	4	2.65	6	2.43	
		95.8	4.2				5.	14.3	65.0		20.1		
65	16	0	0	2.62	2.47	2.35	00	0	0	2.64	0	1.73	ASTM D 1559,

HNRB,
Test
Method:
AASHTO
DESIG
NATIO
NT 209,
Fabrice

66	16	95.8	4.2				4.	13.8	67.6		20.0		AASHTO T 245, RTDA
		0	0	2.62	2.47	2.36	50	0	0	2.64	0	1.47	
67	16	95.8	4.2				4.	13.5	69.2		21.1		
		0	0	2.62	2.47	2.37	20	0	0	2.64	0	1.67	
68	16	95.8	4.2				3.	13.3	70.5		24.0		
		0	0	2.62	2.47	2.37	90	0	0	2.64	0	2.58	
69	16	95.3	4.7				1.	12.5	86.3		20.7		
		0	0	2.62	2.45	2.41	70	0	0	2.63	0	2.42	
70	16	95.3	4.7				1.	12.5	86.1		22.4		
		0	0	2.62	2.45	2.41	70	0	0	2.63	0	2.73	
71	16	95.3	4.7				1.	12.0	90.1		25.5		
		0	0	2.62	2.45	2.42	20	0	0	2.63	0	2.71	
72	16	95.3	4.7				2.	12.8	83.9		14.8		
		0	0	2.62	2.45	2.40	10	0	0	2.63	0	2.30	
73	16	94.8	5.2				0.	13.2	96.8		19.3		
		0	0	2.62	2.41	2.40	40	0	0	2.61	0	2.81	
74	16	94.8	5.2				1.	13.7	92.6		14.4		
		0	0	2.62	2.41	2.39	00	0	0	2.61	0	2.94	
75	16	94.8	5.2				1.	14.4	87.6		22.3		
		0	0	2.62	2.41	2.37	80	0	0	2.61	0	2.50	
76	16	94.8	5.2				0.	13.5	94.4		17.4		
		0	0	2.62	2.41	2.39	80	0	0	2.61	0	2.08	
77	13	94.3	5.7				1.	14.0	88.5		18.2		
		0	0	2.62	2.43	2.39	60	0	0	2.66	0	3.60	
78	13	94.3	5.7				1.	13.8	90.1		19.1		
		0	0	2.62	2.43	2.39	40	0	0	2.66	0	3.07	
79	13	94.3	5.7				1.	14.0	88.6		14.7		
		0	0	2.62	2.43	2.39	60	0	0	2.66	0	2.84	
80	13	94.3	5.7				2.	14.4	86.0		20.0		
		0	0	2.62	2.43	2.39	00	0	0	2.66	0	2.72	
81	13	96.3	3.7				7.	14.4	50.9		31.0		
		0	0	2.62	2.51	2.33	10	0	0	2.66	0	2.10	
82	13	96.3	3.7				6.	14.2	52.0		20.6		
		0	0	2.62	2.51	2.34	80	0	0	2.66	0	2.16	
83	13	96.3	3.7				7.	14.6	50.3		22.4		
		0	0	2.62	2.51	2.33	20	0	0	2.66	0	1.84	
84	13	96.3	3.7				6.	14.2	51.8		21.0		
		0	0	2.62	2.51	2.34	80	0	0	2.66	0	1.85	
85	13	95.8	4.2				5.	14.4	58.7		30.9		
		0	0	2.62	2.49	2.34	90	0	0	2.66	0	1.86	
86	13	95.8	4.2				5.	14.0	60.7		20.7		
		0	0	2.62	2.49	2.34	50	0	0	2.66	0	2.75	
87	13	95.8	4.2				5.	14.2	59.8		19.8		
		0	0	2.62	2.49	2.34	70	0	0	2.66	0	1.83	
88	13	95.8	4.2				6.	14.6	57.8		25.7		
		0	0	2.62	2.49	2.34	20	0	0	2.66	0	2.65	
89	13	95.3	4.7				3.	13.7	71.6		22.1		
		0	0	2.62	2.47	2.38	90	0	0	2.66	0	2.27	
90	13	95.3	4.7				4.	13.9	70.3		23.1		
		0	0	2.62	2.47	2.37	10	0	0	2.66	0	2.86	

		95.3	4.7				4.	13.9	70.3		21.3	
91	13	0	0	2.62	2.47	2.37	10	0	0	2.66	0	2.68
		95.3	4.7				4.	13.9	70.6		23.0	
92	13	0	0	2.62	2.47	2.37	10	0	0	2.66	0	2.11
		94.8	5.2				4.	14.8	72.8		19.9	
93	13	0	0	2.62	2.46	2.36	00	0	0	2.66	0	2.64
		94.8	5.2				3.	14.5	74.4		19.4	
94	13	0	0	2.62	2.46	2.37	70	0	0	2.66	0	2.59
		94.8	5.2				3.	14.3	76.0		21.2	
95	13	0	0	2.62	2.46	2.37	40	0	0	2.66	0	2.55
		94.8	5.2				3.	14.2	76.3		19.4	
96	13	0	0	2.62	2.46	2.37	40	0	0	2.66	0	2.57
		94.3	5.7				3.	15.5	80.3		19.0	
97	13	0	0	2.62	2.43	2.35	10	0	0	2.65	0	3.24
		94.3	5.7				3.	15.6	79.5		22.5	
98	13	0	0	2.62	2.43	2.35	20	0	0	2.65	0	3.48
		94.3	5.7				3.	15.8	78.5		20.0	
99	13	0	0	2.62	2.43	2.34	40	0	0	2.65	0	3.10
		94.3	5.7				3.	15.6	79.5		19.0	
100	13	0	0	2.62	2.43	2.35	20	0	0	2.65	0	2.43
		96.3	3.7				4.	13.8	64.5		34.7	
101	16	0	0	2.62	2.47	2.35	90	0	0	2.66	0	1.22
		96.3	3.7				5.	14.3	62.6		33.8	
102	16	0	0	2.62	2.47	2.34	30	0	0	2.66	0	1.51
		96.3	3.7				6.	15.2	57.8		31.6	
103	16	0	0	2.62	2.47	2.31	40	0	0	2.66	0	1.91
		96.3	3.7				5.	14.5	60.9		30.8	
104	16	0	0	2.62	2.47	2.33	70	0	0	2.66	0	2.63
		95.8	4.2				4.	14.1	66.3		39.2	
105	16	0	0	2.62	2.47	2.35	80	0	0	2.66	0	1.88
		95.8	4.2				5.	14.6	63.9		29.4	
106	16	0	0	2.62	2.47	2.34	30	0	0	2.66	0	2.71
		95.8	4.2				4.	14.2	65.7		34.3	
107	16	0	0	2.62	2.47	2.35	90	0	0	2.66	0	2.57
		95.8	4.2				5.	14.6	63.5		29.6	
108	16	0	0	2.62	2.47	2.34	30	0	0	2.66	0	2.11
		95.3	4.7				3.	13.4	74.1		32.7	
109	16	0	0	2.62	2.47	2.38	50	0	0	2.66	0	2.55
		95.3	4.7				3.	13.6	73.0		21.2	
110	16	0	0	2.62	2.47	2.38	70	0	0	2.66	0	2.52
		95.3	4.7				4.	13.9	71.3		25.0	
111	16	0	0	2.62	2.47	2.37	00	0	0	2.66	0	2.94
		95.3	4.7				3.	13.6	72.6		22.2	
112	16	0	0	2.62	2.47	2.38	70	0	0	2.66	0	2.27
		94.8	5.2				4.	14.6	70.5		25.1	
113	16	0	0	2.62	2.47	2.36	30	0	0	2.66	0	3.19
		94.8	5.2				4.	14.7	70.0		22.6	
114	16	0	0	2.62	2.47	2.36	40	0	0	2.66	0	3.56
		94.8	5.2				3.	14.2	73.0		21.2	
115	16	0	0	2.62	2.47	2.37	80	0	0	2.66	0	2.18

		94.8	5.2				4.	14.5	71.1		25.2		
116	16	0	0	2.62	2.47	2.37	20	0	0	2.66	0	2.62	
		94.3	5.7				5.	15.9	66.8		20.2		
117	16	0	0	2.62	2.47	2.34	30	0	0	2.66	0	2.73	
		94.3	5.7				5.	16.4	64.5		16.0		
118	16	0	0	2.62	2.47	2.32	80	0	0	2.66	0	2.68	
		94.3	5.7				4.	15.5	69.0		18.9		
119	16	0	0	2.62	2.47	2.35	80	0	0	2.66	0	2.66	
		94.3	5.7				5.	15.9	67.0		18.3		
120	16	0	0	2.62	2.47	2.34	20	0	0	2.66	0	2.59	
		95.6	4.4				5.	15.3	62.3				
121	13	0	0	2.57	2.41	2.27	80	0	0	2.58	7.60	1.92	
		95.6	4.4				5.	15.2	62.5				
122	13	0	0	2.57	2.41	2.27	70	0	0	2.58	6.60	1.92	
		95.6	4.4				5.	15.3	62.4				
123	13	0	0	2.57	2.41	2.28	70	0	0	2.58	6.80	1.87	
		95.6	4.4				5.	15.2	62.7				
124	13	0	0	2.57	2.41	2.28	70	0	0	2.58	7.90	2.02	
		95.3	4.7				4.	15.1	67.9		11.8		
125	13	0	0	2.57	2.40	2.29	90	0	0	2.58	0	2.30	
		95.3	4.7				4.	15.0	68.2		11.8		
126	13	0	0	2.57	2.40	2.29	80	0	0	2.58	0	2.34	
		95.3	4.7				4.	15.1	68.1		12.3		
127	13	0	0	2.57	2.40	2.29	80	0	0	2.58	0	2.18	
		95.3	4.7				4.	15.1	67.7		12.6		
128	13	0	0	2.57	2.40	2.29	90	0	0	2.58	0	2.42	
		95.0	5.0				3.	14.9	75.0		14.8		
129	13	0	0	2.57	2.39	2.30	70	0	0	2.57	0	2.70	
		95.0	5.0				3.	14.9	74.8		15.2		
130	13	0	0	2.57	2.39	2.30	70	0	0	2.57	0	2.68	RTDA
		95.0	5.0				3.	14.9	74.7		14.8		Naphtal
131	13	0	0	2.57	2.39	2.30	80	0	0	2.57	0	2.66	
		95.0	5.0				3.	14.9	74.4		14.4		
132	13	0	0	2.57	2.39	2.30	80	0	0	2.57	0	2.61	
		94.7	5.3				3.	15.6	77.7		13.8		
133	13	0	0	2.57	2.37	2.29	50	0	0	2.56	0	3.10	
		94.7	5.3				3.	15.5	78.1		14.1		
134	13	0	0	2.57	2.37	2.29	40	0	0	2.56	0	3.10	
		94.7	5.3				3.	15.6	77.6		14.0		
135	13	0	0	2.57	2.37	2.29	50	0	0	2.56	0	3.00	
		94.7	5.3				3.	15.5	78.1		13.9		
136	13	0	0	2.57	2.37	2.29	40	0	0	2.56	0	3.23	
		95.6	4.4				6.	15.4	58.8		10.2		
137	13	0	0	2.57	2.42	2.27	30	0	0	2.59	0	2.10	
		95.6	4.4				6.	15.4	58.7		11.0		
138	13	0	0	2.57	2.42	2.27	30	0	0	2.59	0	2.00	
		95.6	4.4				6.	15.3	58.9		10.5		
139	13	0	0	2.57	2.42	2.27	30	0	0	2.59	0	2.20	
		95.6	4.4				6.	15.3	58.9		10.4		
140	13	0	0	2.57	2.42	2.27	30	0	0	2.59	0	2.30	

		95.3	4.7				5.	14.9	66.1		14.9	
141	13	0	0	2.57	2.41	2.29	10	0	0	2.59	0	2.53
		95.3	4.7				5.	15.0	65.5		15.2	
142	13	0	0	2.57	2.41	2.29	20	0	0	2.59	0	2.45
		95.3	4.7				5.	15.0	65.5		16.2	
143	13	0	0	2.57	2.41	2.29	20	0	0	2.59	0	2.55
		95.3	4.7				5.	15.0	65.6		14.1	
144	13	0	0	2.57	2.41	2.29	20	0	0	2.59	0	2.59
		95.0	5.0				4.	14.8	72.2		17.8	
145	13	0	0	2.57	2.40	2.30	10	0	0	2.59	0	2.96
		95.0	5.0				4.	14.7	72.5		17.8	
146	13	0	0	2.57	2.40	2.30	10	0	0	2.59	0	2.71
		95.0	5.0				4.	14.8	72.3		18.8	
147	13	0	0	2.57	2.40	2.30	10	0	0	2.59	0	2.70
		95.0	5.0				4.	14.7	72.7		18.7	
148	13	0	0	2.57	2.40	2.30	00	0	0	2.59	0	2.60
		94.7	5.3				3.	14.7	79.7		14.9	
149	13	0	0	2.57	2.38	2.31	00	0	0	2.58	0	2.81
		94.7	5.3				3.	15.2	76.4		14.9	
150	13	0	0	2.57	2.38	2.30	60	0	0	2.58	0	2.80
		94.7	5.3				3.	15.4	75.2		14.9	
151	13	0	0	2.57	2.38	2.29	80	0	0	2.58	0	2.85
		94.7	5.3				3.	15.5	74.7		14.8	
152	13	0	0	2.57	2.38	2.29	90	0	0	2.58	0	2.97
		94.7	5.3				3.	16.0	78.2		12.3	
153	13	0	0	2.57	2.36	2.28	50	0	0	2.57	0	3.21
		94.7	5.3				3.	15.8	79.3		12.4	
154	13	0	0	2.57	2.36	2.29	30	0	0	2.57	0	3.30
		94.7	5.3				3.	15.9	78.5		12.5	
155	13	0	0	2.57	2.36	2.28	40	0	0	2.57	0	3.02
		94.7	5.3				3.	15.9	78.6		12.4	
156	13	0	0	2.57	2.36	2.28	40	0	0	2.57	0	3.14
		95.6	4.4				6.	15.2	60.4			
157	13	0	0	2.57	2.42	2.27	00	0	0	2.59	8.00	1.98
		95.6	4.4				6.	15.2	60.5			
158	13	0	0	2.57	2.42	2.27	00	0	0	2.59	7.60	1.84
		95.6	4.4				5.	15.1	61.2			
159	13	0	0	2.57	2.42	2.28	80	0	0	2.59	7.80	1.98
		95.6	4.4				5.	15.0	61.6			
160	13	0	0	2.57	2.42	2.28	80	0	0	2.59	8.60	1.87
		95.3	4.7				5.	15.0	67.0		13.1	
161	13	0	0	2.57	2.41	2.29	00	0	0	2.58	0	2.20
		95.3	4.7				4.	15.0	67.1		12.8	
162	13	0	0	2.57	2.41	2.29	90	0	0	2.58	0	2.19
		95.3	4.7				5.	15.1	66.9		13.0	
163	13	0	0	2.57	2.41	2.29	00	0	0	2.58	0	2.21
		95.3	4.7				4.	15.0	67.2		13.3	
164	13	0	0	2.57	2.41	2.29	90	0	0	2.58	0	2.18
		95.0	5.0				3.	14.8	74.7		16.2	
165	13	0	0	2.57	2.39	2.30	70	0	0	2.58	0	2.54

		95.0	5.0				3.	14.8	74.8		15.9	
166	13	0	0	2.57	2.39	2.30	70	0	0	2.58	0	2.60
		95.0	5.0				4.	15.0	73.4		16.3	
167	13	0	0	2.57	2.39	2.30	00	0	0	2.58	0	2.56
		95.0	5.0				4.	15.1	72.9		16.3	
168	13	0	0	2.57	2.39	2.29	10	0	0	2.58	0	2.55
		94.7	5.3				2.	14.7	81.8		14.9	
169	13	0	0	2.57	2.37	2.31	70	0	0	2.57	0	2.81
		94.7	5.3				3.	15.6	76.6		14.9	
170	13	0	0	2.57	2.37	2.29	60	0	0	2.57	0	2.80
		94.7	5.3				3.	15.6	76.4		14.9	
171	13	0	0	2.57	2.37	2.29	70	0	0	2.57	0	2.85
		94.7	5.3				3.	15.5	77.1		14.8	
172	13	0	0	2.57	2.37	2.29	50	0	0	2.57	0	2.97
		94.7	5.3				3.	16.1	79.4		12.3	
173	13	0	0	2.57	2.36	2.28	30	0	0	2.59	0	3.21
		94.7	5.3				3.	16.1	79.5		12.4	
174	13	0	0	2.57	2.36	2.28	30	0	0	2.59	0	3.30
		94.7	5.3				3.	16.1	79.4		12.5	
175	13	0	0	2.57	2.36	2.28	30	0	0	2.59	0	3.02
		94.7	5.3				3.	16.2	79.3		12.4	
176	13	0	0	2.57	2.36	2.28	30	0	0	2.59	0	3.14
		95.6	4.4				6.	15.4	58.9			
177	13	0	0	2.57	2.42	2.27	30	0	0	2.59	9.90	2.20
		95.6	4.4				6.	15.3	59.2		10.5	
178	13	0	0	2.57	2.42	2.27	30	0	0	2.59	0	1.99
		95.6	4.4				6.	15.3	59.3		11.3	
179	13	0	0	2.57	2.42	2.27	20	0	0	2.59	0	2.15
		95.6	4.4				6.	15.4	58.9		11.2	
180	13	0	0	2.57	2.42	2.27	30	0	0	2.59	0	2.24
		95.3	4.7				5.	14.9	66.4		14.5	
181	13	0	0	2.57	2.41	2.29	00	0	0	2.59	0	2.63
		95.3	4.7				5.	14.9	66.1		14.4	
182	13	0	0	2.57	2.41	2.29	10	0	0	2.59	0	2.49
		95.3	4.7				5.	15.0	65.8		14.8	
183	13	0	0	2.57	2.41	2.29	10	0	0	2.59	0	2.55
		95.3	4.7				5.	14.9	66.3		14.9	
184	13	0	0	2.57	2.41	2.29	00	0	0	2.59	0	2.60
		95.0	5.0				4.	14.8	72.1		18.2	
185	13	0	0	2.57	2.39	2.30	10	0	0	2.58	0	2.90
		95.0	5.0				4.	14.7	72.9		18.0	
186	13	0	0	2.57	2.39	2.30	00	0	0	2.58	0	2.81
		95.0	5.0				4.	14.8	72.6		17.9	
187	13	0	0	2.57	2.39	2.30	10	0	0	2.58	0	2.80
		95.0	5.0				4.	14.7	72.7		18.4	
188	13	0	0	2.57	2.39	2.30	00	0	0	2.58	0	2.73
		94.7	5.3				3.	14.7	79.4		16.2	
189	13	0	0	2.57	2.38	2.31	00	0	0	2.58	0	2.98
		94.7	5.3				3.	15.4	75.4		14.6	
190	13	0	0	2.57	2.38	2.29	80	0	0	2.58	0	2.91

		94.7	5.3				3.	15.4	74.9		14.4		
191	13	0	0	2.57	2.38	2.29	90	0	0	2.58	0	2.91	
		94.7	5.3				4.	15.6	74.2		14.2		
192	13	0	0	2.57	2.38	2.29	00	0	0	2.58	0	3.10	
		94.4	5.6				3.	15.9	78.4		11.2		
193	13	0	0	2.57	2.37	2.28	40	0	0	2.57	0	3.13	
		94.4	5.6				3.	15.9	78.4		11.3		
194	13	0	0	2.57	2.37	2.28	40	0	0	2.57	0	3.20	
		94.4	5.6				3.	15.9	78.4		11.6		
195	13	0	0	2.57	2.37	2.28	40	0	0	2.57	0	3.17	
		94.4	5.6				3.	15.9	78.7		11.5		
196	13	0	0	2.57	2.37	2.29	40	0	0	2.57	0	3.15	
		95.2	4.8				6.	16.9	62.3		13.7		
197	13	0	0	2.85	2.65	2.48	40	8	1	2.88	0	2.74	
		95.2	4.8				6.	16.8	62.7		14.9		
198	13	0	0	2.85	2.65	2.48	30	9	1	2.88	0	2.46	
		95.2	4.8				5.	16.5	64.2		15.2		
199	13	0	0	2.85	2.65	2.49	92	5	6	2.88	7	2.33	
		95.0	5.0				5.	16.8	65.7		17.6		
200	13	0	0	2.85	2.64	2.49	77	7	8	2.88	4	2.57	
		95.0	5.0				5.	16.8	66.0		17.6		
201	13	0	0	2.85	2.64	2.49	71	2	3	2.88	5	2.68	
		95.0	5.0				5.	16.3	68.1		18.2		
202	13	0	0	2.85	2.64	2.50	21	7	7	2.88	7	2.75	
		94.8	5.2				4.	16.6	71.7		18.6		
203	13	0	0	2.85	2.63	2.50	68	0	9	2.87	5	2.68	
		94.8	5.2				4.	16.3	73.3		19.6		
204	13	0	0	2.85	2.63	2.51	34	0	8	2.87	9	2.79	
		94.8	5.2				4.	16.3	72.9		19.2		
205	13	0	0	2.85	2.63	2.51	44	8	2	2.87	6	2.62	
		94.6	5.4				4.	16.9	73.4		16.8		
206	13	0	0	2.85	2.61	2.50	51	9	4	2.87	9	2.80	
		94.6	5.4				4.	16.5	75.6		17.3		
207	13	0	0	2.85	2.61	2.51	04	8	2	2.87	3	2.86	
		94.6	5.4				4.	16.7	74.8		16.9		
208	13	0	0	2.85	2.61	2.50	21	2	4	2.87	9	2.87	
		94.4	5.6				3.	17.2	76.8		13.6		
209	13	0	0	2.85	2.60	2.49	99	4	5	2.86	5	2.90	
		94.4	5.6				4.	17.6	74.6		13.6		
210	13	0	0	2.85	2.60	2.48	49	7	1	2.86	6	2.97	
		94.4	5.6				4.	17.4	75.9		14.2		
211	13	0	0	2.85	2.60	2.49	19	2	3	2.86	4	3.22	

NPD
MUKO
KIP,
ERIC

APPENDICE B



UNIVERSITY of
RWANDA

P.O Box 3900 Kigali, Rwanda

COLLEGE OF SCIENCE
AND TECHNOLOGY

SCHOOL OF ENGINEERING

Kigali on 20th, May 2025

TO WHOM IT MAY CONCERN

RE: REQUEST FOR FACILITATING OUR STUDENT FOR DATA COLLECTION.

This is to certify that **Mr. SHEMA Richard** is a MSc student of the Department of Civil, Highway Engineering and Management, under the School of Engineering, at University of Rwanda, College of Science and Technology (UR-CST).

As part of the academic requirements for the award of a MSc Degree in Highway Engineering and Management, student is required to work on projects, prepare and defend respective dissertations. It is indeed for this purpose that this student is working on **“DEVELOPING A PREDICTIVE CORRELATION MODEL BETWEEN AGGREGATE CHARACTERISTICS AND MARSHALL PARAMETERS IN ROAD PAVEMENT ASPHALT MIXTURES.**

In this regard, we are requesting you to allow **Mr. SHEMA Richard** to carry out his research work, which is a partial fulfilment for award of MSc degree in the field of study. During that work time, student is required to follow the rules and regulations of your esteemed institution.

Sincerely,

Assoc. Prof. **MBEREYAHU Leopold**
Dean, School of Engineering



REPUBLIC OF RWANDA

29 MAY 2025
Kigali,
Ref No: 1619/Corp.../025



RWANDA TRANSPORT DEVELOPMENT AGENCY
P.O Box 6674
KG 563 St., Queen's Land House
Email: info@rtda.gov.rw
KIGALI

Richard SHEMA
MSc student University of Rwanda (UR-CST)



Dear Sir,

RE: Response to your letter requesting data collection for your MSc Studies

Reference is made to your letter dated 20th May 2025 requesting data collection for your Master's studies in your research project titled "Developing a predictive correlation model between aggregate characteristics and Marshall parameters in road pavement asphalt mixtures";

We hereby inform you that your request is well received and approved. For further information, you can contact **Mr. Emmanuel NIZEYIMANA**, Director of Quality Control and Research Unit on his email: emmanuel.nizeyimana@rtda.gov.rw, or on his phone number: 0788435725.

Sincerely,



Imena MUNYAMPENDA
Director General

CC:

- Hon. Minister of Infrastructure
- Hon. Minister of State/MININFRA
- Permanent Secretary/MININFRA
- Coordinator of Postgraduate Programs/UR-CST

KIGALI

28th May 2025

Ref N^o: SR/NPD/HR & Adm-D/DMD/606/2025

SHEMA Richard

C: +250 788403037

Dear Richard,

Subject: Feedback on your request for Data Collection

Reference is made to your request dated 23rd May 2025, seeking facilitation to conduct academic research (data collection) at NPD in fulfillment of your academic program and to finalize a research project focused on: **“Developing a predictive correlation model between aggregate characteristics and marshall parameters in road pavement asphalt mixtures”**

In line with the academic requirements for the completion of your Master's degree at UR/CST, I am pleased to offer you the above research (Data Collection) under Technical Service Department, and your research will be supervised by **HABIMANA Jean Eric, Material Engineer at KIP**, contact number: **+250789270847**.

Sincerely,



NPD
Reliability is our strength
P.O. Box: 495 KIGALI
TEL: (+250) 790022000 P.O. Box: 495 KIGALI
www.npd.co.rw

Yannick KAYIJUKA ZINGIRO
Ag. Deputy Managing Director

Cc:

- HR & Adm-Director
- Technical Service Director

KIGALI